Coordination Chemistry Reviews 253 (2009) 449–478

Contents lists available at ScienceDirect

Coordination Chemistry Reviews

journal homepage: www.elsevier.com/locate/ccr

Review

Platinum complexes of terpyridine: Synthesis, structure and reactivity

Scott D. Cummings*

Department of Chemistry, Kenyon College, Tomsich Hall, Gambier, OH 43022, United States

Contents

* Tel.: +1 740 427 5355.
E-mail address: cummingss@kenyon.edu.

0010-8545/$ – see front matter
doi:10.1016/j.ccr.2008.04.013

ARTICLE INFO

Article history:
Received 18 September 2007
Accepted 16 April 2008
Available online 2 May 2008

Keywords:
Platinum complexes
Tridentate nitrogen ligands
Ligand substitution reactions
Kinetics
Crystal structures
Stacking interactions

ABSTRACT

With a rich history spanning over 75 years, platinum terpyridine complexes are a diverse and versatile family of coordination compounds. This review addresses the burgeoning field of research aimed at exploring synthesis and characterization, structure and bonding, thermodynamics and kinetics of ligand substitution, and stacking in solution and in the solid state.

1. Introduction

In modern coordination chemistry, transition metal polypyridine complexes [1] play a central role in the analytical detection of metal ions [2], in experiments to understand inorganic reaction mechanisms and kinetics [3], as biochemical electron-transfer reagents [4] and metalloenzyme models [5]. Dyes based on transition metal polypyridine complexes are extensively used in applications ranging from luminescent sensors [6,7] in solar energy conversion schemes [8,9] to molecular photonic devices [10,11], and employed as building blocks for supramolecular [12] and nanoscale [13] chemistry. In particular, metal complexes of the polypyridine ligand 2,2′:6′,2″-terpyridine (terpy), while not as extensively investigated as complexes of bipyridine and other diimine ligands, have a rich history extending back over three quarters of a century [14].

Following an initial report in 1934 of the syntheses of the first platinum terpy complexes [15], over 25 years passed before research continued on the chemistry of these coordination compounds. In recent years, investigations into the synthesis and reactivity of Pt(II) terpy systems have made significant contributions to our understanding of ligand substitution in square-planar d^8 complexes and on how electronic and steric factors within the metal complex affect reactivity. Pt(II) terpy complexes have become important reagents for the study of biomolecules due to their propensity to bind, often by selective modes, to DNA and proteins. Investigations of biomolecular structure and reactivity are facilitated by the useful properties of Pt(II) terpy probes: the spin-active ^{195}Pt nucleus for NMR spectroscopy, the large Pt nucleus to serve as a high-scattering atom for X-ray diffraction studies, and long-wavelength light absorption and emission for identifying binding modes and changes in microenvironment of the probe. Developing concomitantly as an essentially separate field, investigations into the redox and photophysical properties of platinum terpy systems have yielded rich results and have provided a better understanding of how to design reagents having tunable electron-transfer and luminescent properties and excited-state reactivity.

In recent years, an explosion of interest in the platinum terpy family of complexes has resulted in as many as 25 new papers appearing annually in the primary literature. Rapid progress in the three areas of structure/reactivity, interaction with biomolecules and electronic properties offers great potential to expand the applications of this family of coordination compounds. For example, common themes in the platinum terpy systems often emerge from research teams in seemingly disparate areas of chemistry and biochemistry: π–π stacking interactions in crystal structures often share common traits with intercalation in DNA; tailoring luminescent properties through ligand variation may allow for the design of better probes of electron transfer in DNA or active sites of proteins; observations of selective binding to particular amino acid residues in proteins informs investigations of ligand substitution chemistry.

This review aims to present a comprehensive summary of 75 years of research on the synthesis, reactivity and structural characterization of diverse members of the family of platinum terpy complexes of the type $[Pt(Yterpy)X]^{n+}$, where X represents ligands occupying the fourth coordination site, Y represents substituents on the terpy ligand and n is the charge of the complex (Fig. 1). A review summarizing transition metal terpy complexes up to 1986 has been provided by Constable, but few papers involving platinum terpy complexes had been published at that point [16]. Likewise, a recent monograph on terpyridine metal complexes includes only brief mention of platinum complexes [14], and a selective review of Pt(II) pyridine complexes appeared in 1999 [17]. While no comprehensive review of this field has been published, shorter accounts have appeared on the sub-topics of protein binding [18,19], DNA binding [20], and photoluminescence [21].

2. Synthesis

Over 100 different platinum terpy complexes have been prepared, and this section summarizes how they can be assembled from readily available precursors. The vast majority of systems belong to the class of square-planar d^8 $[Pt(terpy)X]^{n+}$ complexes having a tridentate terpy ligand with the fourth coordination site occupied by a donor ligand X, but Pt(IV) systems and those having other types of terpy coordination are also known.

2.1. Synthesis of $[Pt(terpy)X]^{n+}$ complexes

The first report on the preparation of a Pt(II) terpy complex came in 1934 from Morgan and Burstall, who described the synthesis and reactivity of [Pt(terpy)Cl]Cl [15]. This chloro complex can be regarded as the "parent" compound of a large and growing family of Pt(II) terpy complexes. With high water solubility and a labile chloride ligand, it is a useful reagent for the synthesis of a wide range of other $[Pt(terpy)X]^{n+}$ complexes (see Section 3.2 for a review of reactions involving displacement of Cl^- by other X ligands). Four synthetic methods (A–D) for preparing $[Pt(terpy)X]^{n+}$ complexes differ in their starting materials, conditions and yield.

$$\text{Method A}: \quad K_2PtCl_4(aq) + \text{terpy}(s) \rightarrow [Pt(terpy)Cl]Cl + 2KCl(aq) \quad (1)$$

The method first described by Morgan and Burstall involves the reaction of $K_2PtCl_4(aq)$ with a suspension of terpy in water [15]. Upon heating, an insoluble red Magnus-type double salt $[Pt(terpy)Cl]_2[PtCl_4]$ forms along with an orange solution of [Pt(terpy)Cl]Cl. Yield of the later product can be increased to 65% with prolonged heating (1–4 days), but additional heating may result in decomposition to Pt(0) [22]. The authors also describe the

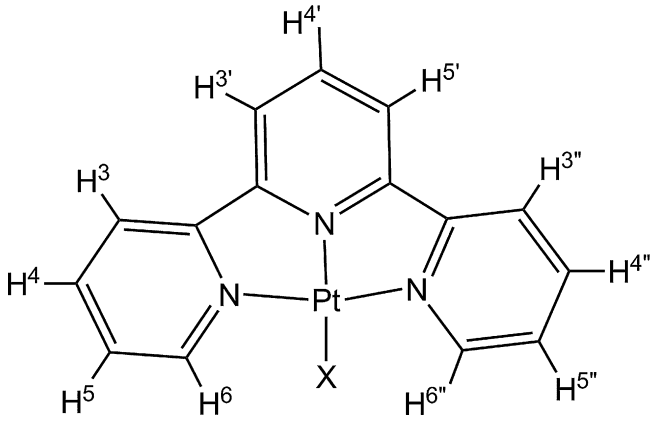

Fig. 1. $[Pt(terpy)X]^{n+}$ complex cation, showing atom numbering scheme.

preparation of a black form of [Pt(terpy)Cl]Cl, but no other reports of this observation have appeared.

The $[Pt(terpy)Cl]_2[PtCl_4]$ double salt, which is the favored kinetic product due to a combination of favorable electrostatic attraction and stacking interactions between the square-planar ions, can be isolated as either a dihydrate or trihydrate and extracted into boiling HCl(aq). The red double salt product also forms from the reaction of [Pt(terpy)Cl]Cl with K_2PtCl_4 [15]. Morgan and Burstall identified a second yellow product, not extractable with HCl(aq), to which they assigned the formula "$[Pt_3$ 2terpy $Cl_6]$". While this has the same empirical formula as the red double salt but differs by its solubility, an isomorphic solid-state structure seems likely (see Section 4.2.4). Reaction of the double salt with pyridine yields additional [Pt(terpy)Cl]Cl along with *trans*-$Pt(py)_2Cl_2$ [23].

Two interesting variations on this method have been reported. First, the use of microwave dielectric loss heating in the preparation of [Pt(terpy)Cl]Cl from K_2PtCl_4 with terpy in water has been reported to offer a 47% yield after two 30-s irradiations [24]. Also, passing SO_2(g) through a solution of K_2PtCl_4 in 4:1 EtOH/water followed by the addition of terpy results in the formation of $[Pt(terpy)(SO_3H)]Cl$ [25]. Addition of CO_2(g) prior to the addition of terpy yields a product identified as $[Pt(terpy)(SO_3H)_2]$, but the coordination mode of the terpy ligand was not discussed.

$$\text{Method B}: \quad [PtL_2Cl_2] + \text{terpy} \rightarrow [Pt(terpy)Cl]Cl + 2L, \quad L = \text{dmso, NCPh} \tag{2}$$

The reaction of *cis*-$[Pt(NCPh)_2Cl_2]$ with terpy in DMF also results in the formation of a double salt $[Pt(terpy)Cl]_2[PtCl_4]$ as the major product [26]. Similarly, using *cis*-$[Pt(dmso)_2Cl_2]$ in MeOH leads to the formation of [Pt(terpy)Cl] $[Pt(dmso)Cl_3]$ precipitate (28% yield) in addition to [Pt(terpy)Cl]Cl (30% yield) [26], but the same reaction in acetone is reported to produce the double salt product with 94% yield [27]. In contrast, the reaction of $[Pt(dmso)_2Cl_2]$ with a cationic terpy derivative proceeds with good yield in $CHCl_3$ to form the monometallic complex [28]. The use of $PtCl_2$ and 10% dmso in a 1:1 water/CH_3CN solvent mixture was reported to react quantitatively with terpy in a few hours [29]. The reaction of *trans*-$[Pt(dmso)_2(R)Cl]$ (R = Me, Ph) with terpy in methanol yields $[Pt(terpy)(R)]^+$ [30,31], but using *cis*-$[Pt(dmso)_2(CH_3)_2]$ results in completely different chemistry [32], as described in Section 2.5.2.

Alternatively, *cis*-$[Pt(NCPh)_2Cl_2]$ can be combined with 1 equiv. AgA (A = SbF_6^- or $CF_3SO_3^-$) in CH_3CN, the resulting AgCl solid removed by filtration and terpy added to prepare [Pt(terpy)Cl]A [33]. Similar chemistry using *cis*-$[Pt(dmso)_2Cl_2]$ has been reported [34].

$$\text{Method C}: \quad \textit{cis}\text{-}[Pt(COD)X_2] + \text{terpy} \rightarrow [Pt(terpy)(X)]X + \text{COD}, \quad X = \text{Cl, I} \tag{3}$$

An efficient preparation has come from Annibale et al., who reported rapid (15 min) and nearly quantitative formation of $[Pt(terpy)Cl]^+$ from the reaction of $[Pt(COD)Cl_2]$ (COD = 1,5-cyclooctadiene) with terpy in water [26]. The COD complex is first prepared from K_2PtCl_4 in 95% yield [35]. The high *trans*-labilizing effect of the COD ligand allows for easily displacement of chloride by terpy. Addition of a few drops of HCl(aq) catalyzes the reaction by protonation if an N atom of terpy to form water-soluble terpyridinium cations. Importantly, at no point is an anionic complex formed that is capable of precipitating as a double salt with the cationic product.

A report by Lowe describes a similar approach, involving the reaction of $[Pt(COD)X_2]$ (X = Cl or I) with 2 equiv. of $AgBF_4$ in acetone, followed by removal of AgX(s) and addition of terpy in CH_3CN to prepare $[Pt(terpy)(CH_3CN)]^{2+}$, which they did not isolate but allowed to react with 4-picoline [29]. The starting material $[Pt(COD)X_2]$ undergoes more rapid reaction for X = I than for X = Cl. Similar reactions using $AgNO_3$ in 20% aqueous acetone [36], $AgSbF_6$ in dry acetone [37], or $AgCF_3SO_3$ in dimethylacetamide [34] provide intermediates described as $[Pt(terpy)(solvent)]^{2+}$, which then reacts with a variety of nucleophilic ligands. One research group has indicated that rigorously dry acetone be used to avoid the formation of substitutionally inert aqua complexes, and also suggested that using $AgPF_6$ may result in fluoride abstraction by the cationic platinum intermediate [38].

The organometallic complex cation $[Pt(terpy)(CH_2SiMe_3)]^+$ can be prepared similarly using $[Pt(COD)(CH_2SiMe_3)I]$ as a starting material [39], and tritium-labeled terpyridine was used to prepare ^{3}H-labeled [Pt(terpy)Cl]Cl by method C [40].

$$\text{Method D}: \quad \textit{cis/trans}\text{-}[PtCl_2(SMe_2)_2] + \text{terpy} \rightarrow [Pt(terpy)Cl]Cl{\cdot}2H_2O + 2SMe_2 \tag{4}$$

Another efficient preparation utilizes *cis*/*trans*-$[PtCl_2(SMe_2)_2]$ [41], dissolved in warm MeOH/H_2O and combined with terpy and heated for 30–40 min [35]. Removal of solvent and recrystallization from MeOH/Et_2O affords $[Pt(terpy)Cl]Cl{\cdot}2H_2O$ in 95% yield (83–87% overall). Interestingly, no double salt formation is observed.

The syntheses of all other $[Pt(terpy)X]^+$ complexes proceeds by substitution of labile chloride from $[Pt(terpy)Cl]^+$ and are described in Section 3.1.

2.2. Crystal structures of $[Pt(terpy)X]^{n+}$ complexes

Commonly, the diffusion of ether into solutions of a Pt(II) terpy complex (MeOH, acetone, DMF, or chloroform solvent) results in crystallization. In other cases, crystals deposit from solutions by slow evaporation of CH_3CN, MeOH or acetone solvent.

The crystal structure of terpy, first reported in 1992, displays near planarity of the three rings but *trans*,*trans*-configuration of the terminal pyridyl rings with the central ring; a bite angle of 128° was estimated for the *cis*,*cis*-configuration of the free ligand [42].

The first crystal structure of a platinum terpy complex was reported by Lippard and co-workers for $[Pt(terpy)(HET)]NO_3$, where HET = hydroxyethanethiol [43], and the structure of the "parent" complex cation $[Pt(terpy)Cl]^+$ has been determined for the $CF_3SO_3^-$ salt [44], the ClO_4^- salt [45], as a double salt with the anion $[Pt(dmso)Cl_3]^-$ [27], as an adduct of AMP [46] and as an intercalation complex [47]. The structure of $[Pt(terpy)Cl]ClO_4$, shown in Fig. 2, displays features common to nearly all other $[Pt(terpy)X]^{n+}$

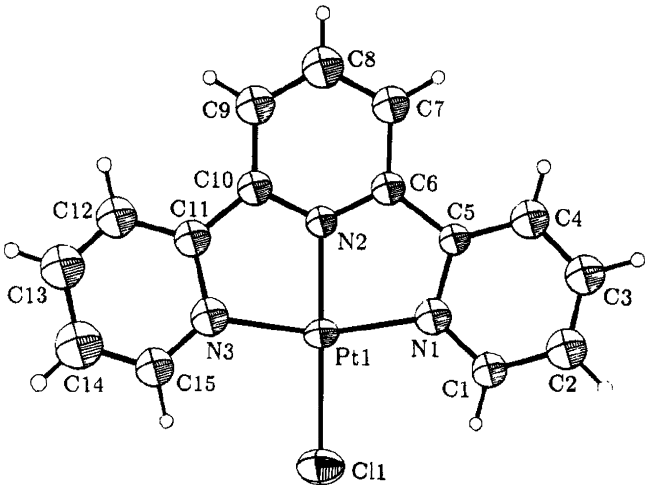

Fig. 2. ORTEP for [Pt(terpy)Cl]ClO_4; from Ref. [45] (reproduced by permission of The American Chemical Society).

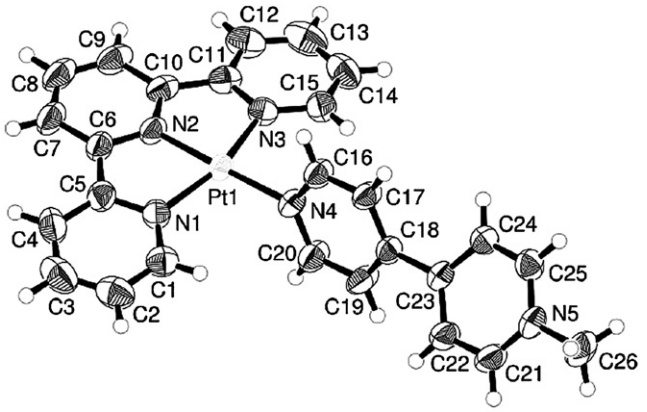

Fig. 3. The crystal structure of $[Pt(terpy)(MQ)]^{3+}$ displays an unusual bent terpy ligand; from Ref. [59] (reproduced by permission of The International Union of Crystallography).

systems that have been solved subsequently. The coordination geometry about the Pt center is essentially square planar. Coordination of the terpy ligand results in a restricted bite angle as indicated by: (1) a Pt–N^2 distance that is smaller than the Pt–N^1 and the Pt–N^3 distances, (2) a N^1–Pt–N^2 angle that is smaller than the theoretical value of 90° and a corresponding N^1–Pt–N^3 angle that is smaller than the theoretical value of 180° expected for a tridentate ligand in a square-planar geometry. Otherwise, the geometry of the terpy ligand changes little upon coordination, although there is some slight ring puckering. This ring strain was postulated by these authors to be a factor in the enhanced reactivity of $[Pt(terpy)X]^{n+}$ complexes toward X ligand substitution reactions, but the discussion in Section 3.2 highlights other factors. Structures for other salts of $[Pt(terpy)Cl]^+$ display very similar geometries for the cation, with the nature of the anion only influencing how the cations pack in the crystal (see Section 4.2.3).

Structures have been determined for numerous other $[Pt(terpy)X]^{n+}$ complexes having X ligands of: OMe [48], 3,4-dimethylphenoxide [49], pyridine-2-thiol [50], pyrimidine-2-thiol [50], cysteine [51], 1-methylcytosine [52], 2-mercapto-5-methyl-1,3,4-thiadiazolate [53], 2,5-dimercapto-1,3,4-thiadiazolate [53], *S*-benzo-15-crown-5 [54], thiourea [55], N_3 [56], N_4CPh [56], diphenyltriazene [57], CH_3CN [33], guanosine [51], 1-methyimidazole [58], *N*-methyl-4,4′-bipyridinium [59], CH_3 [60], CH_2NO_2 [49,61], 1,3-bis(piperidylmethyl)benzene [62], C≡CPh [63,64], C≡CC≡CH [65], and Ph_2P-benzo-15-crown-5 [66]. In some cases, the solid-state structure contains two crystallographically distinct cations having nearly identical structures.

Inspection of this body of crystallographic data for the complex cation structures reveals that the Pt–N^2 bond is shorter (average is 1.951 Å for 33 reported structures) than the Pt–N^1 and Pt–N^3 bonds (average is 2.028 Å) in all but two cations [67,68], but the Pt–N^2 bond length varies from 1.91 Å when X = canavanine [67] to 2.04 Å for an acetylide complex [68]. In general, this bond length appears to be slightly longer when the *trans* donor atom of the X ligand is C, P or S than when it is Cl, N or O, but no obvious correlation with the Pt–X bond length or other structural parameters emerges from these data. Also, the Pt–N^1 and Pt–N^3 bond lengths differ, on average, by less than 0.014 Å. Among nearly 40 reported structures, the N^1–Pt–N^3 bite angle ranges from 158.7° to 163.5° and averages 161.5°. The bite angle does not appear to be specifically influenced by the size or coordination geometry of the X ligand, being shortest for complexes having a bulky PR_3 ligand as well as a small CH_3 ligand and being longest both for a complex with an atomic (Cl^-) X ligand and a bulky 2,5-dimercapto-1,3,4-thiadiazolate ligand with out-of-plane coordination.

The complex salt $[Pt(terpy)(MQ)](ClO_4)_3$ (MQ = *N*-methyl-4,4′-bipyridinium) displays an unusual bent terpy ligand (Fig. 3). The dihedral angles between the central pyridyl ring and the two terminal pyridyl rings are 9.2° and 5.6° and between the two terminal rings it is 14.2° [59].

The coordination geometry of the various X ligands follow established patterns for other metal complexes, including bent geometries for the N_3 [56] and thiourea [55] ligands. The complex salt $[Pt(terpy)(cysteine)](ClO_4)_2{\cdot}0.5H_2O$ crystallizes with 2 independent cations and the cysteine ligand coordinates through the S-atom in both cases, but with different conformations [51]. A similar behavior was found for $[Pt(terpy)(guanosine)](ClO_4)_2{\cdot}0.5guanosine{\cdot}1.5H_2O$, for which the guanosine ligand coordinates through the N^7-atom in both cases but with different conformations [51].

The dihedral angle between the Pt(terpy) plane and the plane of X ligand can have an important influence on packing in the crystal and, in the case of aromatic X ligands, the electronic conjugation between ligands. Crystal structures for phenylacetylide complexes with X=C≡CPhC≡CH [69], C≡CPhNCS-4 [70], and C≡CPh [63,64] all display phenyl rings that are nearly co-planar with the Pt(terpy) plane (dihedral angles of 9.4°, 4.06° and 5.6°, respectively). Likewise, the tetrazole ligand in $[Pt(terpy)N_4CPh](BF_4)$ is nearly co-planar with the Pt(terpy) plane, suggested to be due to weak H-bonding interactions between the tetrazole ligand N^1 and N^3 atoms and the terpy ligand $H^{6,6'}$ atoms [56]. In contrast, other planar X ligands coordinate out of the Pt(terpy) plane, and include pyridine (64.12–69.4° dihedral angle) [34,71,72], 3,4-dimethylphenoxide (~72°) [49], *N*-methyl-4,4′-bipyridinium (81.7°) [59], 1-methylcytosine (84.4°) [52], and 2,5-dimercapto-1,3,4-thiadiazolate and 2-mercapto-5-methyl-1,3,4-thiadiazolate [53].

2.3. *[Pt(terpy)X_3] complexes*

The only reported example of Pt(IV) complexes having tridentate terpy is $[Pt(terpy)Cl_3]^+$, prepared from the addition of Cl_2 to solutions of $[Pt(terpy)Cl]^+$ [15,23]. A number of Pt(IV) complexes having bidentate terpy coordination are described in Section 2.5.1.

2.4. *Synthesis and structures of platinum complexes of terpy derivatives*

Numerous derivatives of 2,2′:6′,2″-terpyridine have been prepared in recent years, and reviews of synthetic approaches have

been presented by Heller and Schubert [73] and Thompson [74]. Substituents on the terpy ligand of Pt(II) complexes offer a means to systematically alter solubility, rates of X ligand substitution, intermolecular stacking interactions, photochemical and electrochemical properties, and binding affinities to biomolecules.

The vast majority of functionalized terpy ligands possess a single substituent at the 4′ position, or three substituents at the 4,4′ and 4″ positions. For simplicity, abbreviations for terpy derivates will assume these substitution patterns, unless otherwise noted. Therefore, 4′-chloro-2,2′:6′,2″-terpyridine will be referred to as Clterpy, and 4,4′,4″-tri-*tert*-butyl-2,2′:6′,2″-terpyridine will be referred to as $^{t}Bu_3$terpy.

Substituents on the terpy ligand can alter its reactivity in the formation of Pt(II) complexes. For example, whereas terpy reacts with $PtCl_2$ in a H_2O/CH_3CN/dmso solvent mixture, the corresponding ligands Clterpy and 4-BrPhterpy lead to low yield and no conversion, respectively [29]. A reduction in the basicity of the immine nitrogen atoms by the chloro and bromophenyl substituents could account for this difference in reactivity, as could decrease water solubility. Synthetic method C, using [Pt(COD)X_2] (X = Cl, I), appears to work well for Yterpy derivatives with Y = halogen [29,75–77], amine [78], alkoxy [29,78], and aryl derivatives [29,78–80]; using K_2PtCl_4 (method A) has also been demonstrated [44,81,82]. The complexes [Pt(Phterpy)X]Cl with X = Cl, Me and Ph have been prepared by method B using *cis*-[Pt(dmso)$_2$(X)Cl] [31], and [Pt(Yterpy)Cl]A complexes with Y = phenyl derivatives have been prepared by method B using *cis*-[Pt(NCPh)$_2$Cl$_2$] with AgA (A = SbF_6^-, $CF_3SO_3^-$, BF_4^-) in CH_3CN [83–85]. Notably, the synthesis of [Pt(Cl_3terpy)Cl]$^+$ could not be achieved using method A or C, and not with method B using [Pt(CNPh)$_2$Cl$_2$] starting material; only [Pt(dmso)$_2$Cl$_2$] was reactive towards the weaker base Cl_3terpy [75].

Numerous Pt(II) complexes of terpy derivatives have been characterized by X-ray crystallography. Comparisons of eight crystal structures for members of the family [Pt(Yterpy)Cl]$^+$ (Y = $^{t}Bu_3$ [81], Ph [83], *o*-CH_3Ph [84], *o*-CF_3Ph [84], *o*-ClPh [31], PhN=NPh [34], and Yterpy = 4,7-Me_2php [86], and btpyxa [87]) with those of [Pt(terpy)Cl]$^+$ reveal very similar structural parameters. Likewise, congruent structures have been reported for 11 Pt(II) $^{t}Bu_3$terpy complexes, ranging from monomers of the type [Pt($^{t}Bu_3$terpy)X]$^+$ (with X = Cl [81], $CH_2C(O)Ph$ [81], C≡CC≡CH [65], C≡CPhC≡CH [69] and C≡CPhNCS-4 [70]) together with a series of unstacked dinuclear complex cations including [{Pt($^{t}Bu_3$terpy)}C≡CC_6H_4N{Pt($^{t}Bu_3$terpy)}]$(PF_6)_3$ [71] and [Pt($^{t}Bu_3$terpy)(C≡C)$_n$Pt($^{t}Bu_3$terpy)]$(CF_3SO_3)_2$ (with n = 1, 2 and 4) [88], and two bimetallic complexes [Pt($^{t}Bu_3$terpy)(C≡C–C_6H_4–C≡C)Re(bpy)(CO)$_3$](CF_3SO_3) [89] and [Pt($^{t}Bu_3$terpy)(C≡C–C_6H_4–C≡C)Re(NO_2phen)(CO)$_3$](CF_3SO_3) [89].

The dihedral angle between the terpy plane and that of 4′-aryl substituents is an important parameter for understanding electronic conjugation between the Pt(terpy)$^{2+}$ unit and the aryl group. For [Pt(Phterpy)Cl]BF_4·CH_3CN, the interannular bond (C^8–C^{16}) between the Y = phenyl substituent and the terpy plane has a dihedral of 33.4°, whereas the dihedral angle in uncoordinated Phterpy is 10.9° [83]. This angle increases for substituted aryl groups, as shown for [Pt(*o*-ClPh-terpy)Cl]SbF_4 (54.5°) [85] and [Pt(*o*-CH_3Ph-terpy)Cl]SbF_4 (65.2°) [84]. Interestingly, the dihedral increases to 69.9° for the latter cation when the anion is changed to BF_4 but decreases to 62.1° when the *ortho*-CH_3 group is replaced with a larger CF_3 group [84]. The azobenzene substituent in [Pt(PhN=NPh–terpy)Cl]PF_6·DMA is co-planar with the terpy ligand while for [Pt(PhN=NPh–terpy)py]$(BPh_4)_2$ it is not, suggesting the configuration of substituents can be sensitive to factors influencing solid-state packing [34].

A chromophore triad reported by Schmehl and Eisenberg and co-workers involves a [Pt(Phterpy)C≡CPh]$^+$ core with a pendant methylpyridinium electron acceptor group on the Phterpy ligand and a trimethoxybenzamide electron donor group on the phenylacetylide ligand [28]. Other variations on the terpy structure are seen in a series of six Pt(II) complexes of "U-shaped" terpy derivatives (Fig. 4) prepared by Risch and co-workers, in which ethylene bridges connect the pyridine rings [80], and a "Me_2php" ligand having an ethyne bridge [86]. It is interesting to note that the crystal structures for these complexes display very similar coordination geometries to the terpy complexes, as well as to another picoline complex, [Pt{bis-hydroxyethyl(amino)-terpy}(4-picoline)]$(BF_4)_2$ [90]. The ligand 2-(8′-quinolinyl)-1,10-phenanthroline coordinates to form Pt(II) complexes having very similar bonding geometry as for terpy complexes but with slightly less ring strain [91].

Quaterpyridine (qtpy = 2,2′:6′,2″:6″,2‴-quaterpyridine) reacts with K_2PtCl_4 to afford [Pt(qtpy)]$^{2+}$, which provides an interesting comparison to the complex cation [Pt(terpy)(pyridine)]$^{2+}$.

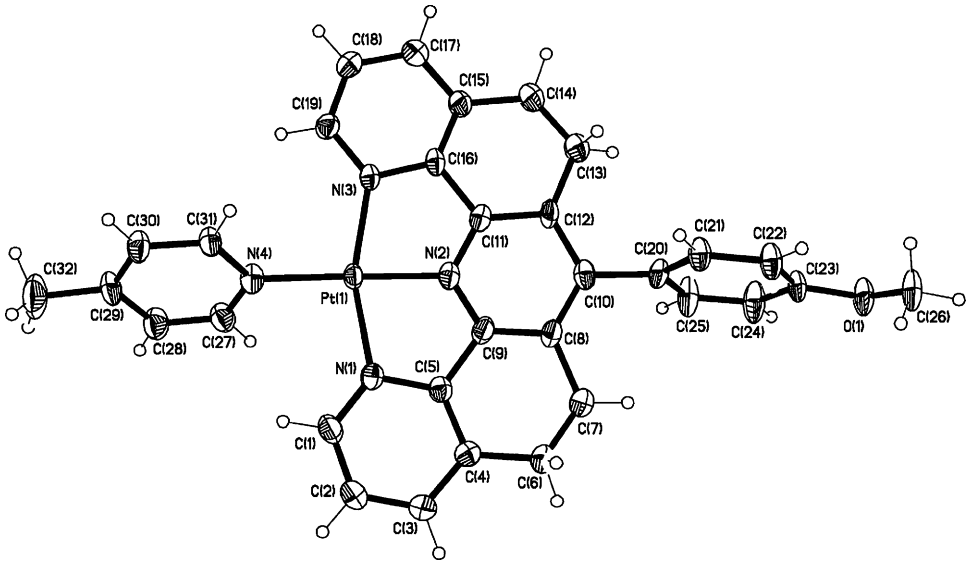

Fig. 4. Pt(II) complex with a U-shaped terpyridine derivative; from Ref. [80] (reproduced by permission of The Royal Society of Chemistry).

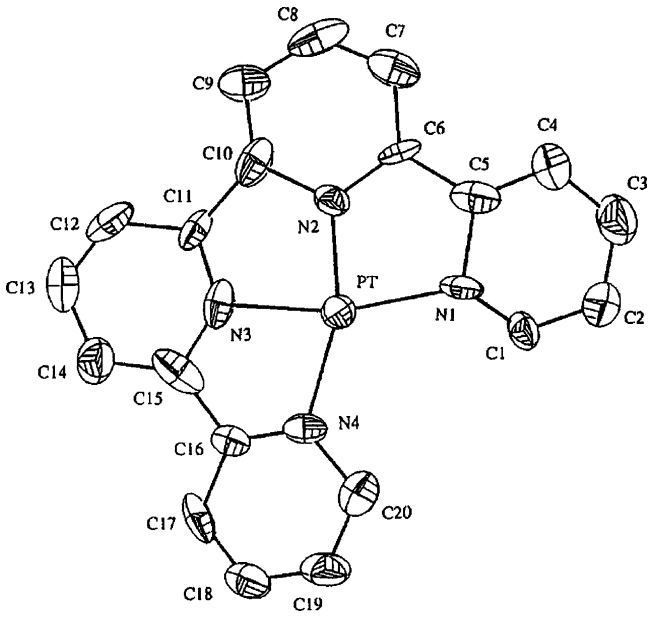

Fig. 5. Crystal structure of a Pt(II) quaterpyridine complex cation; from Ref. [95] (reproduced by permission of The American Chemical Society).

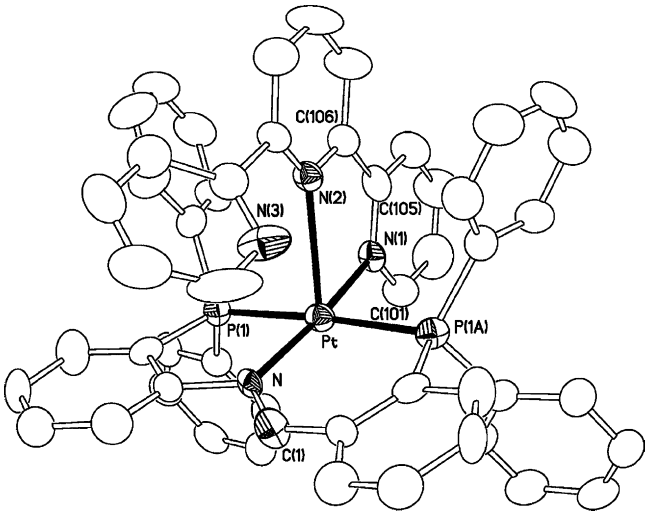

Fig. 6. Structure of $[Pt(terpy)(PNCHP)]^{2+}$ cation, having bidentate terpy coordination; from Ref. [98].

The synthesis was first reported by Burstall in 1938, and a study by Lip and Plowman in 1975 extended the investigations to salts having other anions [92,93]. Results are consistent with four-coordinate qtpy ligand. Constable et al. [94] further characterized this complex using IR and ^{1}H NMR spectroscopies. Substantially different structural parameters are found for the crystal structures of $[Pt(qtpy)](ClO_4)_2$ (Fig. 5) and $[Pt(Me_4qtpy)](ClO_4)_2$ (Me_4qtpy = 3″,5,5′,5‴-tetramethyl-2,2′:6′,2″:6″,2‴-quaterpyridine), for which the Pt–N [1,4] bonds are longer than Pt–N [2,3] bonds [95]. Constable notes that the reaction of qtpy with $[Pt(CH_3CN)_2Cl_2]$ leads to the formation of the double-salt product $[Pt(qtpy)][PtCl_4]$, and that using $[Pt(COD)Cl_2]$ as the starting material yields only protonated qtpy [94].

A Pt(II) complex of a chiral bis-pinene-terpy ligand was mentioned by von Zelewsky, but without any supporting information [96]. Finally, numerous other chelating polypyridines ligands resemble the structure of terpy, but are beyond the scope of this review. Of special relationship are a group of ligands in which one or two pyridyl rings are replaced by phenyl rings. Several Pt(II) complexes of 1,3-di(2-pyridyl)benzene or 4-phenyl-2,2′-bipyridine have been prepared in recent years, and they can serve as interesting organometallic analogs to Pt(II) terpy complexes.

2.5. Unusual binding modes to terpy

While terpy nearly always coordinates as a tridentate ligand to metal ions via its three N atoms, other binding modes have been discovered and designed for platinum complexes.

2.5.1. Bidentate coordination

Although bidentate coordination of terpy is not expected due to the well-established "chelate effect", some Pt(II) and Pt(IV) complexes do exhibit this coordination. Clark and Manzer described a Pt(IV) complex cation $[Pt(terpy)(Me)_2(PMe_2Ph)_2]^{2+}$ as being six-coordinate, with bidentate terpy coordination implied but not addressed specifically by the authors [97]. Stronger evidence is found in the X-ray crystallographic structure for the Pt(II) complex cation $[Pt(terpy)(PNCHP)]^{2+}$, where PNCHP = 2-(diphenylphosphino)-*N*-[2-(diphenylphosphino)benzylidene]benzeneamine (Fig. 6) [98]; in the five-coordinate square-pyramidal structure, the terpy ligand adopts an unusual bidentate coordination.

A series of papers by Orrell and co-workers explored the role of terpy as a fluxional, bidentate ligand in Pt(IV) complexes [99–101]. The reaction of $[(PtClMe_3)_4]$ with terpy in benzene affords *fac*-$[Pt(terpy)ClMe_3]$ in 71% yield [100]. When dissolved in $CDCl_3$, changes in the ^{1}H NMR spectrum with temperature indicated a fluxional process. Cooling to 253 K yielded a spectrum having 11 non-equivalent aromatic resonances, consistent with a static structure having bidentate terpy coordination [99]. Warming the sample solution results in line broadening of all but the signal for the central $H^{4'}$, followed by the emergence at 373 K of a spectrum having only six resonances, consistent with a fast fluxional process giving an averaged structure having tridentate terpy coordination. Fluxional behavior is also evident from the resonances for the two equatorial Me ligands (*trans* to the terpy N atoms), which show large exchange broadening upon warming to 333 K while that for the axial Me ligand (trans to Cl) does not. Therefore, a mechanism of total Me scrambling (as is known for $PtXMe_3$ systems) was ruled out. Instead a "tick-tock" mechanism was proposed, involving oscillation between two different bidentate structures (enantiomers) through a seven-coordinate transition state with elongated Pt–N bonds (Fig. 7). Related $[Pt(terpy)XMe_3]$ complexes with X = Br or I behave similarly [100]. An Eyring analysis of the fluxional terpy binding mode yielded activation parameters of $\Delta H^{\ddagger}$ = 58 kJ/mol, $\Delta S^{\ddagger}$ = −14 J/(K mol) and $\Delta G^{\ddagger}$ = 62 kJ/mol at 298 K for the chloro complex, with similar values for X = Br and I. In the low-T regime, the ^{1}H NMR spectrum indicates another fluxional process is occurring that involves rotation of the uncoordinated pyridyl ring, with a rotational barrier of $\Delta G^{\ddagger}$ = 50 kJ/mol at 298 K.

The complex $[Pt(terpy)IMe_3]$ is the only Pt(IV) terpy complex that has been structurally characterized by X-ray crystallography [100]. The crystal structure shows the pendant pyridine ring adopting an orientation of 52° out of the PtNN plane and with the N atom *cis* to the iodine ligand. Of interest with respect to the discussion of ring strain in tridentate terpy complexes of Pt(II) are the elongated Pt–N^1 and even longer Pt–N^2 distances but short N^1–Pt–N^2 angle in this structure.

The reaction of $[Pt(terpy)Cl]^+$ with PPh_3 in $CDCl_3/CD_3OD$ (1:4, v/v) results in rapid chloride substitution followed by a slower partial de-chelation of the terpy ligand to yield $[Pt(\eta^2\text{-terpy})(PPh_3)_2]^{2+}$, which was characterized by ^{31}P NMR spectroscopy [102].

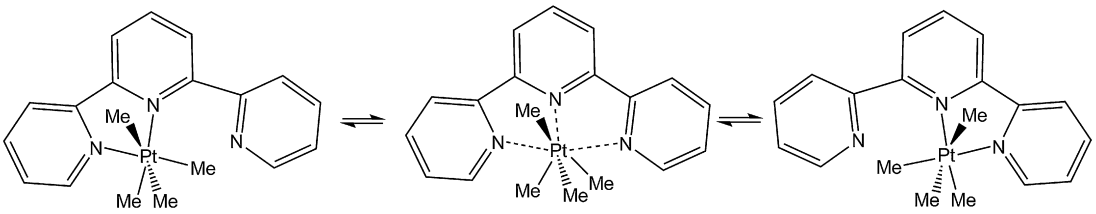

Fig. 7. A "tick-tock" mechanism for fluxional bidentate coordination of terpy.

Orrell and co-workers also have reported on bidentate terpy complexes of Pt(II). The reaction of *trans*-[Pt(C_6F_5)$_2$(1,4-dioxane)] with terpy in Et_2O–CH_2Cl_2 yields the complex *cis*-[Pt(terpy)(C_6F_5)$_2$], isolated in 33% yield [101]. The ^{1}H NMR spectrum for this complex displays 11 non-equivalent aromatic resonances consistent with static structure having bidentate terpy coordination. Broadening of the aromatic signals for solutions at $373 < T \leq 413$ K indicated a fluxional process, but a coalescence temperature could not be reached in the solvent used in their study. Their reported activation parameters $\Delta H^{\ddagger} = 93$ kJ/mol, $\Delta S^{\ddagger} = -3$ J/(K mol) and $\Delta G^{\ddagger} = 94$ kJ/mol at 298 K are moderately higher than those for the Pt(IV) systems. Bidentate terpy coordination is clearly identified in the crystal structure of the related Pd(II) complex *cis*-[Pd(terpy)(C_6F_5)$_2$] [101]. While concentration-dependent changes in ^{1}H NMR spectra are also common for [Pt(terpy)X]$^{n+}$ complexes, these effects can be separated from those due to fluxional coordination geometry [30].

While Orrell and co-workers assigned the fluxional terpy coordination mode to an *associative* "tick-tock" mechanism involving a 1,4-metallotropic shift proceeding through a five-coordinate (tridentate terpy) intermediate, Rotondo et al proposed a *dissociative* mechanism proceeding through a three-coordinate "T-shaped" intermediate having terpy coordinated only through the central pyridyl ring [103]. However, the dissociative mechanism is not supported due to: (1) the lack of significant effect on the rate constant with protonation of the pendant pyridyl ring, (2) a lack of a large positive $\Delta S^{\ddagger}$ expected for a monodentate terpy, and (3) the presumed weaker Pt–N^2 bond [104].

Follow-up studies using unsymmetrical 4-methyl-4′-(4-chlorophenyl)-terpy (mcpt) supported the associative mechanism for both [Pt(L)IMe_3] and *cis*-[Pt(L)(C_6F_5)$_2$], where L = terpy or mcpt, as evidenced by the effect of fluxional terpy coordination on the ^{1}H NMR resonances for the Me and C_6F_5 groups, respectively [105,106]. Both the Pt(IV) complex [Pt(mcpt)IMe_3] and the Pt(II) complex *cis*-[Pt(mcpt)(C_6F_5)$_2$] form as a set of two bidentate products in a 2:1 ratio (Fig. 8) [106]. The major and minor products interconvert via the "tick-tock" mechanism, with an activation barrier of $\Delta G^{\ddagger} = 66$ kJ/mol at 298 K for [Pt(mcpt)IMe_3] and $\Delta G^{\ddagger} = 101$ kJ/mol at 298 K for *cis*-[Pt(mcpt)(C_6F_5)$_2$]. Interestingly these values differ from those for the analogous terpy complexes (above) but in different ways for the Pt(II) and Pt(IV) complexes. The authors point out that the intermediates, having a near-planar five-coordinate geometry for the Pt(II) system and having a stereochemically rigid seven-coordinate geometry for the Pt(IV) system, are worthy of further theoretical consideration.

The work of Orrell and co-workers has been extended to larger systems. Three types of ligands (L^1, L^2 and L^3) having "back-to-back" terpy units (Fig. 9) were prepared along with their mono- and bi-metallic Pt(II) and Pt(IV) complexes [107]. The Pt(II) complexes [PtL($C_6F_4CF_3$)$_2$], [{Pt($C_6F_4CF_3$)$_2$}$_2$L] (where L = L^1 or L^2), [PtL^3(C_6F_5)$_2$], along with the Pt(IV) complexes [($PtClMe_3$)$_2L^1$], [($PtIMe_3$)$_2L^2$], and [($PtIMe_3$)$_2L^3$] all display bidentate and fluxional terpy coordination. A mixed-metal complex [$PtIMe_3L^1ReBr(CO)_3$] was also investigated [107]. As with the systems described above, the activation barrier $\Delta G^{\ddagger}$ strongly depends on the Pt oxidation state, but electronic interaction between metal centers in the bimetallic complexes is negligible. The dinuclear Pt(IV) quaterpyridine complex [($PtIMe_3$)$_2$qtpy] has been prepared and ^{1}H NMR data indicate a structure of bidentate coordination (Fig. 10) [108]. This result is in contrast with tridentate coordination found for Pt(II) qtpy complexes [92–95].

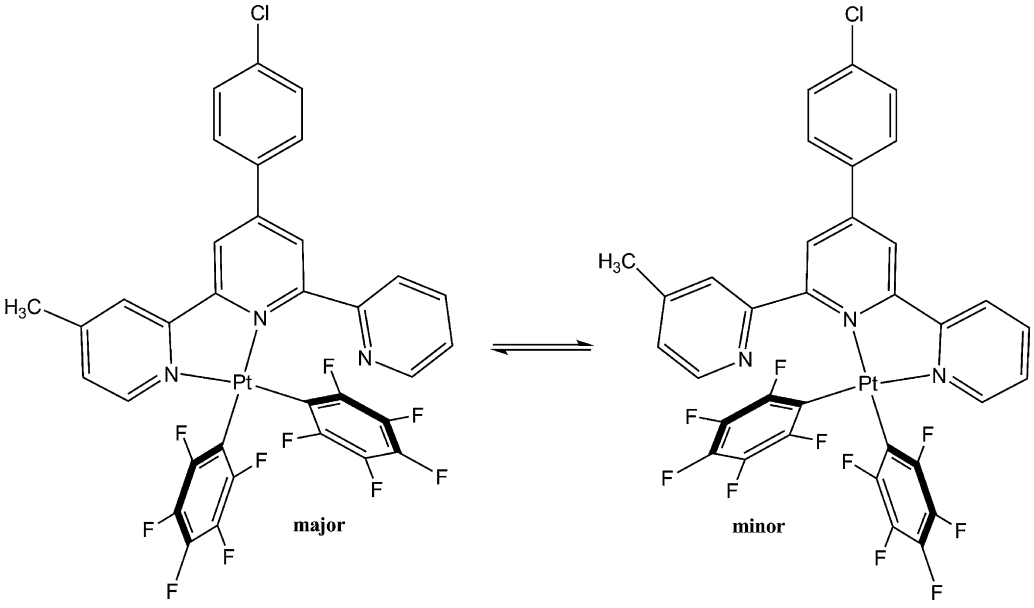

Fig. 8. Favored bidentate coordination for an unsymmetrical terpy.

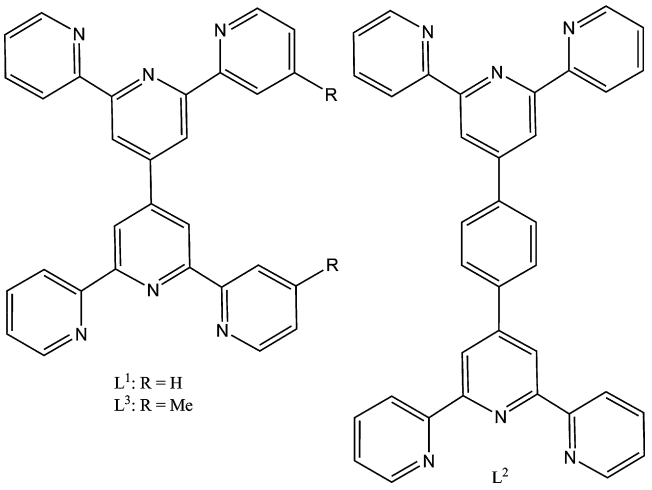

Fig. 9. "Back-to-back" terpy ligands coordinate as fluxional bidentate ligands in Pt(II) and Pt(IV) complexes.

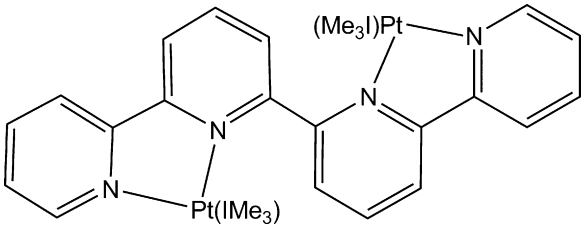

Fig. 10. Bidentate coordination in a quaterpyridine complex.

2.5.2. C–H activation

While coordination to Pt(II) and other metal ions nearly always occurs via the N atoms of terpy, novel cyclometallated products have been reported recently by Minghetti and co-workers (Fig. 11) [32]. The reaction of terpy with *cis*-[Pt(dmso)$_2$Me$_2$] results in C–H activation by Pt(II) and elimination of methane to form a dinuclear complex [(terpy){Pt(dmso)(CH$_3$)}$_2$] in near quantitative yield; no monometallated products or *N*-coordinated [Pt(terpy)Me]$^+$ were detected. In contrast, Arena et al. report that the use of *cis*-[Pt(dmso)$_2$(CH$_3$)Cl] as the starting material results in the formation of [Pt(terpy)(CH$_3$)]$^+$ in high yield [30]. Coordinated dmso in the dinuclear complex can be displaced easily by CH$_3$CN, CO, PPh$_3$ and PCy$_3$, and a crystal structure of [(terpy){Pt(CO)(CH$_3$)}$_2$] displays co-planar pyridine rings for terpy with some distortion of the bond angles in the central pyridine ring [32].

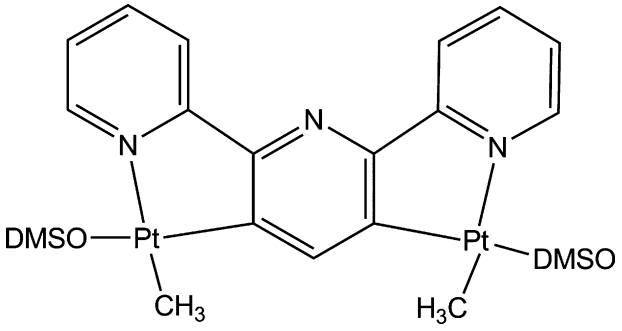

Fig. 11. C–H activation of terpyridine.

2.5.3. Ligands having pendant terpy groups

Terpy derivatives containing reactive substituents can be used to prepare Pt(II) complexes having pendant terpy units. For example, the reaction of 4′-ethynyl-terpy or 4′-butadiynyl-terpy with *cis*- or *trans*-[Pt(PBu$^n_3$)$_2$Cl$_2$] in the presence of CuI catalyst produces *cis*- or *trans*-[Pt(PBu$^n_3$)$_2${–(C≡C)$_n$–terpy}$_2$] (n = 1 or 2) in high yield (Fig. 12) [109]. Subsequent platination of the terpy units appears feasible, but has not yet been reported. Related dimers of the type *trans*-[{Pt(PEt$_3$)$_2$(Ph)}$_2$(C≡CRC≡C)] and oligomers of the type *trans*-[-Pt(PEt$_3$)$_2$(C≡CRC≡C)–]$_n$ (for which R = terpy or Ph-terpy) also have been prepared [110].

The ligand 4′-PPh$_2$-terpy reacts slowly with *trans*-[Pt(NCPh)$_2$Cl$_2$] to yield *cis*-[Pt(PPh$_2$-terpy)$_2$Cl$_2$], and crystal structures (Fig. 13) show the pendant terpy units adopting a *transoid* arrangement of pyridyl rings (as does free terpy) [111]. The pendant terpy ligands can be metallated, and the complex cations *cis*- and *trans*-[Pt{(PPh$_2$-terpy)Ru(terpy)}$_2$Cl$_2$]$^{4+}$ have been prepared [111]; platination of the terpy groups has not yet been reported.

3. Reactivity

Because platinum (II) complexes are generally thermodynamically stable and kinetically inert, ligand substitution reactions tend to be slow and easily monitored. The reactivity of [Pt(Yterpy)X]$^{n+}$ complexes is almost always determined by the ease of displacement of the X ligand by other donor ligands, and the chemistry and kinetics of these X ligand substitution reactions are reviewed first. In a small number of cases, other types of reactivity have been found, including: reactivity within a coordinated X ligand, displacement or reactivity of the terpy ligand, or oxidative addition at the Pt(II) center.

3.1. X ligand substitution reactions

Ligand substitution chemistry can be understood in terms of a combination of thermodynamic factors (relative stability of the bonding between the Pt center and X ligands in reactant and product) and kinetic factors (rate of X ligand displacement by another nucleophile). Many such reactions reach equilibrium, while others are shifted to completion using an excess concentration of entering ligand. Known coordinating X ligands have halogen, O, S, N, P, or C donor atoms, and trends in reactivity inform methods for preparing new types of [Pt(terpy)X]$^{n+}$ complexes and anticipating their reactivity in the presence of potential ligands. Additional examples of reactions of [Pt(terpy)Cl]Cl with biochemically relevant ligands containing heteroatom donors will be presented in a separate review.

3.1.1. Direct displacement of chloride

The chloro complex [Pt(terpy)Cl]Cl is a useful reagent for the synthesis of other [Pt(terpy)X]$^{n+}$ complexes because of its high solubility in water and labile chloride ligand. The addition of nucleophilic molecules or anions in stoichiometric or excess amounts can lead to direct substitution of the chloride ligand. Excess anionic ligand may also replace chloride as the counter ion; larger anions such as ClO$_4^-$, BF$_4^-$ or PF$_6^-$ are often employed for the precipitation of complex cation products.

The chloride ligand of [Pt(terpy)Cl]$^+$ can be displaced by other halide and pseudo-halides. The halide complexes [Pt(terpy)X]$^+$ with X = Br$^-$ and I$^-$ can be prepared from reaction of the chloro complex with 1 equiv. of LiX followed by heating and precipitation of the product using excess LiClO$_4$ [112]. These halide complexes can all be inter-converted by the addition of an excess of a second halide salt to a solution of [Pt(terpy)X]$^+$ with (X = Cl$^-$, Br$^-$ and I$^-$) [44,112–114]. Similarly, addition of excess salts of pseudo-halides

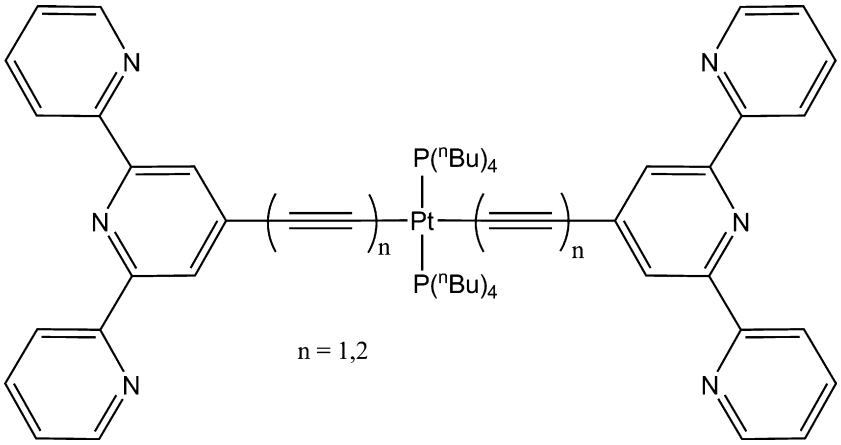

Fig. 12. Pt(II) acetylide complexes having pendant terpy groups.

CN^-, SCN^-, NO_2^-, N_3^- or $S_2O_3^{2-}$ displaces the chloride ligand [23,44,48,56,113,114]. The thiocyanate complex $[Pt(terpy)SCN]^+$ has been characterized as either coordinating through the S atom [23,114] or N atom [48].

Water, hydroxide and alkoxides are also capable of direct displacement of the chloride ligand in $[Pt(terpy)Cl]^+$. While [Pt(terpy)Cl]Cl is soluble in water, it slowly hydrolyzes to form the aqua complex $[Pt(terpy)(OH_2)]Cl_2$ [115,116]. The hydroxide complex cation $[Pt(terpy)(OH)]^+$ can be prepared by direct displacement of the chloride ligand using excess OH^-(aq) [48,117]. Changes in the UV–vis spectrum of $[Pt(terpy)Cl]^+$ upon adsorption on an acidic Nafion membrane (pH 0) suggested acid hydrolysis to form $[Pt(terpy)(OH_2)]^{2+}$ [118]. Reaction of $[Pt(terpy)Cl]^+$ with triflic acid [117] leads to the formation of an *O*-bound triflate complex $[Pt(terpy)(OSO_2CF_3)](OSO_2CF_3)$, which upon reaction with $HClO_4$(aq) yielded crystals of a hydrolysis product presumed to be either $[Pt(terpy)(OH_2)](ClO_4)_2$ or $[Pt(terpy)ClO_4](ClO_4)$ [119].

Numerous thiols are found to react directly with $[Pt(terpy)Cl]^+$ in water or MeOH. The synthesis of thiolato complex cations $[Pt(terpy)(SR)]^+$ by this method have been reported using 2-mercaptoethanol (or HET = hydroxyethanethiol) [22,120]; *n*-PrSH, *i*-PrSH, $HOOCCH_2SH$, $HOCH_2CH_2SH$, $HCl{\cdot}H_2NCH_2CH_2SH$, and PhSH [116]; cysteine, thioglycolic acid and D-penicillamine [121]; *N*,*N*-bis(aminoethyl)aminoethanethiol [122]; pyridine-2-thiol, pyrimidine-2-thiol and quinoline-2-thiol [50]; and 4′-mercaptomonobenzo-15-crown-5 and 3,4-dimethoxythiophenol [54]. Fazlur-Rahman and Verkade investigated the reaction of $[Pt(terpy)Cl]^+$ with seven different thiols by using ^{195}Pt NMR spectroscopy to monitor the rate of loss of the −2694 ppm resonance for the chloro complex and growth of the resonance at ∼−3150 ppm for the thiol complexes [123]. Displacement of chloride by a thiol is proposed to involve a five-coordinate transition state involving hydrogen bonding between the thiol proton and the chloride-leaving group, leading to release of HCl. Thus, thioethers are generally unreactive toward $[Pt(terpy)Cl]^+$ presumably due to the instability of the dication $[Pt(terpy)(SR_2)]^{2+}$ [116]. However, one paper does refer to the preparation of a thioether complex [Pt(terpy)(1,4-thioxane)] [121], and Mureinik and Bidani mention direct displacement of chloride by both thiourea and tetrahydrothiophen [23]. Likewise, solvolysis of $[Pt(terpy)Cl]^+$ by dmso is very slow at room temperature [78]. Similar substitution reactions using thiolate salts are also known. For example, the reaction

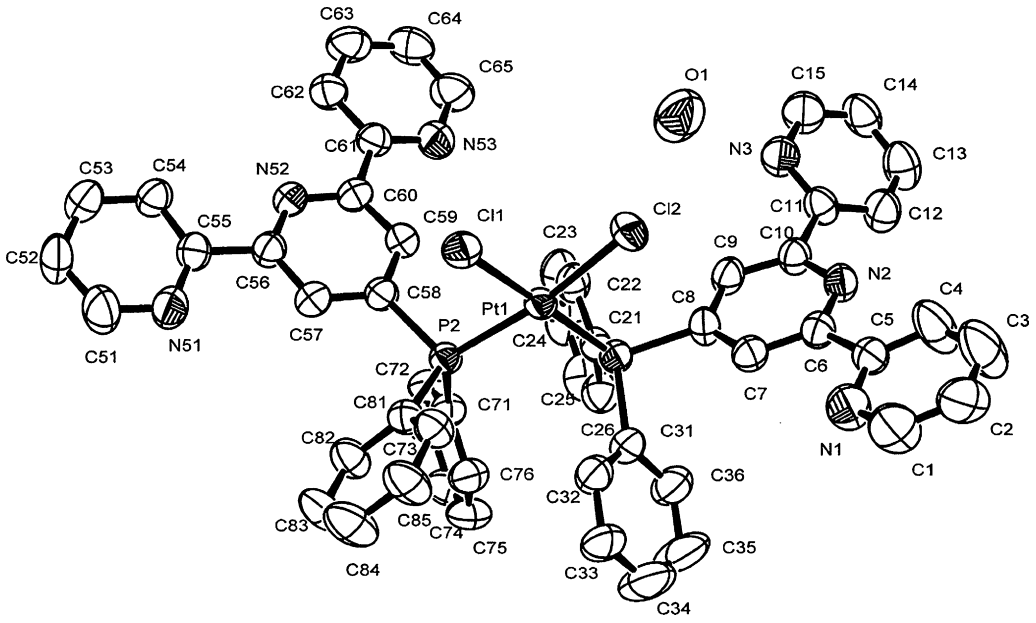

Fig. 13. Crystal structure of Pt(II) phosphine complexes having pendant terpy ligands; from Ref. [111].

of $[Pt(terpy)Cl]^+$ with NaSMe in MeOH to form $[Pt(terpy)(SMe)]^+$ is driven by precipitation of NaCl(s) [124]. Also, a suspension of [Pt(terpy)Cl]Cl in EtOH/water reacts with a mixture of thiophenols and base [125].

Morgan and Burstall prepared $[Pt(terpy)(NH_3)]Cl_2$ from the direct displacement of the chloride ligand in $[Pt(terpy)Cl]^+$ by ammonia [15]. Subsequent investigations [44,126] have confirmed this reactivity, while others have established direct chloride ligand displacement by pyridines [113,126,127], and aliphatic amines *n*-propylamine and α-picoline [23]. Displacement of chloride by 1-methylimidazole (MeIm) yields $[Pt(terpy)(MeIm)]^{2+}$ [58], while the reaction with 1,3-diphenyltriazene (dpt) in the presence of NEt_3 leads to the formation of $[Pt(terpy)(dpt)]^{2+}$ [57].

Mureinik and Bidani first reported the direct displacement of chloride ligand of $[Pt(terpy)Cl]^+$ by PPh_3 [23], but a more recent study indicates that the reaction in $CDCl_3/CD_3OD$ (1:4 v/v) results in rapid chloride substitution followed by a slower de-chelation of the terpy ligand to yield $[Pt(\eta^2\text{-terpy})(PPh_3)_2]^{2+}$ and eventually $[Pt(PPh_3)_3Cl]^+$ and free terpy [102].

Finally, the chloride ligand of $[Pt(terpy)Cl]^+$ can be displaced by ketones and acetylides. Che and co-workers reported that the reaction of $[Pt(^tBu_3terpy)Cl]^+$ with excess NaOH(aq), which would presumably form the hydroxo complex cation $[Pt(^tBu_3terpy)(OH)]^+$, instead yields the ketonyl products $[Pt(^tBu_3terpy)\{CH_2C(O)R\}]^+$ (R = Me, Ph) when either acetone or acetophenone is added and the solution stirred for 12 h [81]. The reaction of $[Pt(Yterpy)Cl]^+$ with acetylenes HC≡CR in DMF/triethylamine in the presence of CuI catalyst or in MeOH with KOH and CuI catalyst yields acetylide complex cations $[Pt(Yterpy)C{\equiv}CR]^+$ [28,89,128,129].

3.1.2. Removing chloride ligand using Ag(I) reagents

A second approach for the preparation of $[Pt(terpy)X]^{n+}$ complex cations involves the use of Ag(I) salts to abstract the chloride ligand from $[Pt(terpy)Cl]^+$, forming AgCl(s) precipitate and the aqua (or other solvent) complex $[Pt(terpy)(OH_2)]^{2+}$. This method has been described for the preparation of numerous thiolate complexes of the general type [Pt(terpy)(SR)]A (A = NO_3^-, PF_6^-, or $CF_3SO_3^-$) using 2 equiv. of $AgNO_3$ in water [43], 10-fold excess of $AgPF_6$ in water [123], or 2 equiv. of $AgCF_3SO_3$ in DMF [130,131], respectively. Similarly, the reaction of [Pt(terpy)Cl]Cl with Ag_2O (molar ratio unreported) affords the hydroxo complex [Pt(terpy)(OH)]OH [15]. Continuous extraction of solid $[Pt(terpy)Cl]SbF_6$ into refluxing CH_3CN having an excess of $AgSbF_6$ has been reported as a means of preparing $[Pt(terpy)(CH_3CN)](SbF_6)_2$, with subsequent addition of a nucleophilic ligand X resulting in rapid formation of $[Pt(terpy)X]^{n+}$ complexes in high yield [33]. In contrast, thioethers, disulfides and sterically bulky thiols are unreactive under these conditions [123].

A large number of pyridyl complex cations of the type $[Pt(terpy)(py)]^{2+}$ (py = pyridine, substituted pyridines, ammonia) have also been prepared from $[Pt(terpy)Cl]ClO_4$ using 1 equiv. of $AgBF_4$ in DMF [126,132] and from [Pt(terpy)Cl]Cl using 2 equiv. of $AgClO_4$ in water [59] or excess $AgBF_4$ in MeOH [127]. However, Pitteri et al. have reported that this general procedure does not work for nucleophiles such as aniline, morpholine, methylamine or piperidine, which act as bases to deprotonate the $[Pt(terpy)(OH_2)]^+$ intermediate to give $[Pt(terpy)(OH)]^+$ [126]. Lowe et al. corroborated this observation, also noting that it is not possible to form complexes with X = secondary or tertiary amines, presumably due to steric hindrance between the R groups of the tetrahedral N atom of the amine ligand and the 6 and 6″ H atoms of the terpy ligand [133].

The reaction of [Pt(terpy)Cl]Cl with 1 equiv. of $AgCF_3SO_3$ is reported to produce [Pt(terpy)Cl] [O_3SCF_3], indicating the selectivity of precipitating the chloride counter ion before removing the coordinated chloride ligand [44]. However, van Eldik and co-workers reported that the reaction of [Pt(terpy)Cl]Cl with "an equivalent" of $AgClO_4$ (but which appears to be 1.7 equiv. according to the amounts listed) in 95% MeOH results in formation of the aqua complex, which was not isolated but rather underwent rapid reaction with added thiourea, cysteine or guanosine [51,55]. Mureinik and Bidani asserted that they could not completely remove chloride using $AgNO_3$ [23]. However, Lippard and co-workers characterized the product of the reaction between [Pt(terpy)Cl]Cl and 2 equiv. of $AgNO_3$ as "platinum terpyridine nitrate" and tentatively assign the formula $[Pt(terpy)(OH_2)]NO_3$ [43]. Conversion of [Pt(terpy)Cl]Cl to the corresponding nitrate salt results in a product that is identified as $[Pt(terpy)Cl]NO_3$, but the formula $[Pt(terpy)NO_3]Cl$ may also apply and the presence of small amounts of the related aqua or hydroxo complexes (with either anion) are difficult to rule out [40]. Clarifying this ambiguity is the recently reported crystal structure of $[Pt(terpy)(ONO_2)]$ $[H(ONO_2)_2]$, prepared from the reaction of [Pt(terpy)Cl]Cl with 2 equiv. of $AgNO_3$ followed by precipitation from a solution of $HNO_3/NaNO_3$ [129].

3.1.3. Displacing hydroxide and alkoxide ligands

The equilibrium between $[Pt(terpy)(OH)]^+$ and $[Pt(terpy)(OH_2)]^{2+}$ plays an important role in the substitution chemistry because the hydroxo complex is thought to be relatively inert towards substitution compared to the aqua species [134]. For example, the measurement of solution pH for $[Pt(terpy)(OH_2)]^{2+}$(aq) resulted in formation of $[Pt(terpy)Cl]^+$(aq) from the NaCl electrolyte in the electrode [134]. The pK_a value of ~4.5 for $[Pt(terpy)(OH_2)]^{2+}$(aq) [135] indicates that the hydroxo complex $[Pt(terpy)(OH)]^+$ is expected to be the dominant species when solution pH is much above 3. With this in mind, the reaction of $[Pt(terpy)(OH)]^+$ with HCl(aq), HBr(aq) or HI(aq) is reported to yield $[Pt(terpy)X]^+$ (X = Cl, Br, I) [15,23]. In MeOH, $[Pt(terpy)(OH)]^+$ is converted to the methoxide complex $[Pt(terpy)(OMe)]^+$, which can revert to the hydroxide complex in acetonitrile (presumably from trace water) [48]. Phenolate complexes can be prepared from the slow reaction of $[Pt(terpy)(OH)]^+$ with phenols in CH_2Cl_2, but the authors note that similar reactions using $[Pt(terpy)Cl]^+$ did not yield clean products [49]. McMillin and co-workers observed that $[Pt(terpy)(OH)]^+$ is stable for days in EPPS buffer but unstable in organic solvents such as dmso and CH_3CN over the course of hours; no products of this reaction were identified [136].

Thiols can also displace the hydroxide ligand [53,124], as in the reaction of $[Pt(terpy)(OH)]^+$ with excess PhSH in MeOH to yield $[Pt(terpy)(SPh)]^+$ [116]. The effect of pH on this substitution chemistry is highlighted by a study by Annibale et al. who observed that the reaction of $[Pt(terpy)(OH)]^+$ with *S*-methyl-3-acyl-2-methyldithiocarbazate derivatives results in the formation of the complex cation $[Pt(terpy)(SMe)]^+$ whereas using $[Pt(terpy)(OH_2)]^{2+}$ yields a SMe-bridged dinuclear complex $[\{(terpy)Pt\}_2SMe]^{3+}$ [124]. More on this chemistry is presented in Section 4.1.1. Finally, nitromethane was reported to displace hydroxide or phenoxide ligand of $[Pt(terpy)(OR)]^+$ during a recrystallization procedure to yield $[Pt(terpy)(CH_2NO_2)]^+$ suggesting that perhaps other weak acids could also displace alkoxide ligands [49,61].

3.1.4. Displacing nitrogen ligands

Pyridine (py) ligands in complex cations of the type $[Pt(terpy)(py)]^{2+}$ can be displaced by other nucleophilic ligands. Reports indicate that chloride displaces picoline in $[Pt(terpy)(4\text{-picoline})]^{2+}$ when $[Cl^-] > 150$ mM in water [127], and that chloride (but not water) slowly displaces pyridines in $[Pt(terpy)(Rpy)]^{2+}$ (R = H, 2-CH_3, 4-CH_3) [137,138]. Nucleobases can also substitute for picoline [139], and cyanide displace pyridines [140]. Most facile appear to be the displacement of pyridine ligands

by thiols [140], such as in the rapid displacement of the 4-picoline ligand in $[Pt(terpy)(4\text{-picoline})]^{2+}$ by 2-mercaptoethanol or dithiothreitol [127]. The pyridine ligand in the complex cation $[Pt(Clterpy)(pyridine\text{-}4\text{-}thione)]^{2+}$ is completely displaced upon addition of 1 equiv. of glutathione, but the reverse reaction (displacement of glutathione ligand by pyridine-4-thione) does not occur even with excess of the pyridine [36]. Sulfur nucleophiles L-cysteine, glutathione, thiourea, thiosulfate, and diethyldithiocarbamate can displace N^7-bound guanosine ligand in $[Pt(terpy)(guanosine)]^{2+}$ at pH 6 [51].

Amine complexes $[Pt(terpy)(NH_2R)]^{2+}$ (R = H, *n*Pr) are reported to come into equilibrium with the aqua complex in water [133], but are stable with respect to solvolysis in dmso [78].

The labile acetonitrile ligand makes $[Pt(terpy)(CH_3CN)]^{2+}$ a versatile precursor for the formation of acetylide complex cations of the type $[Pt(terpy)(C{\equiv}CR)]PF_6$ [63,68–70], diynyl complexes $[Pt(terpy)(C{\equiv}CC{\equiv}CH)]^+$ [65], thiolate [141,142], phosphine [66], and pyridine complexes [66,71,72].

3.1.5. Displacing thiolate ligands

In the $[Pt(terpy)X]^{n+}$ family, complexes having X = thiolate appear to be the most substitutionally inert, but some examples of displacement reactions have been found. Basolo et al. observed that the thiocyanate ligand of $[Pt(terpy)(SCN)]^+$ can be displaced by pyridine in water [113]. For the complex cation in $[Pt(terpy)(SPh)]^+$, the displacement of the phenylthiolate ligand by excess chloride is very slow even at low pH, while non-coordinating acids such as $HClO_4$ and $MeSO_3H$ quickly react to release PhSH [116].

Thiolate substitution reactions for complexes of the type $[Pt(Clterpy)(SR)]^+$ (where SR are aliphatic thiolates $^-SCH_2CH_2OH$, $^-SCH_2CH_2CH_2OH$, or glutathione) were investigated by Lowe and co-workers [36]. Reactions of each of these three complex cations with either of the other two free thiols results in a rapid reaction to produce a 1:1 equilibrium mixture when up to 1 equiv. of thiol is added. With excess thiol, decomposition and the release of free Clterpy is observed. The results of this study indicate that thiolate exchange reactions may occur for *S*-bound Pt(II) terpy complexes of proteins *in vivo*. The strong nucleophiles diethyldithiocarbamate, thiosulfate and thiourea are capable of slowly ($k = 1\text{–}9\ M^{-1}\ s^{-1}$) displacing cysteine from $[Pt(terpy)(cysteine\text{-}S)]^{2+}$ (at pH 6) [51].

Cheng and Lu reported that the cleavage of Pt–S bonds in $[Pt(terpy)SR]^+$ complexes, with SR = 2-aminoethanethiol (AET) and *N*,*N*-bis(aminoethyl)aminoethanethiol (BAT), is facilitated by Zn^{2+}, Cu^{2+} and Ni^{2+} [122]. The reaction of the BAT complex with 1 equiv. of $ZnCl_2$ is complete in 10 min to yield $[Pt(terpy)Cl]^+$, but slower rates were observed using Cu^{2+} and Ni^{2+}. Slower rates for the AET complex and pH-dependence of the rates for the BAT complex suggested a mechanism involving metal ion coordination to the amino group of the thiolate ligand.

3.1.6. Displacing alkyl or aryl ligands

The only example of displacement of a carbon donor X ligand comes from Romeo et al., who noted that $[Pt(terpy)Me]^+$ is stable toward hydrolysis for weeks at room temperature, but addition of HCl(aq) results in the clean formation of $[Pt(terpy)Cl]^+$ with $k = 0.10\ M^{-1}\ s^{-1}$ [60].

3.2. Kinetics of X ligand substitution

Among these numerous examples of X ligand substitution reactions, a select group of studies have addressed the kinetics and mechanism for the displacement of ligand X by an incoming nucleophilic ligand Z, with most studies focusing on examples of X = chloride or water:

$$[Pt(Yterpy)X]^{n+} + Z \rightleftharpoons [Pt(Yterpy)Z]^{n+} + X \quad (5)$$

Kinetic investigations have established that the rates of X ligand substitution reaction are influenced by: (1) the nucleophilicity and steric bulk of the entering ligand Z, (2) the nucleophilicity and steric bulk of the leaving group X, and (3) on a combination of steric effects and electronic effects of terpy ligand that can be modulated by the Y substituent.

3.2.1. Kinetics of halide ligand substitution

The first kinetic study of ligand substitution reactions of Pt(II) terpy complexes came from Basolo et al. [113]. By measuring changes in electrical conductivity of aqueous reaction solutions, they determined pseudo-first order rate constants, k_{obs}, for the reaction of $[Pt(terpy)Cl]^+(aq)$ with excess pyridine. The group also reported that chloride substitution by pyridine occurs 10^3 to 10^4 times faster for $[Pt(terpy)Cl]^+$ than for the related complex cation $[Pt(dien)Cl]^+$ having a saturated diethylenetriamine (dien) ligand, and that substitution for the analogous $[Pd(terpy)Cl]^+$ complex cation is much faster than for the Pt(II) systems. This work represents one of the major contributions to understand the ligand substitution kinetics of coordination compounds and presented the two-term rate law now frequently encountered for square-planar d^8 complexes:

$$\text{rate} = k_{obs}[Pt] \quad \text{with } k_{obs} = k_1 + k_2[Z] \quad (6)$$

Under conditions of excess concentration of entering ligand Z, substitution of X follows a kinetic rate law that is first-order in $[Pt(terpy)X]^+$ ("[Pt]") but with a overall rate constant k_{obs} that depends on [Z], so that plots of k_{obs} vs. [Z] are used to obtain k_1 (intercept) and k_2 (slope). A mechanism of two parallel substitution pathways (Scheme 1) is consistent with this observed rate law. A solvolysis path, in which solvent (S) displaces the leaving group X but does not involve the entering ligand Z, gives rise to the unimolecular rate constant k_1, which are often small and less certain. An associative path involving direct displacement of X by the entering ligand Z gives rise to the bimolecular rate constant k_2 and typically dominates the kinetics (except at very small [Z], for which k_{obs} approaches k_1). The overall rate constant derived from this mechanism is $k_{obs} = k_1k_3[Z]/(k_{-1}[X] + k_3[Z]) + k_2[Z]$, which reduces to $k_{obs} = k_1 + k_2[Z]$ when $k_{-1}[X] \ll k_3[Z]$ (e.g. low [X]).

Using UV–vis spectroscopy, Mureinik and Bidani followed changes in absorption for solutions containing $[Pt(terpy)Cl]^+(aq)$ and excess halide or pseudo-halide anion Z (Z = Br^-, SCN^-, NO_2^- or N_3^-) to obtain the pseudo-first order rate constants, k_{obs}, for the complete displacement of chloride by these nucleophilic ligands [114]. In the absence of excess chloride, the reactions follow the standard two-term rate law (above), but the authors highlight some "unusual substitution behavior" of the $[Pt(terpy)Cl]^+$ cation. First, k_1 was found to depend on the nature of Z, in contrast to the prediction of the mechanism in Scheme 1. Addition of excess chloride

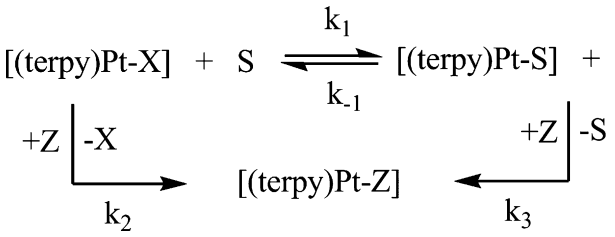

Scheme 1. A mechanism for ligand substitution reactions of Pt(II) terpy complexes showing an associative path involving direct displacement of X by incoming ligand Z, and a solvolysis path involving solvent coordination prior to ligand substitution.

Table 1
Relative substitution lability for $[Pt(terpy)X]^+ + Z^- \rightarrow [Pt(terpy)Z]^+ + X^-$; from Ref. [112]

X	Z = Cl	Z = Br	Z = I
Cl	1	1	1
Br	7.8	3.4	1.4
I	106	22	3.7

(leaving group) decreases the value of k_1 according to the equation $k_1 = (a[Cl^-] + b)^{-1}$, where a and b are empirical fitting parameters, while k_2 is unaffected. A suggestion of pre-association of Z in the solvent path was postulated to explain this chloride dependence. A second unusual result was that the values for k_2 follow a different relative ordering for the Z anions than had been found for other Pt(II) systems, highlighting the importance of the terpy ligand or complex charge in modulating X ligand substitution rates.

Investigations by Pitteri et al. using UV–vis spectroscopy showed that halide exchange for $[Pt(terpy)X]^+$ with (X,Z = Cl^-, Br^- and I^-) in MeOH also follows the standard two-term rate law [112]. Relative rates depend on the nature of the entering group Z, increasing in the order $Z = Cl^- < Br^- < I^-$ (Table 1). Using second order rate constants and nucleophilicity index values for Pt with each of the halides, the researchers calculated the discrimination parameters (s), which indicate the ability of $[Pt(terpy)X]^+$ to discriminate kinetically among each of the halide entering group. Their data indicate that s increases along the series $X = Cl^- < Br^- < I^-$, suggesting an increasing effect of the halide leaving group in determining the transition state energy and a substitution mechanism that has some associative character. Using second order rate constants for forward and reverse halide exchange $[Pt(terpy)X]^+ + Z^- \rightleftharpoons [Pt(terpy)Z]^+ + X^-$, they calculated equilibrium constants and Gibbs energies of reaction. The effect of the halide on the ground state energies, while correlating well with the polarizabilities of the halide atoms, are smaller for the $[Pt(terpy)X]^+$ system than for other Pt(II) complexes—an effect attributed to the importance of the *ortho* H atoms of the terpy ligand in destabilizing the larger halide ligands. Ground state and transition state Gibbs energies (relative to $G = 0$ for $[Pt(terpy)Cl]^+$) are summarized in Fig. 14. Noteworthy is that the energy difference between $[Pt(terpy)Cl]^+$ and $[Pt(terpy)I]^+$ four-coordinate ground states is much smaller than the energy difference between [Pt(terpy)Cl,Cl] and [Pt(terpy)I,I] transition states, highlighting the importance of the halides in controlling $\Delta G^{\ddagger}$ and the reactions rates for substitution.

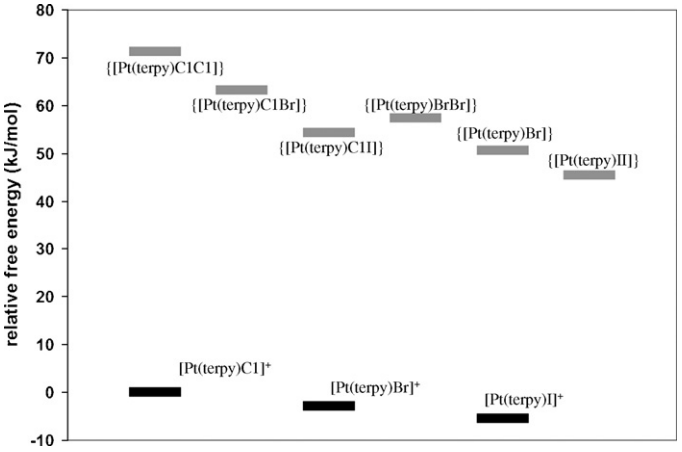

Fig. 14. Free energy levels for ground states of $[Pt(terpy)X]^+$ and transition states {[Pt(terpy)X,Z]} (X,Z = Cl, Br, I), relative to that for $[Pt(terpy)Cl]^+$; data from Ref. [112] (reproduced by permission of The Royal Society of Chemistry).

A subsequent study by Pitteri et al. explored the kinetics of chloride substitution in $[Pt(terpy)Cl]^+$ by excess pyridines (Z = pyridine; 3-methylpyridine; 4-methylpyridine; 4-cyanopyridine; 4-aminopyridine; 4-acetylpyridine; methylisonicotinate; 2-methylpyridine; 2,4-dimethylpyridine and ammonia) in MeOH, and their work revealed additional factors controlling ligand substitution rates [126]. The second-order rate constant k_2 increases with the basicity of the pyridine, following the linear free energy relationship for all of the pyridines lacking substituents at the 2 and 4 positions:

$$\log k_2 = \alpha pK_a + \text{constant} \quad (7)$$

Steric hindrance in these positions slows the reaction, as expected. This reaction between a monocationic complex and a neutral Z entering group is not influenced by ionic strength (μ). Pseudo-first order rate constant for chloride substitution by imidazole and histidine have also been reported [143].

Several studies have explored the kinetics of displacement of chloride in $[Pt(terpy)Cl]^+$ by thiols. Brothers and Kostic reported pseudo-first order rate constant for chloride substitution by excess $^-SCH_2CH_2OH$, cysteine and two cysteine-containing tripeptides [143]. Using ^1H NMR spectroscopy, Bugarcic et al. measured bimolecular rate constants for the reaction of $[Pt(terpy)Cl]^+$ with equimolar amounts of the thiols L-cysteine, thioglycolic acid and D-penicillamine (Table 2); the thioether L-methionine was found to be unreactive, even when in excess concentration [115,121]. In a series of related studies, the researchers used UV–vis spectroscopy to monitor the reactions in MeOH solutions of excess thiol (*n*-PrSH, *i*-PrSH, $HOOCCH_2SH$, $HOCH_2CH_2SH$, $HCl{\cdot}H_2NCH_2CH_2SH$, or PhSH [116]; L-cysteine, thioglycolic acid or D-penicillamine [115]; and thiourea [144], 1,3-dimethyl-2-thiourea, 1,1,3,3-tetramethyl-2-thiourea [145]). In each case, kinetics are a pseudo-first order with the standard two-term rate law (Eq. (6)) dominated by the k_2 terms. Not discussed was why the rate constants obtained by the two methods differ significantly for some of the thiols (Table 2). Substitution rates are slowed by steric bulk of the entering thiol (slowest for D-penicillamine), and enhanced by an anchimeric effect by which certain thiols (such as glutathione) stabilize the transition state via hydrogen bonding to the chloride-leaving group. While chloride substitution by halides and pseudo-halides occurs 10^3 to 10^4 times faster with $[Pt(terpy)Cl]^+$ than with $[Pt(dien)Cl]^+$, thiol displacement rates are enhanced only 10-fold, suggesting that thiols may have lower nucleophilicity or larger steric hindrance with the terpy systems. Activation parameters of $\Delta H^{\ddagger} = 34 \pm 4\ kJ\ mol^{-1}$ and $\Delta S^{\ddagger} = -144\ J\ K^{-1}\ mol^{-1}$, calculated from the temperature-dependence of the k_2 value for reaction with 1-propanethiol [116], are consistent with an associative substitution mechanism; similar results were found for other thiols [115]. The reverse reaction was also investigated, but excess chloride was not capable of displacing thiolate ligands. However, PhSH could be released by reacting $[Pt(terpy)(SPh)]^+$ with $HClO_4$ or $MeSO_3H$.

3.2.2. Kinetics of aqua ligand substitution

Related studies on the substitution of the aqua ligand in $[Pt(terpy)(OH_2)]^{2+}$ by thiols and thiourea, I^- and SCN^-, and nucleobases have been conducted to obtain rates constants (Table 3) and activation parameters [51,55,134,146]. In general, substitution of the aqua ligand is 10^3 to 10^4 times faster than displacement of chloride ligand. But in both cases rates are enhanced for entering ligands that are stronger σ-donors and less sterically hindered. Negative volumes of activation ($\Delta V^{\ddagger} \approx -10\ cm^3/mol$) and entropies of activation ($\Delta S^{\ddagger} \approx -75\ J\ K^{-1}\ mol^{-1}$) are consistent with an associative mechanism.

In contrast, kinetic studies by van Eldik and co-workers using stopped flow UV–vis methods to investigate aqua lig-

Table 2
Rate constants for chloride ligand substitution in $[Pt(terpy)Cl]^+$ by nucleophilic ligands Z at 298 K

Z	Solvent	k_2 (M^{-1} s^{-1})	Ref.
$[Pt(terpy)Cl]^+ + Z^- \rightarrow [Pt(terpy)Z]^+ + Cl^-$			
Br^-	4.5×10^{-3} M $NaNO_3$(aq)	10.2	[114,112]
	0.1 M $MeSO_3Na$ in MeOH	8.10 (±0.50)	[148]
	0.1 M $LiSO_3CF_3$ in MeOH	6.5 (±0.1)	
I^-	0.1 M $MeSO_3Na$ in MeOH	303.00 (±11.00)	[112,148]
	0.1 M $LiSO_3CF_3$ in MeOH	267 (±1)	
SCN^-	4.5×10^{-3} M $NaClO_4$(aq)	2.69 (±0.16)	[114]
NO_2^-	4.5×10^{-3} M $NaClO_4$(aq)	2.66 (±0.12)	[114]
N_3^-	4.5×10^{-3} M $NaNO_3$(aq)	18.73 (±0.70)	[114]
OH^-	Water, pH > 10	0.7	[117]
$[Pt(terpy)Cl]^+ + Z^- \rightarrow [Pt(terpy)Z]^{2+} + Cl^-$			
Pyridines			
4-Cyanopyridine	0.1 M $MeSO_3Na$ in MeOH	0.069 (±0.002)	[126]
Methylisonicotinate	0.1 M $MeSO_3Na$ in MeOH	0.200 (±0.020)	[126]
4-Acetylpyridine	0.1 M $MeSO_3Na$ in MeOH	0.202 (±0.007)	[126]
Pyridine	0.1 M $MeSO_3Na$ in MeOH	0.432 (±0.008)	[126]
3-Methylpyridine	0.1 M $MeSO_3Na$ in MeOH	0.597 (±0.006)	[126]
4-Methylpyridine	0.1 M $MeSO_3Na$ in MeOH	0.654 (±0.003)	[126]
4-Aminopyridine	0.1 M $MeSO_3Na$ in MeOH	4.900 (±0.200)	[126]
2-Methylpyridine	0.1 M $MeSO_3Na$ in MeOH	0.0247 (±0.006)	[126]
2,4-Dimethylpyridine	0.1 M $MeSO_3Na$ in MeOH	0.038 (±0.001)	[126]
NH_3	0.1 M $MeSO_3Na$ in MeOH	4.100 (±0.100)	[126]
Imidazole	85 mM phosphate (pH 7)	0.125 (±0.005)[a]	[143]
Histidine	85 mM phosphate (pH 7)	0.0425 (±0.005)[a]	[143]
Thiols			
Cysteine	MeOH	0.049 (±0.003)	[121,115]
	0.1 M $MeSO_3H$ in MeOH (5% H_2O)	0.0106 (±0.002)	[143]
	85 mM phosphate (pH 7)	6.5 (±1.5)[a]	
Thioglycolic acid	MeOH	0.052 (±0.002)	[121]
n-PrSH	0.1 M $MeSO_3H$ in MeOH (5% H_2O)	0.220 (±0.002)	[116]
i-PrSH	0.1 M $MeSO_3H$ in MeOH (5% H_2O)	0.225 (±0.003)	[116]
PhSH	0.1 M $MeSO_3H$ in MeOH (5% H_2O)	0.0488 (±0.0008)	[116]
$HOCH_2CH_2SH$	0.1 M $MeSO_3H$ in MeOH (5% H_2O)	0.188 (±0.006)	[116,143]
	85 mM phosphate (pH 7)	12.5 (±1.5)[a]	
$HOOCCH_2SH$	MeOH	0.052 (±0.004)	[115]
	0.1 M $MeSO_3H$ in MeOH (5% H_2O)	0.057 (±0.002)	[116]
$HCl{\cdot}H_2NCH_2CH_2SH$	0.1 M $MeSO_3H$ in MeOH (5% H_2O)	0.0263 (±0.0008)	[116]
Glutathione	0.1 M $MeSO_3H$ in MeOH (5% H_2O)	0.0777 (±0.008)	[115]
D-Penicillamine	MeOH	0.0018 (±0.0001)	[115]
	0.1 M $MeSO_3H$ in MeOH (5% H_2O)	0.0061 (±0.0001)	
Thiourea	0.1 M $LiSO_3CF_3$ in MeOH	1494 (±10)	[145]
1,3-Dimethyl-2-thiourea	0.1 M $LiSO_3CF_3$ in MeOH	448 (±10)	[145]
1,1,3,3-Tetramethyl-2-thiourea	0.1 M $LiSO_3CF_3$ in MeOH	82 (±4)	[145]

[a] Calculated from pseudo-first order rate constants.

Table 3
Rate constants for aqua ligand substitution in $[Pt(terpy)(OH_2)]^{2+}$ by nucleophilic ligands Z at 298 K

Z	Solvent	k (M^{-1} s^{-1})	Ref.
Halides/pseudohalides			
I^-	0.10 M $NaClO_4$(aq) pH 2–3	224,000 (±4000)	[134]
SCN^-	0.10 M $NaClO_4$(aq) pH 2–3	119,400 (±1000)	[134]
Thiols			
L-Cysteine	0.10 M $HClO_4$(aq) pH 1	37.8 (±0.1)	[55,146]
	$HClO_4$(aq)	29.7 (±0.2)	
L-Glutathione	0.10 M $HClO_4$(aq) pH 1	580 (±10)	[55,146]
	$HClO_4$(aq)	711.9 (±18.3)	
DL-Penicillamine	0.10 M $HClO_4$(aq) pH 1	12.8 (±0.1)	[55,146]
	$HClO_4$(aq)	10.7 (±0.7)	
Thiourea	0.10 M $HClO_4$(aq)	172,000 (±200)	[55,135,134]
	0.10 M $NaClO_4$(aq) pH 2–3	163,400 (±2230)	
1,3-Dimethyl-2-thiourea	0.10 M $NaClO_4$(aq) pH 2–3	216,970 (±2980)	[135,134]
1,1,3,3-Tetramethyl-2-thiourea	0.10 M $NaClO_4$(aq) pH 2–3	152,900 (±2700)	[135,134]
Nucleobases			
Guanosine-5′-monophosphate	0.10 M $NaClO_4$(aq) pH 2.5	616 (±9)	[51]
Inosine-5′-monophosphate	0.10 M $NaClO_4$(aq) pH 2.5	564 (±8)	[51]
Inosine	0.10 M $NaClO_4$(aq) pH 2.5	402 (±7)	[51]

and substitution in $[Pt(terpy)(OH_2)]^{2+}$ by excess thiourea (TU), 1,3-dimethyl-2-thiourea (DMTU), 1,1,3,3-tetramethyl-2-thiourea (TMTU), I^- and SCN^-, found that rates do *not* vary significantly with the nature of the entering nucleophile Z [134,135].

3.2.3. Kinetics of pyridine ligand substitution

Pitteri et al. found that the kinetics for displacement of pyridine ligands in $[Pt(terpy)(py)]^{2+}$ by excess chloride also follow a two-term rate law with a second order rate constant that depends on the nature of the pyridine ligand leaving group [126]. Comparing kinetics among a series of isosteric leaving groups (pyridine, 3-methylpyridine, 4-methylpyridine, or 4-aminopyridine) indicates rates decrease with increased pyridine basicity, following a linear free energy correlation seen for the forward reaction (above). The systems with 4-cyanopyridine, 4-acetylpyridine, and methylisonicotinate, display slower rates presumably due to an effect of increased conjugation of the π system, and the sterically hindered 2-methylpyridine and 2,4-dimethylpyridine again display slower rates. In contrast to the forward reaction, this reaction between a dicationic complex and an anionic Z entering group *is* influenced by ionic strength. An analysis of these rate constants along with discrimination parameters among isosteric pyridines led the authors to conclude that the rate-determining transition state for this reversible substitution reaction involves a partial formation of a Pt–N bond with little change in the Pt–Cl bond.

A report by Cusumano et al. illustrates the separate effect of X and Z groups on ligand substitution kinetics [138]. Using stopped-flow UV–vis spectroscopy, the researchers determined that the reaction $[Pt(Yterpy)X]^{2+}$ (Y = H or *o*-tolyl; X = pyridine or 2-picoline) with excess nucleophile (Z = I^- or thiourea) follows pseudo-first order kinetics. Plots of k_{obs} vs. [Z] were linear with an intercept of zero, indicating that there is no contribution from a solvolysis path (independent of [Z]). Thiourea is a better nucleophile than iodide, while the displacement of pyridine is faster than that of 2-picoline. Intercalation of the metal complex cation into calf thymus DNA inhibits the reaction rate due to both steric shielding of the metal center from incoming nucleophiles, and (in the case of I^-) an electronic repulsion from the anionic DNA backbone. Whether or not other types of host–guest supramolecular interactions can affect ligand substitution kinetics of $[Pt(Yterpy)X]^{n+}$ systems remains unanswered. In this study, the Y substituents on terpy had no effect on the 2-picoline displacement rate.

Kinetic studies of other X ligand displacement reactions are less common, but the *S*-bound cysteine ligand in $[Pt(terpy)(cysteine)]^{2+}$ can be slowly substituted by diethyldithiocarbamate ($k = 8.884\ M^{-1}\ s^{-1}$), thiosulfate ($k = 5.997\ M^{-1}\ s^{-1}$), and thiourea ($k = 0.936\ M^{-1}\ s^{-1}$) at pH 6, and the N^1-bound guanosine ligand in $[Pt(terpy)(guanosine)]^{2+}$ can be slowly substituted by sulfur nucleophiles L-cysteine ($k = 1.843\ M^{-1}\ s^{-1}$), glutathione ($k = 4.724\ M^{-1}\ s^{-1}$), thiourea ($k = 4.871\ M^{-1}\ s^{-1}$), and more rapidly by thiosulfate ($k = 121\ M^{-1}\ s^{-1}$), and diethyldithiocarbamate ($k = 595\ M^{-1}\ s^{-1}$) at pH 6 [51]. Hydrolysis of $[Pt(terpy)(OSO_2CF_3)]^+$ in $HClO_4$(aq) occurs with a pseudo-first order rate constant of $0.10\ s^{-1}$ [119].

3.2.4. Influence of the terpy ligand on kinetics of X ligand substitution

A kinetic study of propylamine hydrolysis in dmso/water (1:1, v/v) solutions of complex cations of the type $[Pt(Yterpy)(NH_2\text{-}nPr)]^{2+}$ (Y = H, NH_2, NHN=CMe_2, OEt, 4-BrC_6H_6) provided important insight into the role of electronic effects of the terpy ligand in controlling ligand substitution rates [78]. In this study, the leaving group X = propylamine was the same through the series and the terpy substituents Y were all in the 4′ position and should introduce no steric effects on the reaction. Pseudo first-order rate constants ranged from $2–125 \times 10^{-6}\ s^{-1}$ and were larger for complexes having electron-withdrawing Y substituents and lower for those having electron-donating Y substituents. A linear correlation of the log *k* values with the Hammet σ_p parameters for the Y group indicates that the ligand substitution reactions share a common rate-limiting step; a five-coordinate transition state having an increase in electron density is consistent with an associative mechanism.

In a study by van Eldik and co-workers, the rates of displacement of chloride in $[Pt(Yterpy)Cl]^+$ systems (with Y = H, Ph, or 2-CF_3Ph) by thiourea derivatives depended only slightly on the Y substituents of the terpy ligand (enhanced by the 2-CF_3Ph group and inhibited by the Ph group) [145]. The authors attributed this effect to changes in σ-donicity of the terpy ligand but ruled out any π electronic effect of the phenyl substituents because the crystal structures for these systems show an out-of-plane phenyl ring; electronic communication in solution may be facilitated by thermally accessible phenyl ring rotation, however. In contrast, Cusumano et al. found no difference between the terpy complex and one having *o*-tolyl-terpy in their study of the kinetics for displacement of X = pyridine or 2-picoline by Z = I^- or thiourea [138]. Together, these three studies suggest that the influence of terpy Y substituents on ligand substitution kinetics may depend on a combination of factors, including: (1) the magnitude of the electronic effect of the Y substituent, (2) the nature of X ligand, and (3) the charge of the complex. No study has systematically investigated all three factors.

In several studies, researchers have observed and commented on the enhanced ligand substitution reactivity of $[Pt(terpy)Cl]^+$ compared to that of $[Pt(dien)Cl]^+$, containing the saturated analog diethylenetriamine (dien); the terpy complex displays reaction rates that are up to 10^3 to 10^4 times faster [78,114,115,123]. Chloride substitution rates are also faster than other Pt(II) *tris*-chelate systems [147]. This difference has been attributed to the *trans* effect, a combination of a ground-state labilization (σ-*trans* influence) and a transition-state labilization (π-*trans* influence) by which empty π^* molecular orbitals of the terpy ligand can accept electron density from platinum d orbitals of appropriate symmetry ($5d_{xz}$ and $5d_{yz}$). An early study posited the lack of significant differences between the Pt–Cl vibrational energy for the terpy and dien systems as evidence against differences in ground-state labilization [114]. Some authors [123,133] have suggested that ring strain of the terpy ligand enhances the lability of the chloride ligand in $[Pt(terpy)Cl]^+$; ring strain is supported by crystallographic data (see Section 2.2), which reveal a shorter bond between the Pt center and the central nitrogen atom of terpy and a long Pt–Cl bond [43].

More recently, the dominant effect has been attributed to the role of the terpy ligand in effectively delocalizing the increased electron density present in the five-coordinate transition state structure of an associative ligand substitution mechanism [147]. Studies by van Eldik and co-workers highlight the unique ability of the delocalized terpy π system to markedly increase ligand substitution rates compared to other *tris*-chelating ligands [134,135]. The group investigated a series of six aqua complexes of the type $[Pt(NNN)(OH_2)]^{2+}$, where NNN are chelating ligands having various combinations of pyridine and donors in *cis* and *trans* positions (ranging from terpy to dien). Aqua ligand substitution follows pseudo-first-order rate laws that depended on the entering Z nucleophile concentration ($k_{obs} = k_2[Z]$). The terpy system has the fastest ligand substitution rates ($k_2 \approx 2 \times 10^5\ M^{-1}\ s^{-1}$), which do *not* vary significantly with the nature of the nucleophile Z. In contrast, rates for the dien complex were a factor of 10^4 slower and decreased significantly with

increasing steric bulk of the Z ligand. Systematic variation in the position of pyridyl or amine donors in the *cis* and *trans* positions highlighted the larger importance of *cis* π-acceptors on enhancing ligand substitution rates. The pK_a values of the aqua ligands can serve as an indication of electron density at the metal center (more electron withdrawing NNN ligands resulting in a more electrophilic Pt center and increased acidity of the aqua ligand). For the series of NNN systems, k_2 values were found to increase with decreasing pK_a values, but with the terpy system having an enhancement beyond that predicted by the trend – shown by the other four members of the series – for the sum of three pyridyl rings. This "unusual" reactivity, therefore, was attributed to the delocalized π system in the terpy ligand, and frontier orbital energy calculations suggest that charge stabilization in the transition state by the terpy ligand may involve the Pt $6p_z$ orbital [134]. The authors refute the notion that labilization of the leaving group is due to ground state effects of ring strain or a *trans* σ-donor effect. The second-order rate constant was also found to be affected by solvent, increasing with increasing carbon chain length of a series of alcohols [144]. Studies involving related systems having cyclometallated phenylpyridine ligands in place of terpy further explored the role of the σ-donor and π-acceptor effects in the *cis* and *trans* positions of the *tris* chelate [148].

3.3. Reactions involving the X ligand

In addition to displacement of the X ligand by other nucleophiles, unique reactivity of the coordinated X ligand has been found in several cases. Perhaps the simplest example of this is the decrease in pK_a of water from 15.7 to 4.5 when coordinated to Pt(terpy)$^{2+}$ [135]. Due to this, the aqua complex [Pt(terpy)(OH_2)]$^{2+}$ is converted to the hydroxo complex [Pt(terpy)(OH)]$^+$ unless solution pH is kept below ~3. Annibale et al. reported that protonation of [Pt(terpy)(OH)]$^+$ using HBF_4 gives [Pt(terpy)(OH_2)]$^{2+}$, which was isolated from solution and fully characterized [124]. A pK_a value of about 5.2 has been found for water ligand in [Pt(Clterpy)(OH_2)]$^{2+}$ [149] although an electron-withdrawing substituent on the central terpy ring would be expected to increase the acidity of the aqua ligand. The equilibrium between [Pt(terpy)(OH)]$^+$ and [Pt(terpy)(OH_2)]$^{2+}$ plays an important role in ligand substitution chemistry, as described above [116,124,134].

The carboxaldehyde group of the coordinated ligand 2-pyridinecarboxaldehyde (pyCHO) in the pyridine complex [Pt(terpy)(pyCHO)]$^{2+}$ is observed to react with water to quantitatively form a 2-pyridinemethanediol [132]. During the preparation of [Pt(terpy)(NH_2R)]$^{2+}$ complexes from the reaction of the acetonitrile complex starting material [Pt(terpy)$(NCCH_3)$]$^{2+}$ with alkylamines or ammonia, Lowe and co-workers observed interesting reactivity of the ammine ligand to yield coordinated amidines (Scheme 2) [78].

While stable in refluxing toluene or DMF, the azido ligand in the complex cation [Pt(terpy)N_3]$^+$ reacts in refluxing MeCN (or more slowly at room temperature) to form a tetrazole coordinated to Pt as N^2-bound (major) and N^1-bound (minor) isomers of [Pt(terpy)N_4CMe]$^+$ (Scheme 3) [56]. Heating the azido complex in PhCN results in the formation of only the N^2-bound phenyltetrazole complex [Pt(terpy)N_4CPh]$^+$, as steric effects prevent N^1 coordination [56]. In addition to these solution phase reactions, Wee et al. also reported on gas phase collision-induced dissociation (CID) reactions of the ligands. Upon CID, [Pt(terpy)N_3]$^+$(g) fragments to form the nitride complex cation [Pt(terpy)N]$^+$(g) and N_2(g), but is not reactive with MeCN, Me_2CO or MeOH. The nitride complex cation does reacts with these to form [Pt(terpy)N + L]$^+$(g) (L = MeCN, Me_2CO or MeOH) adducts. The tetrazole complex cations [Pt(terpy)N_4CR]$^+$ (R = Me, Ph) undergo a complex sequence of fragmentation under CID that, depending on the R group, yields acetylide or carbyne products as shown in Scheme 3.

3.4. Reactions involving the terpy ligand

Tridentate coordination of terpy to Pt(II) leaves this ligand inert to displacement due to the well-established chelate effect, while aromatic stability limits its reactivity. And yet, a few examples of terpy ligand reactivity have been discovered.

Displacement of the terpy ligand can be accomplished by the addition of excess NaCN [23,150] or PPh_3 [23,102] to [Pt(terpy)Cl]$^+$, yielding [Pt$(CN)_4$]$^{2-}$ and [Pt$(PPh_3)_2Cl_2$], respectively. Similarly, dithioethane (DTE) displaces terpy in [Pt(terpy)(4-picoline)]$^{2+}$ to yield Pt$(DTE)_2$, and thiols 2-mercaptoethanol and trypanothione do the same [76]. Excess thiolate added to a solution of [Pt(Clterpy)SR]$^+$ results in release of free Clterpy [36]. The reaction of [Pt(terpy)Cl]$^+$ with 1 equiv. of 8-quinolinethiolate (8-QNS) in CH_2Cl_2/MeOH involves terpy displacement to yield [Pt$(QNS)_2$] [Pt(terpy)Cl]$_2^{2+}$ [47].

Mureinik and Bidani posited some unusual reaction of the terpy ligand in their early report on ligand substitution chemistry, reporting that addition of concentrated NaSCN(aq) to [Pt(terpy)Cl]$^+$(aq) results in cleavage of the C^2–C2′ bond to form [Pt(bpy)$(SCN)_2$] [23]. This remarkable transformation has been unsubstantiated by any other study. They also suggested that C–H bond activation in the C^6 positions of the terpy ligand upon reaction of [Pt(terpy)Cl]$^+$ with $AgNO_3$. Reaction with OH^- is described as reversible upon acidification, and the authors postulated that hydroxide attacks the C^6 position of the terpy ligand, which is activated by coordination to Pt(II). A recent paper by Gameiro et al. [151] provides ^{1}H NMR and CD spectroscopic data to support this interpretation, but others attribute the reaction of [Pt(terpy)Cl]$^+$ with hydroxide as involving chloride displacement to yield [Pt(terpy)(OH)]$^+$ (Section 3.1) [48,117].

A gas-phase reaction of a Pt(II) terpy complex having a deoxyguanine ligand involves a fluxional terpy ligand that undergoes C–H activation in a so-called "roll-over 3-metallation" mechanism, as supported by electrospray ionization and collision-induced mass spectrometry data [152].

3.5. Oxidative addition

Reaction of Cl_2(aq) with [Pt(terpy)Cl]Cl(aq) results in oxidative addition to yield the Pt(IV) product [Pt(terpy)Cl_3]Cl, which can be isolated as a colorless dihydrate or trihydrate solid [15] or as [Pt(terpy)Cl_3]PF_6 [23]. The Pt(IV) complex slowly converts back to the Pt(II) starting material upon standing. No other oxidative addition reactions have been reported.

4. Bimolecular complexes and interactions

One of the central themes in the chemistry of the Pt(II) terpy family of compounds is the propensity for these square-planar complexes to "stack" with other [Pt(Yterpy)X]$^{n+}$ cations or with other planar molecules. Numerous [Pt(Yterpy)X]$^{n+}$ systems are found to bind with planar organic π systems, the prototypical example being intercalation between DNA bases. In concentrated solutions, Pt(II) terpy homo-dimers can spontaneously form, and this is believed to preclude subsequent intercalation in DNA [153]. Similarly, Pt(II) terpy complex cations often pack in the solid state into homo-dimers or extended chains. Related to these non-covalent bimolecular interactions are dinuclear complexes having covalently linked Pt(II) terpy units (commonly called "dimers"), which can offer insight into how specific stacking interactions affect electronic properties.

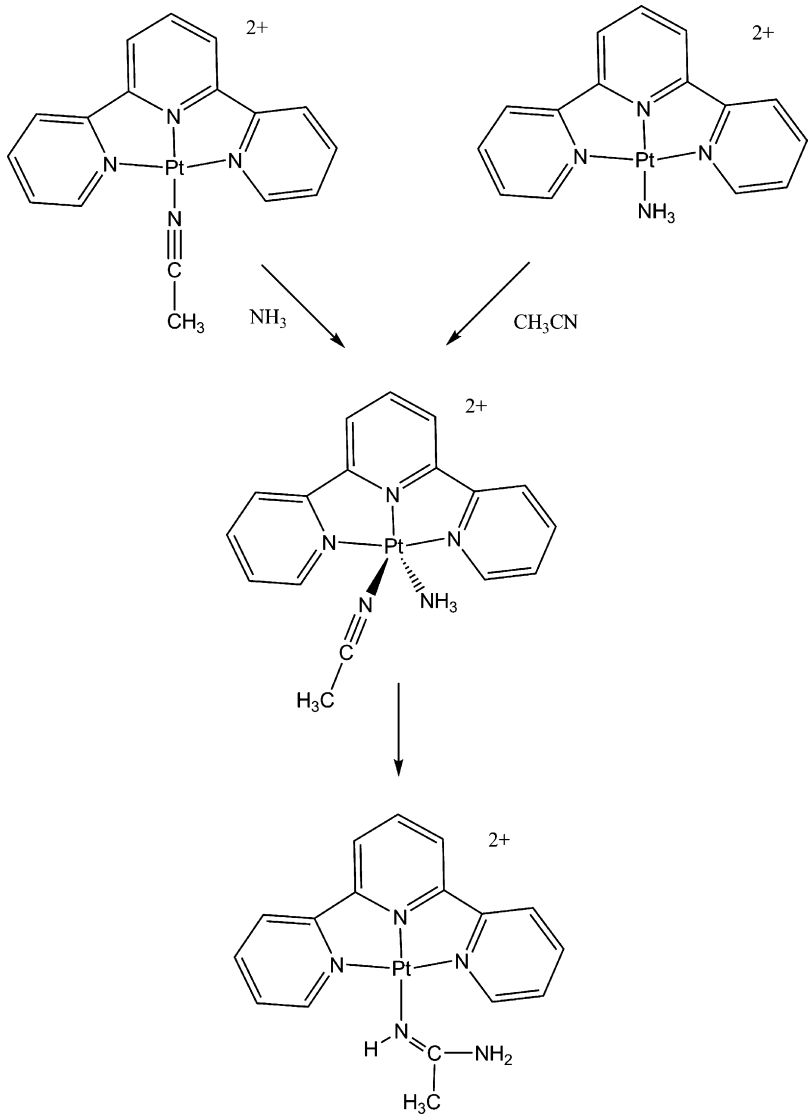

Scheme 2. Formation of amidine complex; adapted from Ref. [78].

4.1. Covalently linked dinuclear complexes

While not all covalently linked Pt(II) terpy dimers involve stacking interactions between metal centers, a diverse family of dinuclear systems is reviewed in this section. Linking two $[Pt(Yterpy)X]^{n+}$ units can be accomplished using a bridging ligand in the X position or using terpy derivatives that are covalently linked. No examples of using bridging ligands in the axial positions of Pt(IV) terpy complexes have been reported.

4.1.1. Dimers linked through bridging X ligands

The geometry of a bridging X ligand determines if $[Pt(terpy)X]^{+}$ units in a dimer adopt a stacked or un-stacked relative orientation. Characteristics of stacked dimers include: long-wavelength visible absorption, upfield shifts for the terpy resonances in ^{1}H NMR spectra, and downfield shift of ^{195}Pt resonances relative to related monomers [52]. Although ^{1}J coupling between two Pt atoms is diagnostic for Pt···Pt distances, values have not been reported for dinuclear Pt(II) terpy complexes.

Crystal structures have been solved for numerous dinuclear complexes in which Pt(terpy) units are held in a stacked orientation by a bridging X ligand. These systems provide a most interesting opportunity to model the spontaneous stacking of monomeric Pt(terpy) cations in the solid state and in solution (Section 4.2). The coordination geometry of the bridging ligand can be used to tune the separation and torsion angle between the Pt(terpy) planes and the Pt···Pt distance, as indicated in Table 4. This spacing plays an important role in controlling color and luminescence properties.

Gray and co-worker investigated a series of $[\{Pt(terpy)\}_2X]^{n+}$ dimers having bidentate N-donor X bridging ligands. For example, the reaction of $[Pt(terpy)Cl]^{+}$ with 0.5 equiv. of pyrazole (pz) at pH 9 for 5 days at 348 K yields $[\{Pt(terpy)\}_2(\mu\text{-pz})](ClO_4)_3{\cdot}CH_3CN$ [154]. The crystal structure displays the small two-atom pz bridge holding together two Pt(terpy) units that are eclipsed but inclined by a 48° dihedral angle, which results in a Pt···Pt separation of 3.432(1) Å (Fig. 15). Pt···Pt distances below 3.5 Å are considered indicative of weak bonding [38].

The Gray lab also reported on dimers having X = μ-azaindole, μ-*N*,*N*-diphenylformamide and μ-arginine [155,156] while reactions involving the potentially bridging ligand 1,3-diphenyltriazene (dpt) formed only the mononuclear complex $[Pt(terpy)(dpt)]^{2+}$ [57]. Kostic and co-workers also investigated the dimer having X = μ-arginine, along with X = μ-canavanine and μ-methylguanidine [67].

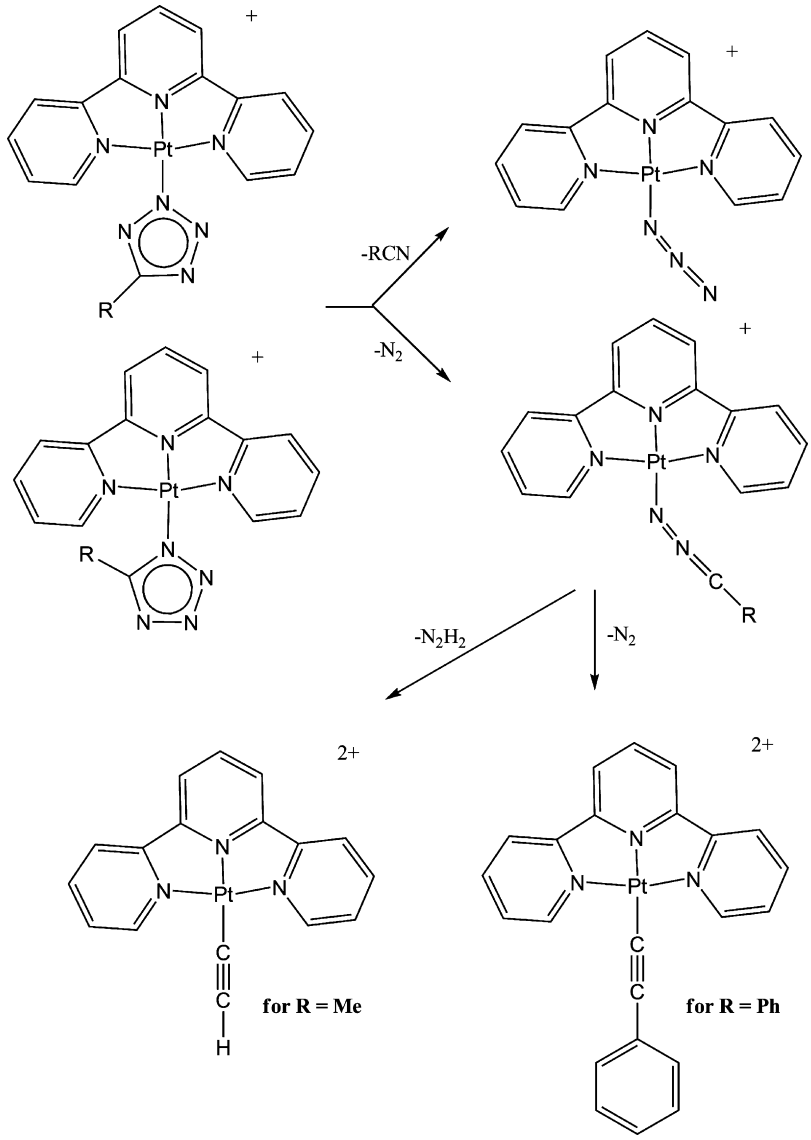

Scheme 3. Pt(II) terpy methyltetrazole and phenyltetrazole complexes and subsequent gas-phase reactivity; adapted from Ref. [56].

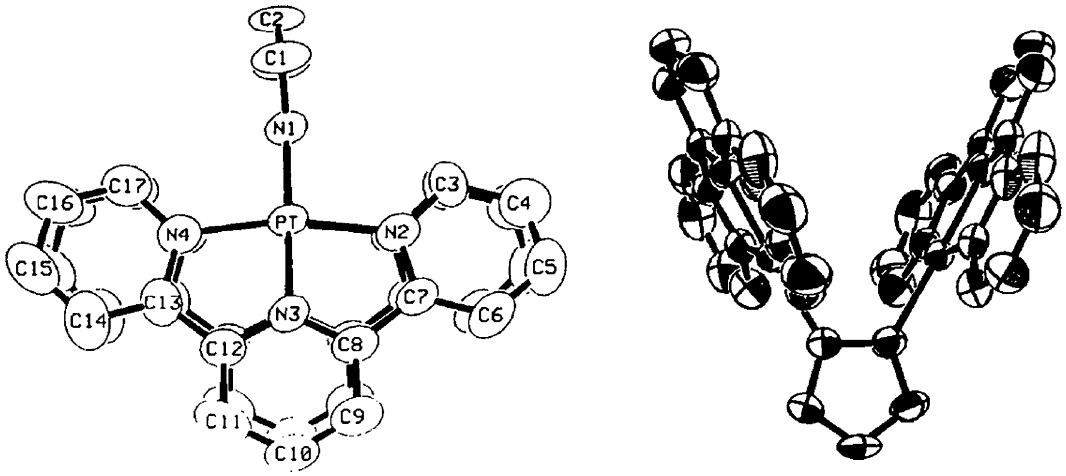

Fig. 15. Two views of the crystal structure of the dinuclear complex $[\{Pt(terpy)\}_2(pz)](ClO_4)_3{\cdot}CH_3CN$; from Ref. [154] (reproduced by permission of The International Union of Crystallography).

Table 4
Selected structural parameters for dinuclear $[\{Pt(Yterpy)\}_2(X)]^{n+}$ cations (X = bridging ligand)

Complex	d_{Pt-Pt} (Å)	Dihedral	Torsion	Ref.
$[\{Pt(terpy)\}_2(\mu$-can$)](ClO_4)_3 \cdot 5.5H_2O$	2.9872(8) 2.9884(7)	9	21	[67]
$[\{Pt(terpy)\}_2(\mu\text{-dpf})](ClO_4)_3 \cdot H_2O$	3.049(1)	16.8, 9.7	7.4	[155]
$[\{Pt(terpy)\}_2(\mu\text{-mcty-}N^3,N^4)](ClO_4)_3$	3.0350(10)	17.1(4)	18	[52]
$[\{Pt(terpy)\}_2(\mu\text{-dtc})](PF_6)_3$	3.052(1)	9.0(1)	33.9	[159]
$[\{Pt(terpy)\}_2(\mu\text{-guanidine})](ClO_4)_3$	3.090(1)	12	28.6	[158]
	3.071(1)	9	22.1	
$[\{Pt(terpy)\}_2(\mu\text{-pz})](ClO_4)_3 \cdot CH_3CN$	3.432(1)	47.7(12)	~0	[154]
$[\{(terpy)PtSCH_2CH_2NH_2\}_2Pt](BF_4)_4$	4.420			[161]
$[\{Pt(terpy)\}_2(\mu\text{-dithiouracil})](ClO_4)_3$	4.501	14.0	~0	[50]
$\{Pt_2(\mu\text{-dppm})_2(C{\equiv}CC_5H_4N)[Pt(terpy)]_4\}(CF_3SO_3)_8$	5.079			[72]
$[\{Pt(Clterpy)\}_2(2\text{-mercaptoimidazole})](PF_6)_3$	3.2903	7.5(5)		[153]
$[(btpyxa)\{PtCl\}_2]PF_6$	4.38			[87]

Dihedral angles describe the inclination between the two Pt(terpy) planes, and the torsion angle describes the twist of the coordination planes along the Pt···Pt axis away from an eclipsed orientation. Complexes are arranged in order of increasing Pt···Pt distance (d_{Pt-Pt}).

Similarly, guanidine can serve as a bridging ligand [157,158]. ^{195}Pt chemical shifts for $[\{Pt(terpy)\}_2X]^{3+}$ dimers with X = guanidine ligands are found in the −975 to −994 ppm range, which is more than 200 ppm lower than the chemical shift for the corresponding $[Pt(terpy)X]^{2+}$ monomer complexes, indicating that the guanidine ligand is more weakly coordinated as a bridging ligand in the dimer complex than as a terminal ligand in the monomer complex [67].

In contrast to the pyrazole complex, the crystal structures of dinuclear complexes having three-atom bridges reveal more closely stacked Pt(terpy) units with significant Pt···Pt interaction. The crystal structure for the dinuclear complex $[\{Pt(terpy)\}_2(canavanine)](ClO_4)_3 \cdot 5.5H_2O$ displays two independent cations differing slightly in the torsion angle within the canavanine ligand [67]. For both, the Pt(terpy) units are very close to being co-planar and eclipsed, giving a short Pt···Pt distance of 2.99 Å. An unusual aspect of the terpy coordination not addressed by the authors is a longer Pt–N^3 distance relative to nearly equal Pt–N^1 and Pt–N^2 distances. Two years later, the crystallographic data for the related complex $[\{Pt(terpy)\}_2(guanidine)](ClO_4)_3$ were reported, revealing a nearly identical dimer structure [158].

Nucleosides adenosine (A), 2′-deoxyadenosine (dA), and 2′-deoxycytidine (dC) can serve as bridging ligands in reactions to form $[\{Pt(terpy)\}_2X]^{3+}$, where X = A, dA or dC as shown in Fig. 16 [139].

Crystal structures for similar stacked dinuclear complexes with short Pt···Pt separation have been found for systems having three-atom N–C–N bridging units 1-methylcytosine [52] and *N*,*N*′-diphenylformamide [155], and S–C–S bridge of a diethyldithiocarbamate (dtc) ligand in $[\{Pt(terpy)\}_2(dtc)](PF_6)_3$ [159]. A longer Pt···Pt separation (3.2903 Å) is present in the crystal structure of the dinuclear complex $[\{Pt(Clterpy)\}_2(2\text{-mercaptoimidazole})](PF_6)_3$, which also possesses a three-atom bridge (Fig. 17) [153,160]. However, using thioacetimine as a bridging ligand results in a bridged $[\{Pt(terpy)\}_2(\mu\text{-}N,S\text{-thioacetimine})]^{3+}$ dimer that is unstable in solution, reacting with water to release acetamide and a sulfide-bridged trimer $[\{Pt(terpy)\}_3\mu\text{-}S]^{3+}$, the "propeller-like" structure of which has been characterized by X-ray crystallography [153].

Larger bridging ligands can be used to assemble stacked but more widely spaced Pt(terpy) units. The dinuclear complex $[\{Pt(terpy)\}_2(dithiouracil)](ClO_4)_3$ has been prepared from $[Pt(terpy)Cl]^+$ and 0.5 equiv. of the corresponding dithiol [50]. In the structure (Fig. 18), Pt(terpy) units are eclipsed but non-interacting due to the large distance (4.5 Å) they are held apart by the 5-atom bridging unit of the dithiouracil ligand.

The trinuclear complex $[\{(terpy)PtSCH_2CH_2NH_2\}_2]Pt(BF_4)_4$ was prepared by addition of 1 equiv. of K_2PtCl_4 to a mixture of 2 equiv. each of $[Pt(terpy)Cl]^+$ and 2-aminoethanethio (AET) hydrochloride in NaOH(aq) [161]. A crystal structure (Fig. 19) shows a square-planar $[Pt(SCH_2CH_2NH_2)_2]$ complex serving as a bridging unit of two $[Pt(terpy)]^{2+}$ units that are nearly co-planar but twisted by ca. 90° torsion angle (resulting in a long Pt···Pt distance of 4.420 Å). This complex cation also spontaneously formed from a solution of $[Pt(terpy)(AET)]^+$ and crystallized as an adduct with deoxymethoxy-pTpA. The structure shows A–T base pairs stacked on either side of the platinum complex cation and $[Pt(terpy)]^{2+}$ units that are nearly eclipsed, indicating how stacking can be affected by microenvironment [162].

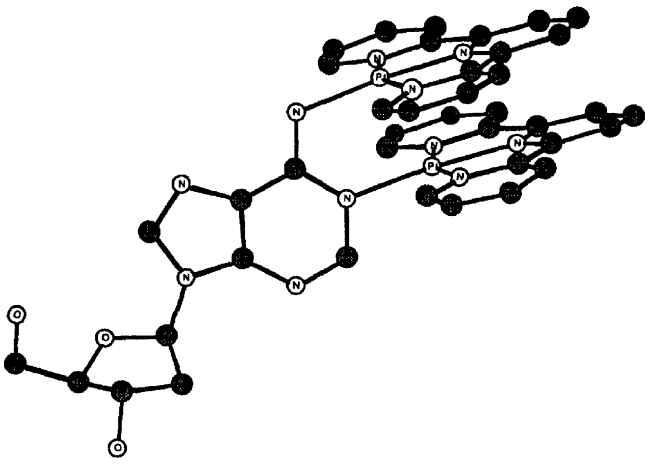

Fig. 16. The proposed conformation of a Pt(II) terpy dinuclear complex bridged by 2′-deoxyadenosine; from Ref. [139] (reproduced by permission of The Royal Society of Chemistry).

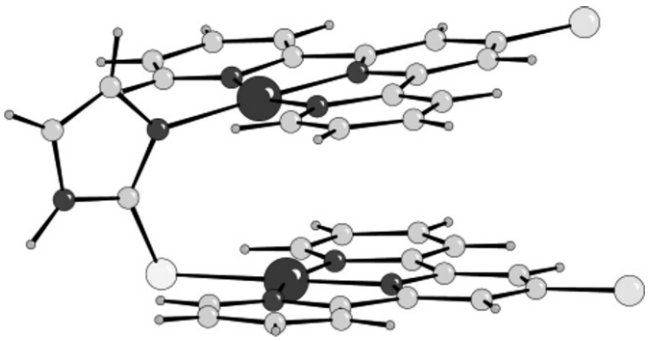

Fig. 17. The X-ray crystal structure of $[\{Pt(Clterpy)\}_2(2\text{-mercaptoimidazole})](PF_6)_3$; from Ref. [153] (reproduced by permission of The Royal Society of Chemistry).

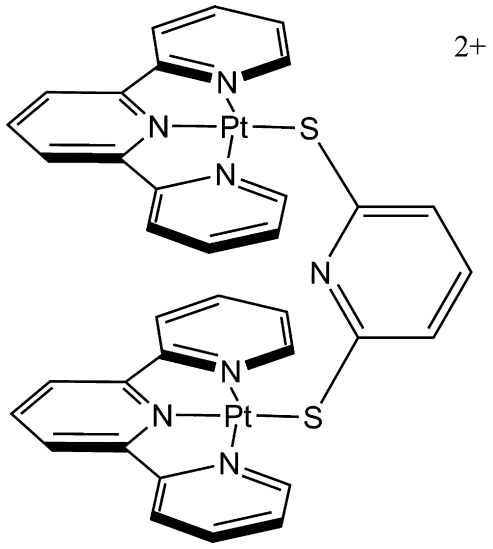

Fig. 18. A dithiouracil-bridged Pt(II) terpy dimer complex.

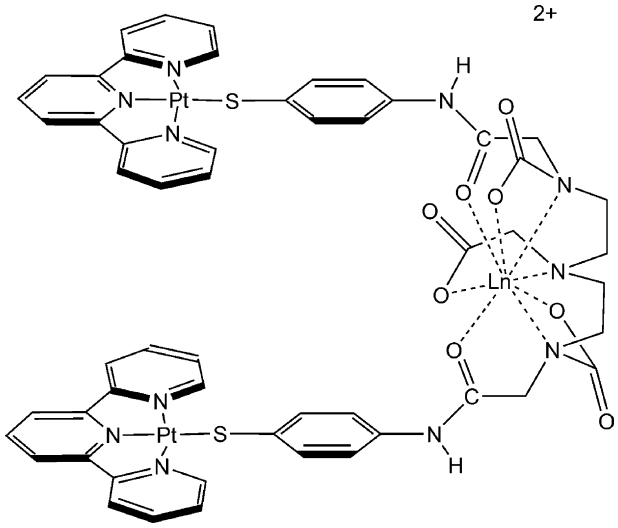

Fig. 21. A Pt(II) terpy dimer having a lanthanide complex spacer.

With the goal of developing synthetic routes to supramolecular Pt(II) complexes, Yam and co-workers have recently prepared a hexanuclear Pt(II) complex $\{[Pt_2(\mu\text{-dppm})_2(C{\equiv}CC_5H_4N)][Pt(terpy)]_4\}(CF_3SO_3)_8$ [72]. Two pair of face-to-face $[Pt(terpy)]^{2+}$ units are parallel with a close inter-plane distance indicative of π-stacking, but a long Pt···Pt distance precludes inter-metallic interaction (Fig. 20).

A seven-coordinate luminescent lanthanide complex serves as a large spacer between two $[Pt(terpy)(SPh)]^+$ units in a trimetallic complex cation (Fig. 21) prepared using the flexible synthetic strategy of Pikramenou and co-workers [163]. Molec-

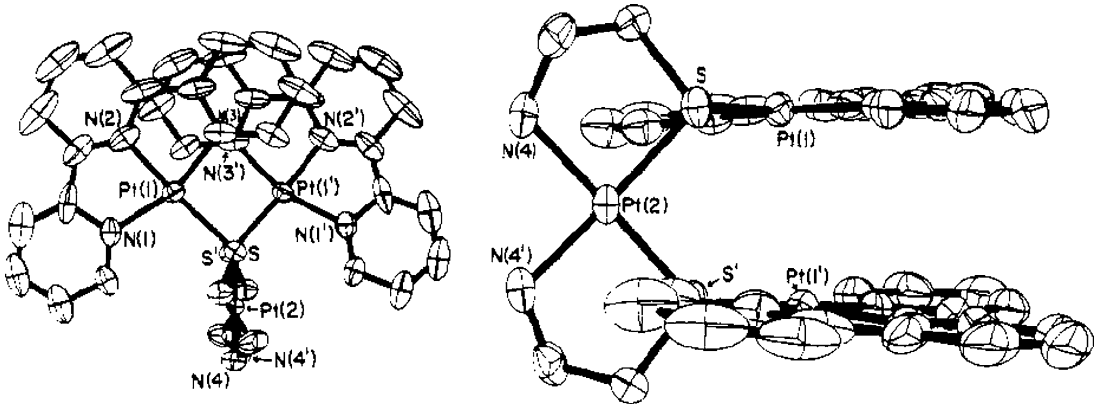

Fig. 19. A trinuclear complex cation containing two co-planar Pt(II) terpy units; from Ref. [161] (reproduced by permission of The American Chemical Society).

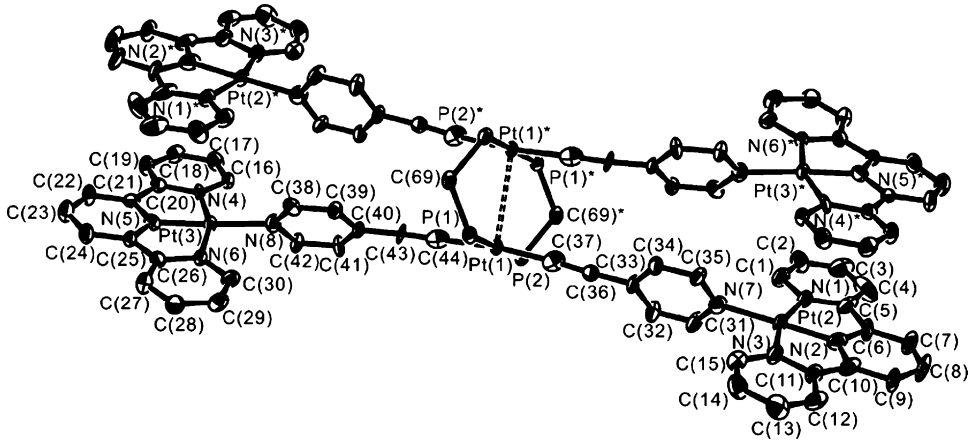

Fig. 20. Crystal structure of the complex cation of $[Pt_2(\mu\text{-dppm})_2(C{\equiv}CC_5H_4N)_4\{Pt(trpy)\}_4](CF_3SO_3)_8$, with H and C atoms of phenyl rings of dppm omitted for clarity; from Ref. [72] (reproduced by permission of The American Chemical Society).

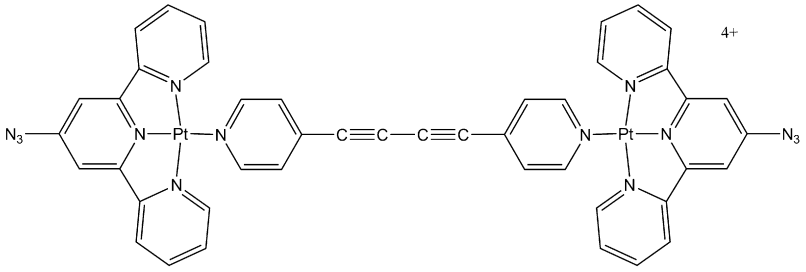

Fig. 22. $[\{Pt(N_3terpy)\}_2L]^{4+}$ dimer having a dipyridyldiethynyl spacer.

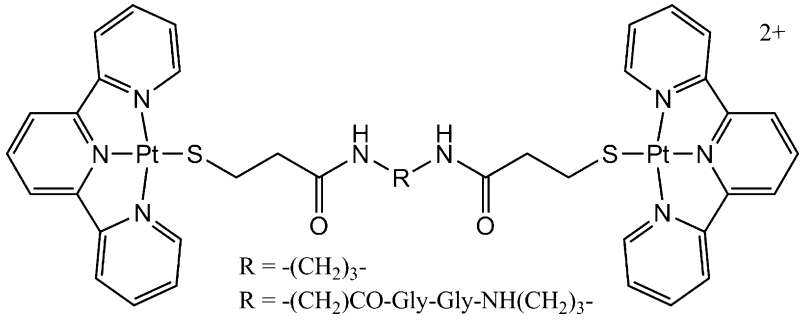

Fig. 23. A Pt(II) terpy dimer having a peptide dithiols spacer.

ular modeling suggests that the two $[Pt(terpy)(SPh)]^+$ units are co-planar.

Bridging ligands having well-separated donor atoms form dimers with unstacked $[Pt(terpy)X]^+$ units. Pyridyl bridging ligands have been used to prepare the dinuclear complex $[\{Pt(terpy)\}_2$-*N*,*N*-4,4′-vinylenedipyridine$]^{4+}$ [133,152] and a series of five $[\{Pt(N_3terpy)\}_2L]^{4+}$ complexes for which the bridging L ligand contains pyridine endcaps with either diethynyl (Fig. 22), *para*-phenylenediethynyl, *para*-biphenyldiethynyl or *trans*-$[Pt(pyridine)_2(NH_3)_2]^{2+}$ spacer groups [140]. The thallium salt of the 2,5-dimethyl-1,4-dicyanamidebenzene anion (Me_2dicyd^{2-}) slowly reacts with $[Pt(terpy)Cl](PF_6)_2$ to yield the dinuclear complex cation $[\{Pt(terpy)\}_2(\mu\text{-}Me_2dicyd)]^{2+}$ [164].

Alkane dithiols allow for the formation of un-stacked dimers of the type $[(terpy)PtS(CH_2)_nSPt(terpy)]^{2+}$ having $n = 4$–10, but those for $n = 2$ and 3 were not isolable [165]. Dimers constructed using bridging dithiols with peptide chain spacers (Fig. 23) [166] and several different carborane dithiols (Fig. 24) [142] have been reported. The ligand 2,5-dimercapto-1,3,4-thiadiazole ($DMcTH_2$) can serve as either a monodentate or bridging ligand in the preparation of $[Pt(terpy)(DMcTH)]^+$ and $[\{Pt(terpy)\}_2(DMcT)]^{2+}$, while the related 2-mercapto-5-methyl-1,3,4-thiadiazole (McMTH) yields only the mononuclear complex cation $[Pt(terpy)(McMT)]^+$ [53]. The crystal structure of $[\{Pt(terpy)\}_2(DMcTH)](PF_6)_2$ reveals two Pt(terpy) units parallel to each other but on opposite ends of a perpendicular bridging DMcTH ligand [53]. The reaction of 2 equiv. of $[Pt(terpy)(OH_2)]^{2+}$ with *S*-methyl-3-acyl-2-methyldithiocarbazate derivatives results in the formation of the complex cation $[\{(terpy)Pt\}_2SMe]^{3+}$, the crystal structure of which shows the single S atom of the methanethiolate ligand serving as a bridge of two nearly orthogonal Pt(terpy) units (Fig. 25) [124]. The use of the 1,3,4-oxadiazoline-5-thione bi-products for pharmaceutical and biological applications highlights the importance of the ability of $[Pt(terpy)(OH_2)]^{2+}$ to facilitate in this cyclization reaction.

A series of alkynyl-bridged dinuclear cations of the type $[Pt(^tBu_3terpy)(C{\equiv}C)_nPt(^tBu_3terpy)]^{2+}$ ($n = 1$, 2, 4) have been prepared by Yam et al. [88], as has a dinuclear complex having a 4-ethynylpyridine ligand bridging two $[Pt(^tBu_3terpy)]^{2+}$ units [71]. Bimetallic complexes of the type $[Pt(^tBu_3terpy)(C{\equiv}C\text{–}C_6H_4\text{–}C{\equiv}C)Re(NN)(CO)_3]^+$, where NN = bipyridine and phenanthroline derivatives, have been prepared by similar methods [89].

A tetranuclear complex cation [3,6-$\{Pt(^tBu_3terpy)(C{\equiv}CPhC{\equiv}C)Pt(PEt_3)_2(C{\equiv}C)\}_2$-9-butylcarbazole$]^{2+}$ prepared by Yam and coworkers contains two $[Pt(^tBu_3terpy)]^{2+}$ units with phenylacetylide ligands in the fourth coordination site that connect to $[Pt(PEt_3)_2(C{\equiv}C)_2]$ units which in turn bridge to a carbazole core (Fig. 26) [69].

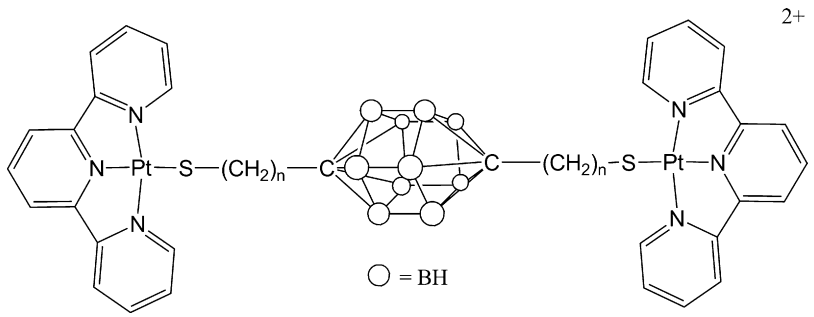

Fig. 24. A Pt(II) terpy dimer having a carborane dithiols spacer; from Ref. [142] (reproduced by permission of The Royal Society of Chemistry).

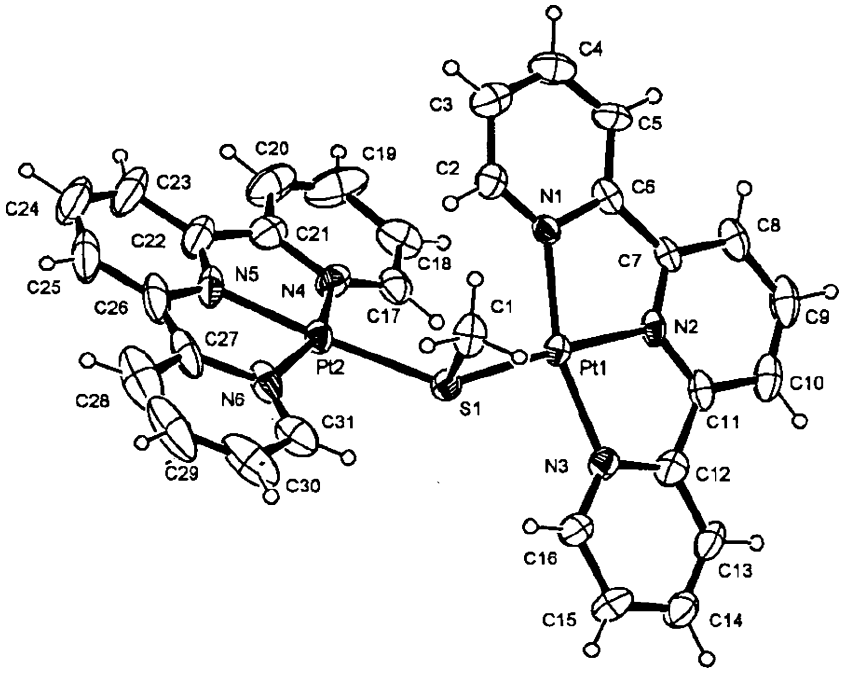

Fig. 25. A Pt(II) terpy dimer having a SMe complex spacer; from Ref. [124] (reproduced by permission of The Royal Society of Chemistry).

4.1.2. Dinuclear complexes linked via the terpy substituent

New synthetic strategies for preparing terpy derivatives have opened the door for the design and synthesis of covalently linked terpy ligands and the preparation of dinuclear Pt(II) terpy complexes.

The Bosnich group has prepared a dinuclear system $[L\{(terpy)PtCl\}_2]^{2+}$ (Fig. 27) using a spacer (L) connecting two terpy ligands via the 4′ positions from the reaction of $Pt(COD)I_2$ with $AgSbF_6$ in acetone followed by addition of 0.5 equiv. of $L(terpy)_2$ [38]. Further descriptions of binding of other metal complexes to this "molecular cleft" receptor is described in Section 4.2. Lowe has reported on cytotoxicity studies involving the dimer $[L\{(terpy)Pt(NC_6H_4Me\text{-}4)\}_2]^{4+}$ having a spacer L = butanediamide (Fig. 28) [133].

Tanaka and co-workers have built a $L(terpy)_2$-type ligand "btpyxa" with L being a planar xanthene unit bridging two terpy rings capable of single or double platination [87]. In the crystal structure of the $[(btpyxa)PtCl]PF_6$, a bridging planar and perpendicular xanthene unit holds a $[Pt(terpy)Cl]^+$ cation co-planar to a second terpy unit but too apart (>4.1 Å) for π-stacking. The crystal structure for the dinuclear complex $[(btpyxa)\{PtCl\}_2]PF_6$ (Fig. 29) shows a large Pt···Pt separation (4.38 Å). Reaction of the former with $RuCl_2(dmso)_4$ produces $[(dmso)Cl_2Ru(btpyxa)PtCl]^+$ which, in turn, can react with 3,5-$^tBu_2$catechol to yield $[(dmso)(^tBu_2catechol)Ru(btpyxa)PtCl]^{2+}$.

A linear non-stacked dinuclear Pt(II) terpy complex has been prepared by Risch and co-workers using a terphenyl linkage between terpyridine ligands [167].

4.2. Non-covalent intermolecular interactions

The examples of face-to-face stacking of $[Pt(terpy)X]^{n+}$ units described in the last section rely on bridging ligands to secure the metal complexes in a co-planar orientation. Similar stacking is now considered for non-covalent interactions to form dimers and aggregates of $[Pt(terpy)X]^{n+}$ complex cations in solution and the solid state. Also considered are bimolecular pairing involving $[Pt(terpy)X]^{n+}$ complex cations with other planar molecules. This latter effect is of special importance to understanding how $[Pt(terpy)X]^{n+}$ systems intercalate between base pairs of DNA.

Stacking of square-planar d^8 platinum complexes is well known for a wide variety of ligand systems, including polypyridines such as terpy. The stability of these dimer or aggregate structures is commonly attributed to a combination of favorable orbital interactions between the Pt d orbitals and between terpy π orbitals. Specifically, the interaction between adjacent Pt centers split the occupied $5d_{z^2}$ orbitals into a dσ bonding and dσ* antibonding MOs, while the unoccupied $6p_z$ orbitals split into a pσ bonding and pσ* antibonding MOs. Stability from Pt···Pt interactions is thought to occur for systems having Pt···Pt distances ≤3.5 Å [38]. Likewise, the π systems of aromatic ligands such as terpy can interact and split to yield a bonding and anti-bonding combination. In addition, interactions between Pt d and ligand π orbitals have been considered. For some systems, hydrophobic interactions and hydrogen bonding may also stabilize dimers and aggregates. The net effect of these combinations of interactions determines the stability of the dimers or aggregates relative to the monomer complexes.

4.2.1. Solution-phase stacking of $[Pt(Yterpy)X]^{n+}$ cations

Many (but not all) $[Pt(Yterpy)X]^{n+}$ systems display dimer or aggregate formation in solution, and a survey of this growing body of literature offer insight into how various properties of the complex cation or solution medium can influence the magnitude of the dimerization constant or dimer structure. Dimers and aggregates are often in equilibrium with monomers, and are less favored at higher T as π-stacking interactions are weakened [30].

Jennette and Lippard reported on the concentration-dependence of the UV–vis absorption spectra for $[Pt(terpy)Cl]^+$ and $[Pt(terpy)HET]^+$, for which linear Beer's Law plots are observed only for solution concentrations below 15 μM [43]. Molar absorptivity data were used to calculate dimerization constants of $K_d = (4 \pm 2) \times 10^3\ M^{-1}$ and $K_d = (7 \pm 5) \times 10^3\ M^{-1}$, respectively [43]. The authors note that these values depend somewhat on the wavelength used, suggesting that more than one type of aggregate may exist in solution. Conductivity measurements for 10^{-2} M solutions were consistent with dimer formation.

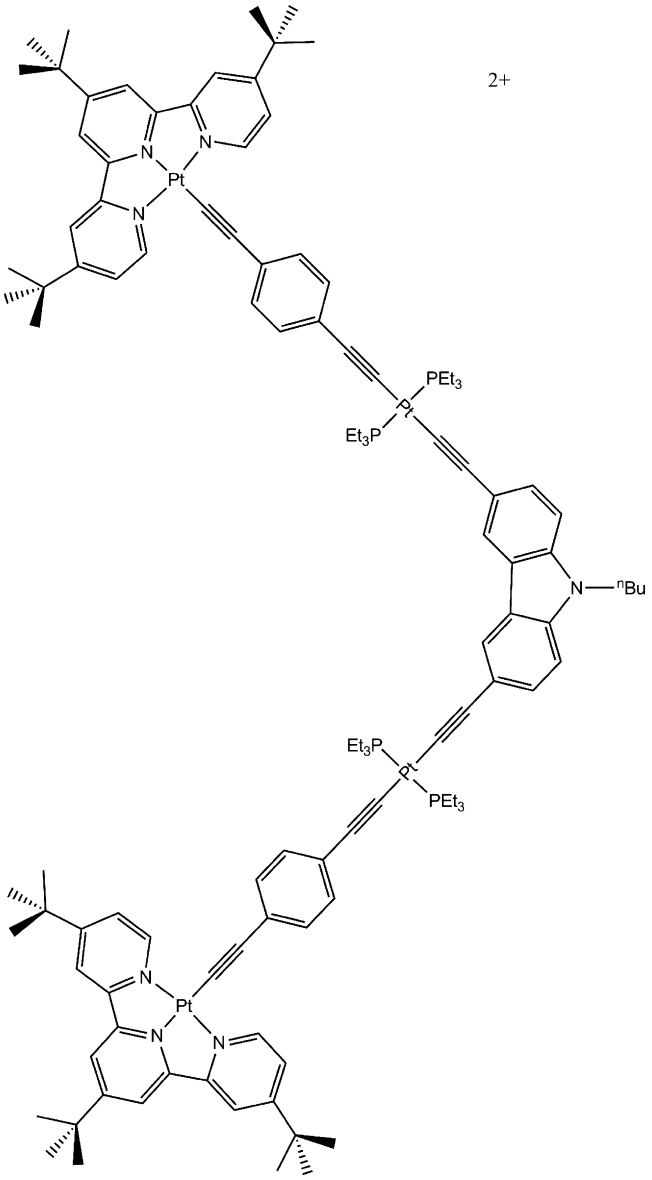

Fig. 26. A supramolecular Pt(II) terpy dimer.

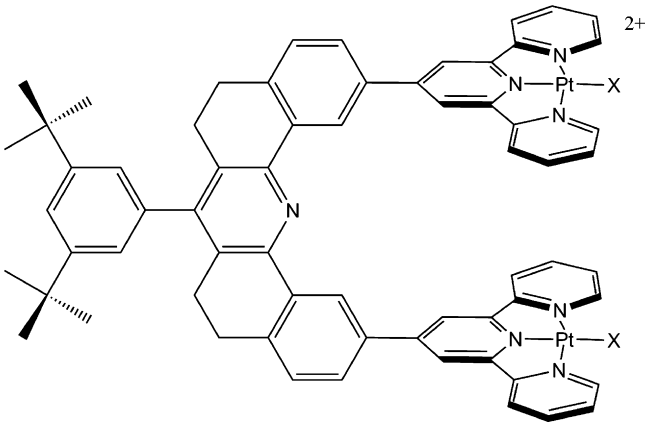

Fig. 27. A Pt(II) terpy dimer having an aromatic organic bridge spacer.

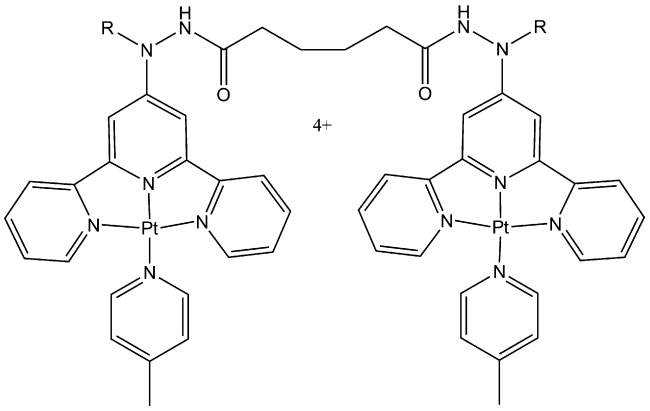

Fig. 28. A Pt(II) terpy dimer having butanediamide spacer.

Gray and co-workers characterized dimer formation from observations of a new absorption band at ~470 nm for 10 mM aqueous samples of the reduced complex $[Pt(terpy)Cl]^+$ and at ~570 nm for 0.15 mM solutions in frozen solvent at 77 K and reported a dimerization constant of $K_d = (3 \pm 2) \times 10^3\ M^{-1}$ [45]. They propose two types of dimers: one assembled through Pt···Pt interaction and the other through π–π interaction of terpy ligands. The medium has a strong effect on dimerization, with K_d dropping to only $80\ M^{-1}$ in 0.1 M $(Bu_4N)PF_6$/DMF [168]. The Gray group investigated the role of charge of the complex on dimerization, finding that K_d increases 10-fold for the neutral complex [Pt(terpy)Cl] in 0.1 M $(Bu_4N)PF_6$/DMF [168]. In addition, they spectroscopically identified a mixed-valence dimer [Pt(terpy)Cl]–$[Pt(terpy)Cl]^+$.

Does increasing the hydrophobicity of the X ligand favor dimerization? The K_d value for the complex cation $[Pt(terpy)(SPh)]^+$, having a more hydrophobic SPh ligand, is $6.3 \times 10^3\ M^{-1}$ (pH 7 aqueous buffer; 20 °C; $\eta = 0.01$), nearly the same as that for $[Pt(terpy)HET]^+$ [169]. The dimerization constant increases with increasing ionic strength (at constant $T = 20$ °C), and decreases with increasing temperatures (at constant ionic strength of $\mu = 0.01$). van't Hoff plots reveal a small negative ΔH and a positive ΔS for dimerization, but ΔS becomes negative at higher ionic strength. The phenyl ring of the thiol X ligand may have a minor de-stabilizing

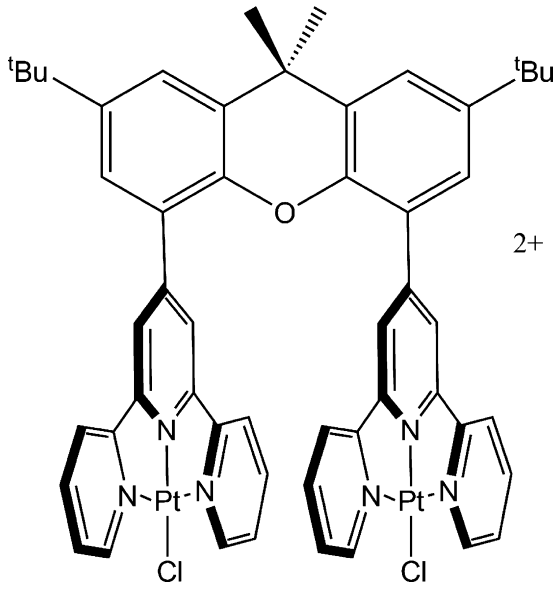

Fig. 29. A Pt(II) terpy dimer having a xanthene spacer.

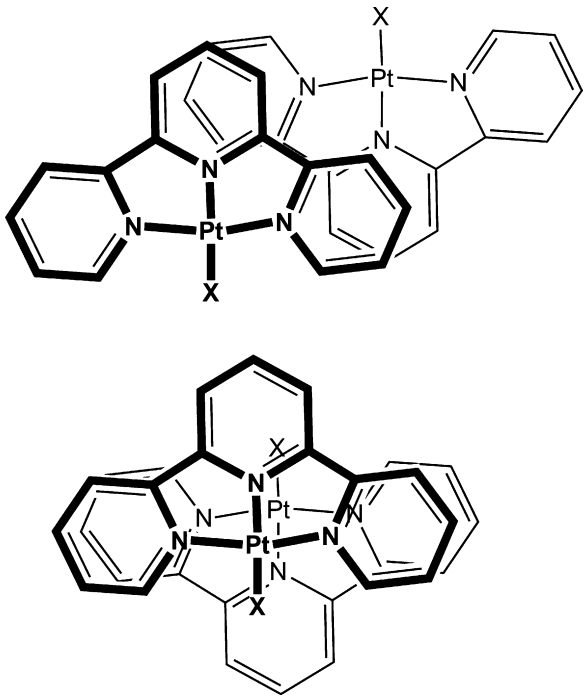

Fig. 30. Two types of head-to-tail stacking orientation proposed for dimers and aggregates.

influence on dimer formation, as indicated by $K_d = 1.0 \times 10^4\ M^{-1}$ ($\mu = 0.01$) for $[Pt(terpy)SC_4H_9]^+$ in KFH(aq) buffer [165,170]. Aggregation is also disrupted by organic solvents such as EtOH, dmso and DMF or the addition of a surfactant.

At concentrations below 0.25 mM, the organometallic complex cation $[Pt(terpy)Me]^+$ dimerizes with $K_d = 1.0 \pm 0.8 \times 10^4\ M^{-1}$ (from UV–vis data) or $2.6 \pm 0.1 \times 10^4\ M^{-1}$ (from NMR data), but at higher concentrations (or higher ionic strength) evidence for aggregation comes from resonance light scattering and changes to the NMR spectrum [30,60,171]. Specifically, observations of large changes in the ^1H chemical shift of the methyl group were used to postulate a head-to-tail structure for dimer and aggregate formation (Fig. 30) [171]. Comparing the results for the methyl complex with those for the thiol systems described above suggests that greater planarity of the methyl complex may be the dominant effect in favoring aggregate formation rather than differences in hydrophobicity of the various ligands as was originally hypothesized [30]. Again, solvent has a large influence, with the extent of aggregation in CH_3CN found to be significantly less ($K_d = 180 \pm 52\ M^{-1}$) than in water [60].

A comparative study on aggregate formation for $[Pt(terpy)Me]^+$, $[Pt(Phterpy)Me]^+$, $[Pt(terpy)Ph]^+$, and $[Pt(Phterpy)Ph]^+$ indicated that while only the two methyl complexes display evidence of both dimer and aggregate formation, the two phenyl complexes do not dimerize but do aggregate highly in aqueous solution [172]. A perpendicular orientation of Pt(Phterpy) units was postulated. For all of these systems, aggregate formation was enhanced by alcohols but inhibited by dmso and dioxane.

In the ^1H NMR spectra of several $[Pt(Yterpy)X]^+$ cations (Y = H or Ph and X = Cl or Me; but *not* for X = Ph) dissolved in methanol, chemical shifts move upfield with increasing complex concentration and decreasing *T*, indicative of stacking [31]. However, absorption spectra obey Beer's Law up to 3×10^{-4} M. Differential pulse voltammograms of complexes $[Pt(PhCH_2CH_2CH_2Oterpy)Cl]BF_4$ and $[Pt(CH_3CH_2CH_2Oterpy)Cl]BF_4$ display splitting attributed to an equilibrium mixture of monomer and dimer in solutions [82].

Even the steric bulk of the complex cation $[Pt(terpy)(SCH_2C_2B_{10}H_{11})]^+$ (and two other related complex cations having a carborane-derivatized thiol ligand) does not prevent aggregation, which was detected for solutions of greater than 13 μM concentration [130].

A dramatic demonstration of the effect of solvent on aggregation has been reported for $[Pt(terpy)(C{\equiv}CC{\equiv}CH)]^+$ [65]. The addition of ether to acetonitrile solutions results in significant color changes due to large red-shift in the absorption bands, attributed to the formation of aggregates in the less polar solvent. Interestingly, the color of the solutions containing aggregates also depends on the nature of the anion, ranging from blue for the triflate salt to orange for the BF_4^- salt [64]. This important observation suggests that the structure of aggregates can be controlled by anion size or shape, and effect on absorption may lead to colorimetric anion sensor. A similar aggregation is induced by a polyelectrolyte anion, deprotonated poly(acrylic acid) [173].

Dimerization is *not* evident for $[Pt(^tBu_3terpy)Cl]^+$ [81], $[Pt(terpy)(OH)]^+$ [136] or for a family of $[Pt(terpy)C{\equiv}CR]^+$ [63] complex cations, as UV–vis spectra follow Beer's Law up to concentrations of 10^{-2} M.

Covalently linked dinuclear complexes of the type $[(terpy)PtS(CH_2)_nSPt(terpy)]^{2+}$, having flexible aliphatic dithiolate bridging ligands, also display concentration-dependent UV absorbance, indicative of either intra- or inter-unit aggregation [165,166]. Dimerization constants have been determined for the $n = 4$ ($K_d = 4.4 \times 10^3\ M^{-1}$) and $n = 6$ ($K_d = 6.2 \times 10^3\ M^{-1}$) complexes in KFH(aq) buffer [165]. The much lower dimerization constant ($K_d = 7.0 \times 10^2\ M^{-1}$) found for a related Pt(II) terpy dinuclear complex, having an aromatic 1,4-benzenedimethanethiol bridging ligand, may reflect the effect that the rigidity of the bridging ligand has on the self-association process [174]. Interestingly, the analogous 1,3-benzenedimethanethiol complex does not display evidence of dimerization for concentrations up to 10^{-4} M.

4.2.2. Solution-phase bimolecular stacking interactions

While intercalation of $[Pt(terpy)X]^{n+}$ complexes between base pairs of DNA has been recognized for many years, non-covalent interactions between $[Pt(terpy)X]^{n+}$ and other types of π systems have been explored only recently.

Identification of the contributions of Pt···Pt and π–π interactions in assembling stacked structures led Bosnich and co-workers to design and investigate "molecular cleft" receptors of type $[L\{(terpy)MCl\}_2]^{2+}$ (Fig. 27) where L = spacer and M = Pd(II) and Pt(II) [38]. While $[Pt(terpy)Cl]^+$ does not bind to either the M = Pd(II) or Pt(II) receptors due to unfavorable electrostatic repulsion between the cationic guest and the dicationic receptor, the addition of the neutral square-planar complex $[Pt(salap)NH_3]$ to the Pt terpy receptor in CH_3CN results in immediate color change due to new absorption bands with λ > 500 nm. Data from variable-temperature ^1H NMR spectroscopy established a 1:1 host–guest binding stoichiometry with a 51,000 (±8400) M^{-1} association constant. This association constant is significantly higher than ones found for similar receptors with organic aromatic guests, suggesting appreciable stabilization via Pt···Pt···Pt interactions in addition to π–π interactions between terpy and salap ligands and charge-induced dipole interactions between guest and host. Results of ^1H NOESY experiments were consistent with the $[Pt(salap)NH_3]$ guest binding only in the molecular cleft between the $[Pt(terpy)Cl]^+$ units, and with an orientation having the ammine ligand of the guest pointing along the same direction as the chloride ligands of the host, a structure confirmed using X-ray crystallography (Fig. 31). Near-linear alignment of Pt(II) centers with Pt···Pt distances of 3.303 and 3.262 Å suggest that Pt···Pt interactions are more significant for stability than π–π interactions. The importance of the charge of the

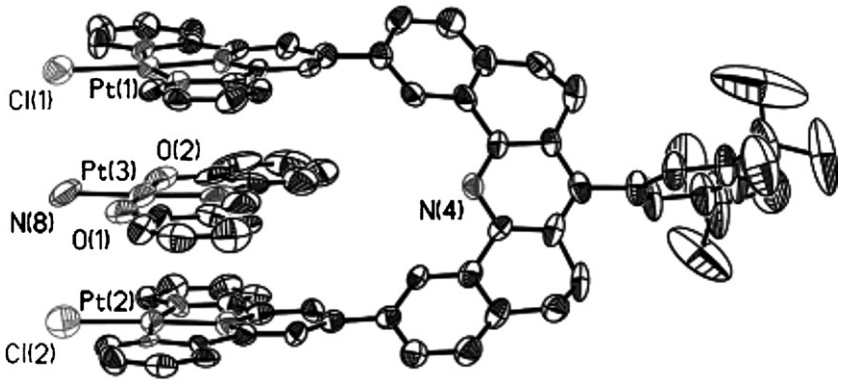

Fig. 31. Crystal structure of a host–guest complex formed between $[Pt(salap)NH_3]^{2+}$ and a Pt(II) terpy dimer; from Ref. [38] (reproduced by permission of The American Chemical Society).

guest and the resulting net charge of the host–guest complex was highlighted by investigations using anionic guests $[Pt(salap)CN]^-$ and $[Pt(salap)Cl]^-$. In addition to guest binding within the host cleft, aggregation between monocationic host–guest units was evident from concentration-dependent absorption spectra and was not observed for the dicationic host–guest complex. The addition of dianionic complexes $[Pt(CN)_4]^{2-}$ or $[Pt(oxalate)_2]^{2-}$ to the dicationic receptors results in the immediate formation of an insoluble precipitate indicative of binding due to favorable electrostatics. These results emphasize the importance of overall complex charge in controlling inter-complex aggregation. Also, two of these "molecular clefts" can be connected through bridging dipyridyl ligands to form "molecular rectangles" capable of binding other Pt(II) complexes [37]. Interestingly, pairs of molecular clefts interlock to form chains of $[Pt(terpy)Cl]^+$ units in the solid-state structure [175], and this common solid-state stacking phenomenon is reviewed in the next section.

4.2.3. Solid-state stacking of $[Pt(Yterpy)X]^{n+}$ cations

Stacking of $[Pt(Yterpy)X]^{n+}$ cations in the crystal structure can have a large influence on color and luminescence properties of solids and relate to the propensity for dimerization in solution. As with the covalently linked dinuclear systems described above, interaction between $[Pt(Yterpy)X]^{n+}$ cations in the crystal packing structure is characterized by three important parameters: the dihedral angle, torsion angle and the distance between cation planes (which together determine Pt···Pt separation). Cations almost always pack in a face-to-face arrangement, with deviation from co-planarity described by the dihedral angle between the cation planes. In addition, cation stacks most often have a torsion angle close to 180°, giving a "head-to-tail" relative orientation in which the Pt–X bonds of adjacent cations point in opposite directions about a center of inversion; importantly, this is the opposite orientation from the majority of the covalently bridged dinuclear complexes having *syn* orientation (above). These two parameters along with the inter-plane separation of cations planes determine the Pt atom spacing, which is typically either extended chains of evenly spaced and co-linear Pt atoms or groupings of dimers having alternating short and long Pt···Pt spacing; for the later, cations planes may still be evenly spaced due to a zigzag arrangement of Pt atoms. In general, Pt···Pt distances less than 3.5 Å are considered indicative of direct overlap of Pt d_{z^2} orbitals [38]. In addition to Pt···Pt interactions, π orbitals of adjacent terpy ligands can overlap to stabilize cation stacking, and some solid-state structures reveal that π-stacking is the dominant interaction. This π-stacking is generally regarded as occurring when inter-plane distances are less than 3.8 Å [57]. These solid-state stacking parameters can depend on four factors: (1) the nature of the X ligand, (2) Y substituents on the terpy ligand, (3) the nature of the anion, and (4) the solvent used in recrystallization. Some examples of these effects follow.

The crystal structures of salts of the complex cation $[Pt(terpy)Cl]^+$ consist of chains of dimers, arranged in a head-to-tail orientation with short Pt···Pt distances (Fig. 32), stacked along one axis resulting in chains having longer Pt···Pt distances between dimers but nearly constant terpy···terpy inter-plane distances. Differences in the stacking arrangements for the $CF_3SO_3^-$ [44], ClO_4^- [45] and $[Pt(dmso)Cl_3]^-$ salts [27] are summarized in Table 5. The later salt also displays anion–cation interactions.

The importance of the anion is also illustrated by differences between $[Pt(terpy)(CH_2NO_2)]BPh_4$, which is a red solid

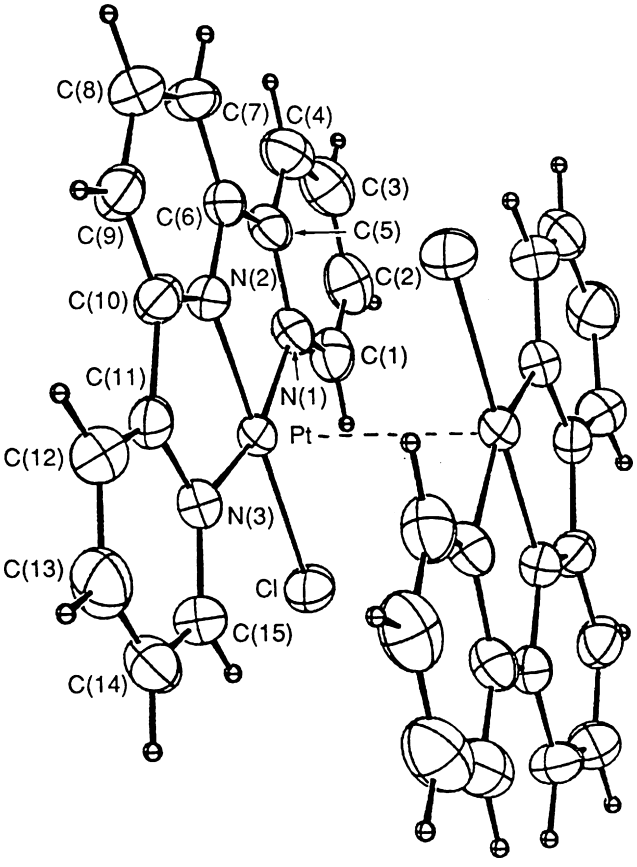

Fig. 32. The solid-state dimer structure for $[Pt(terpy)Cl][CF_3SO_3]$; from Ref. [44] (reproduced by permission of The Royal Society of Chemistry).

Table 5
X-ray crystallographic data for stacking between $[Pt(terpy)Cl]^+$ cations

Anion	Cl–Pt···Pt–Cl torsion angle (°)	$d_{Pt\cdots Pt}$ (intra-dimer) (Å)	$d_{Pt\cdots Pt}$ (inter-dimer) (Å)	terpy···terpy (Å)	$Pt^1\cdots Pt^2\cdots Pt^1$ angle (°)	Ref.
$CF_3SO_3^-$	180	3.329(1)	3.575(1)	~3.5	169	[44]
ClO_4^-	160	3.269(1)	4.197(1)	~3.4	143	[45]
$[Pt(dmso)Cl_3]^-$	180	3.338(1)	3.419(1)			[27]

having dimers stacked in head-to-tail orientation [61], and $[Pt(terpy)(CH_2NO_2)]BF_4$, which is a yellow solid having co-parallel dimers offset from each other [49].

Two types of stacking interactions were found in the crystal structure of $[Pt(terpy)(HET)](NO_3)$ (Fig. 33) [43]. Within the unit cell, complex cations stack in a head-to-tail fashion, with inter-plane separation of 3.43 Å and Pt···Pt distance of 3.5721 Å. Cations in adjacent unit cells display π–π stacking via partial overlap of the terpy ligands, with inter-plane separation of 3.42 Å but a longer Pt···Pt distance (>3.65 Å). In the crystal lattice, the cations pack in sheets (not columns) with Pt centers that are laterally displaced due to the influence of the HET "tail". Other examples of head-to-tail stacking of dimers are found for [Pt(terpy)(pyridine-2-thiol)]ClO_4 [50] and $[Pt(terpy)(C{\equiv}CPh)]PF_6$ [63].

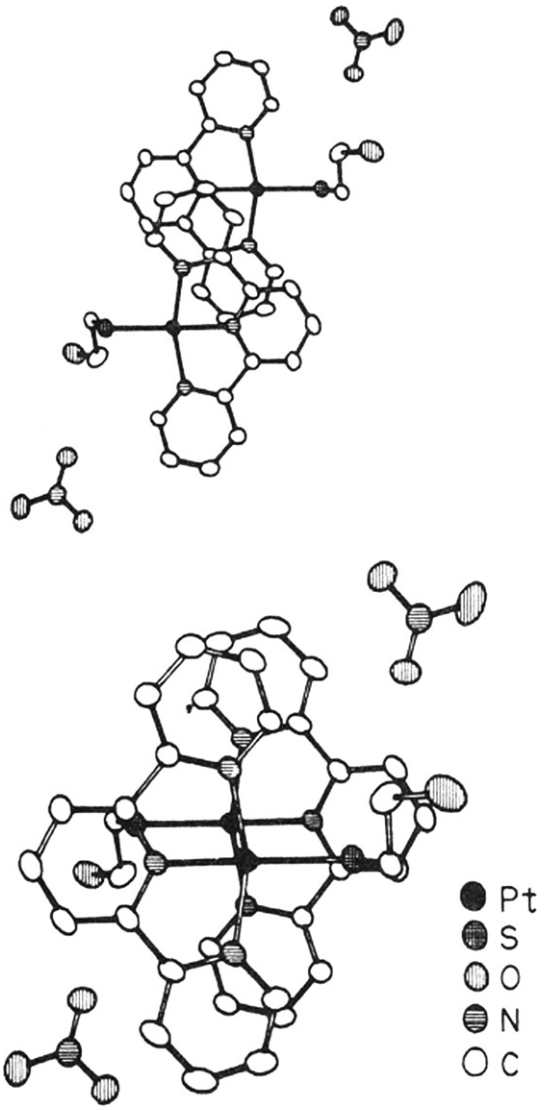

Fig. 33. Two different stacking interactions found for the crystal structure of $[Pt(terpy)(HET)](NO_3)$; from Ref. [43] (reproduced by permission of The American Chemical Society).

The sensitivity of solid-state packing to subtle changes in molecular structure is quite striking. Cations in crystals of [Pt(*o*-CH_3Ph-terpy)Cl]SbF_4 stack with evenly spaced (3.368 Å) Pt atoms in head-to-tail orientation, while in crystals of the BF_4^- salt the same cations display only π-stacking with uneven and larger Pt···Pt spacing (3.573 and 3.827 Å) [84]. Crystals of a related complex [Pt(*o*-CF_3Ph-terpy)Cl]SbF_4 displays head-to-tail cations with uneven and large Pt···Pt spacing (3.629 and 3.685 Å) [84], while that for [Pt(*o*-ClPh-terpy)Cl]SbF_4 displays close but uneven Pt···Pt spacing (3.374 and 3.513 Å) so as to be intermediate between dimers and extended linear chains [85]. In contrast, cations in $[Pt(Phterpy)Cl]BF_4{\cdot}CH_3CN$ stack in extended chains of tetramers, having π–π stacking and Pt···Pt interactions (3.303 Å) [83].

Stacking between complex cations of the type $[Pt(terpy)(SR)]^+$ displays an interesting sensitivity to the nature of the thiol ligand. When SR = pyridine-2-thiol, the cations stack in a standard head-to-tail fashion, but the cations exist as discreet monomers when SR = pyrimidine-2-thiol; in both cases the aromatic ring is perpendicular to the terpy plane [50].

Solid-state structures having long (>3.5 Å) Pt···Pt separation but close (<3.8 Å) terpy–terpy distances are considered to be π-stacked. Examples include $[Pt(terpy)(CH_3)]BH_4$ [60], $[Pt(Clterpy)\{SP(O)(OEt)_2\}]BPh_4$ [77], $[Pt(terpy)N_3](PF_6)$ [56], and $[Pt(terpy)(N_4CPh)](BF_4)$ [56]. Parallel head-to-head dimers of $[Pt(terpy)OPh(Me)_2\text{-}3,4]BF_4$ π-stack with close 3.3–3.4 Å interplane distance, but the out-of-plane phenoxide ligand causes adjacent cations to be offset so as to have long Pt···Pt distances (5.3 Å) [49]. For $[Pt(terpy)(MeIm)]^+$ cations, the out-of-plane coordination of the 1-methyimidazole (MeIm) ligand (66.5° torsion angle) results in only partial π-stacking of the terpy ligands, which are close (~3.5 Å) but offset to accommodate the MeIm ligand [58]. Two different types of π-stacking interactions in the solid state are observed for $[Pt(terpy)(MQ)](ClO_4)_3$ (MQ=*N*-methyl-4,4′-bipyridinium): stacks with 3.43(2) Å separation between terpy planes, and no Pt···Pt interaction (7.6 Å) (Fig. 34) [59].

In some cases, additional interactions can facilitate π-stacking in solids. For $[Pt(terpy)(McMT)]^+$ (where McMT = 2-mercapto-5-methyl-1,3,4-thiadiazolate), π-stacking is accompanied by H-bonding between DMcTH ligands [53], while H-bonding between the two thioamide ligands accompanies π-stacking between dimers in $[Pt(terpy)(DMcTH)](PF_6)$ [53]. Cations in [Pt{bis-hydroxyethyl(amino)-terpy}(4-picoline)]$(BF_4)_2$ are assembled via π-stacking as well as H-bonding between ethanolamine substituents [90]. In the solid state, $[Pt(terpy)(dpt)](ClO_4)$ units assemble into tetramers showing π-stacking both between the terpy rings and between terpy and the phenyl rings of the 1,3-diphenyl-2-triazeno (dpt) ligand [57].

Finally, some crystal structures involve discreet $[Pt(Yterpy)X]^{n+}$ cation monomers, without Pt···Pt or terpy···terpy stacking. Examples include $[Pt(terpy)(CH_3CN)](SbF_6)_2$ which contains parallel sheets of cations and anions [33], $[Pt(terpy)(thiourea)](ClO_4)_2$ [55], and $[Pt(4,7\text{-}Me_2php)Cl]BPh(CF_3)_2$ [86]. Cations in $[Pt(terpy)(Ph_2P\text{-}benzo\text{-}15\text{-}crown\text{-}5)](CF_3SO_3)_2$ [66] and $[Pt(terpy)(S\text{-}benzo\text{-}15\text{-}crown\text{-}5)]PF_6$ [54] do not stack due to large out-of-plane crown ether groups on the X ligands.

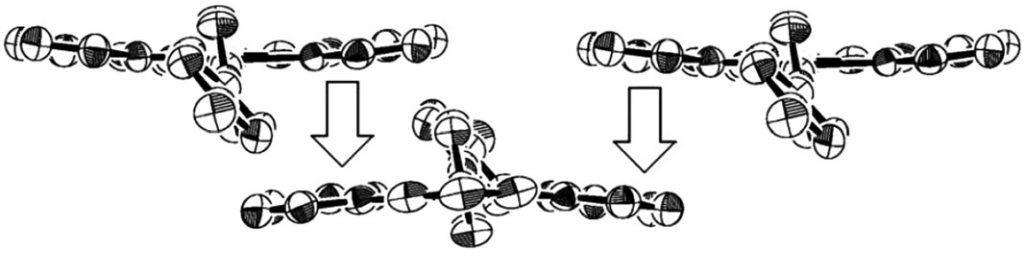

Fig. 34. Solid-state π-stacking for $[Pt(terpy)(MQ)]^{3+}$ cation; from Ref. [59] (reproduced by permission of The International Union of Crystallography).

In addition to ligand bulk, H-bonding with anions can stabilize non-stacked crystal structures. The cations of [Pt(terpy)(Hmcyt)] $[NO_3]_2{\cdot}5H_2O$ stack in columns with a head-to-head geometry, but having a separation of over 7.5 Å and assembled through hydrogen bonding interactions between nitrate, water and the methyl cytosine (Hmcyt) ligand [52] (Fig. 35) while [Pt(terpy)(cysteine)]$(ClO_4)_2{\cdot}0.5H_2O$ packs with a 3D network involving several H-bonding interactions between the amine group of the cysteine ligand and the ClO_4^- anion [51].

Likewise, bulky Y substituents of the terpy ligand can prevent stacking. For example, unlike the related terpy complex, the tri-^{t}butylterpyridine complexes of the type $[Pt(^tBu_3terpy)X]^+$ (R = Cl [81], C≡CC≡CH_3 [65], C≡CPhC≡CH [69], C≡CPhNCS-4 [70]) and the dinuclear complex $[Pt(^tBu_3terpy)(C{\equiv}C)_nPt(^tBu_3terpy)](CF_3SO_3)_2$ (n = 1, 2, 4) [88] display no stacking of cations, and yet cations of the related acetonyl complex $[Pt(^tBu_3terpy)CH_2C(O)Me]ClO_4{\cdot}C_2H_5OH$ are π-stacked with an inter-plane distance of 3.5 Å and a close Pt···Pt distance of 3.584 Å [81]. The azostilbene group in [Pt(PhN=NPh-terpy)py]$(BPh_4)_2$ results in large separation between cations and a Pt···Pt distance of 10.9 Å [34].

The structures of $[Pt(qtpy)](ClO_4)_2$ (qtpy = 2,2′:6′,2″:6″,2‴-quaterpyridine) and $[Pt(Me_4qtpy)](ClO_4)_2$ (Me_4qtpy = 3″,5,5′,5‴-tetramethyl-2,2′:6′,2″:6″,2‴-quaterpyridine) have a long Pt···Pt distance of 5.904 Å. While this is much longer than expected for Pt···Pt interactions, it is also shorter than the inter-plane separation in the crystal structure of uncoordinated qtpy, suggesting some inter-metallic interaction [95].

4.2.4. Dimorphism

Adding to the complexity of understanding how molecular structure affects solid-state packing is the observation of dimorphism for several Pt(II) terpy systems. The complex [Pt(terpy)Cl]Cl crystallizes in both red and yellow forms. Slow evaporation of a solution prepared by dissolving the red form in 1:1 H_2O–EtOH results in the formation of yellow crystals [176]. Repeatedly heating the red solid to 150 °C and cooling to RT also causes conversion to the yellow form, suggesting that the later is the more stable form. The two forms differ from each other only in the solid state. Gillard postulates that they are either dimorphs, having the same molecular structure but packing in different crystal lattices, or that the red form consists of twinning [176]. Occasionally, the solid is isolated as a brown solid, presumably a mixture of the red and yellow forms [151]. Red and yellow forms of the organometallic complex $[Pt(terpy)CH_3]Cl$ have been noted [30], and the diynyl complex $[Pt(terpy)(C{\equiv}CC{\equiv}CH)]CF_3SO_3$ crystallizes in two forms: as a green solid having a linear chain of evenly spaced Pt atoms separated by 3.388 Å, and as a red solid having dimers with short Pt···Pt separation of 3.394 Å and a 49.7° torsion angle which stack along an axis forming a zigzag Pt chain [65]. Significant Pt···Pt interactions are expected to red-shift the lowest-energy absorption band, so the red solids are anticipated to involve closer stacking than the yellow solids [44].

4.2.5. Solid-state bimolecular stacking interactions

As noted in Section 2.1, the reaction of terpy with certain platinum reagents produces insoluble products of the type $[Pt(terpy)Cl]_2[PtCl_4]$ and [Pt(terpy)Cl] $[Pt(dmso)Cl_3]$. Double-salt formation is certainly driven by highly favorable electrostatic interactions between cations and anion and possibly stabilized by Pt···Pt interactions, similar to those found for Magnus's salt $[Pt(NH_3)_4]_2[PtCl_4]$.

The crystal structure of a 2:2 intercalation complex, formed upon mixing $[Pt(terpy)Cl]^+$ and adenosine-5′-monophosphate (AMP), was the first structure of "parent" chloro complex characterized

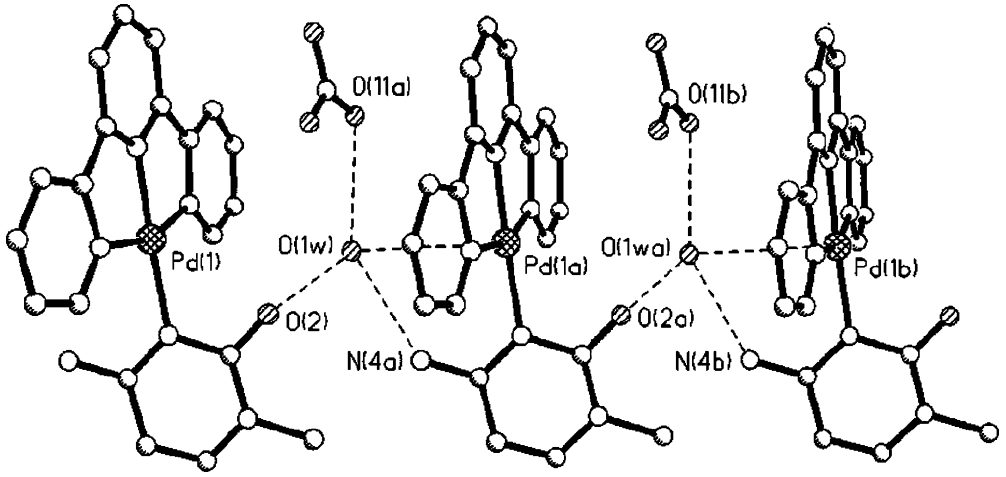

Fig. 35. Hydrogen bonding interactions control solid-state stacking of $[Pt(terpy)(Hmcyt)][NO_3]_2{\cdot}5H_2O$; from Ref. [52] (reproduced by permission of The Royal Society of Chemistry).

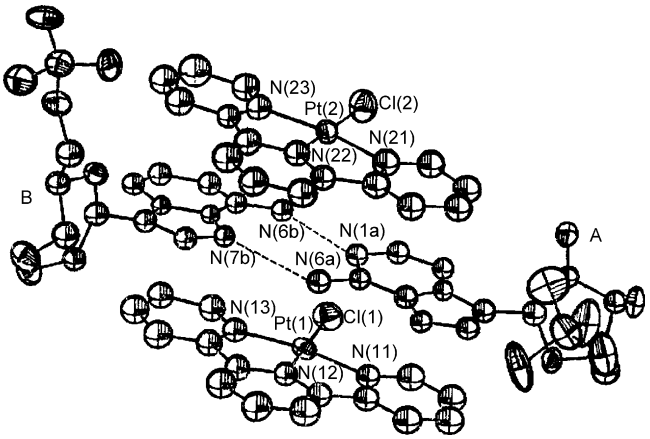

Fig. 36. Crystal structure of the 2:2 [Pt(terpy)Cl]$^+$–AMP intercalation complex, omitting the water molecules in the lattice and showing hydrogen bonding. Translation of this unit in the vertical direction produces additional head-to-head stacking of the [Pt(terpy)Cl]$^+$ species; from Ref. [46] (reproduced by permission of The Royal Society of Chemistry).

(Fig. 36) [46]. Although stacking in the unit cell is certainly influenced by the AMP pair, it is interesting to note that the [Pt(terpy)Cl]$^+$ units orient in a head-to-head arrangement with overlapping terpy ligands.

The crystal structure for a 2:2 complex formed between [Pt(terpy)(HET)]$^+$ and the base-paired DNA fragment deoxycytidyl-(3′,5′)-deoxyguanosine (dCpG) reveals both intercalation of [Pt(terpy)(HET)]$^+$ between base-pairs and π-stacking of [Pt(terpy)(HET)]$^+$ on each ends of the base pairs [177]. The authors postulate that stability of this intercalation complex results from π-interactions between the central pyridyl group of the terpy and bases pairs, interaction between the O atoms of guanines and the Pt center, and H-bonding between the HET ligand "tail" and a cytosine O atom.

Tzeng et al. have reported that when [Pt(terpy)Cl]$^+$ reacts with 1 equiv. of 8-quinolinethiolate (8-QNS) in CH_2Cl_2/MeOH an unusual rearrangement occurs to produce [Pt(QNS)$_2$] [Pt(terpy)Cl]$_2{}^{2+}$, which crystallizes in stacked "sandwich" chains of [Pt(terpy)Cl]$^+$ cation pairs with an intercalated neutral [Pt(QNS)$_2$] unit [47]. The [Pt(terpy)Cl]$^+$ pairs stack in head-to-tail orientation, suggesting minimal terpy–terpy π–π interaction, but with short Pt···Pt distances (3.353 Å) indicating substantial d-orbital interaction (Fig. 37). The intercalated [Pt(QNS)$_2$] complex appears to interact with adjacent [Pt(terpy)Cl]$^+$ units by Pt–S interactions and terpy–QNS π–π interaction.

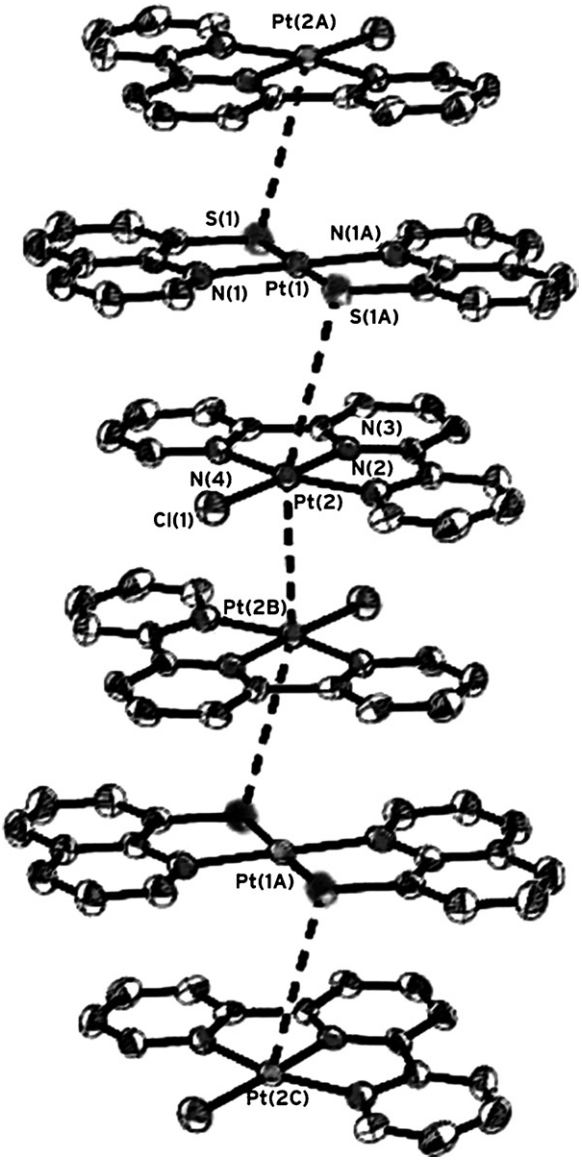

Fig. 37. Solid-state "sandwich" structure [Pt(QNS)$_2$][Pt(terpy)Cl]$_2{}^{2+}$; from Ref. [47].

5. Characterization

5.1. ^{1}H, ^{13}C, ^{195}Pt NMR spectroscopy

Reports by Lippard and co-workers on [Pt(terpy)SR]$^+$ complexes [43] and by Romeo and co-workers on [Pt(terpy)Me]$^+$ [30,171] note that ^{1}H NMR chemical shifts are dependent on solvent, ionic strength, solute concentration and temperature, typically moving upfield with increasing concentration and lower T due to staking in solution [176]. Therefore, consideration of these conditions should accompany comparisons of chemical shift values.

For [Pt(terpy)X]$^+$ complex cations having symmetric X ligands, six ^{1}H resonances typically lie between 7.8 and 9.0 ppm as three doublets and three multiplets, though not all are resolved. The chemical shift of the terpy H$^{6,6''}$ resonance moves downfield upon coordination to platinum and is particularly sensitive to the nature of the X ligand. For example, a large downfield shift of H$^{6,6''}$ resonance is observed upon displacement of chloride by nitrogen [178] and thiolate [179] donors. Asymmetric X ligands may make H^6 and H$^{6''}$ inequivalent enough to observe two resonances. Even between complexes having ligands having the same donor atoms in the fourth coordination site, more subtle differences in the nature or conformation of the X ligand can be elucidated from the H$^{6,6''}$ chemical shift. For example, N^2-bound and N^1-bound isomers of [Pt(terpy)(N$_4$CMe)]$^+$ display large difference due differences in coordination geometry of tetrazole ligand [56]. For the N^2-bound (major) isomer, for which the tetrazole ligand is co-planar with the terpy ligand, the H^6 resonance is found at δ 9.96 ppm; while for the N^1-bound (minor) isomer steric effects cause the tetrazole to coordinate perpendicular to the terpy plane and ring current shielding of the H^6 proton results in a chemical shift of δ 7.74 ppm. Browlee, Rook and co-workers published a full study on the effects of substituents on the thiol ligand of [Pt(terpy)(SPh)]$^+$ complex cations have on ^{13}C and ^{195}Pt NMR spectra [180].

The spin-active (I = 1/2) ^{195}Pt isotope, present in 33.8% natural abundance, can result in ^{195}Pt satellites for the terpy H$^{6,6''}$ resonance and provide useful characterization of terpy coordi-

nation to the Pt ion [31,43,56,81,130,174,181]. Systems for which these satellites are resolved show coupling constants ranging from J_{Pt-H} = 35 Hz for $[Pt(terpy)Cl]^+$ [31] to J_{Pt-H} = 56 Hz for $[Pt(terpy)(pip_2NCN)]^+$ [62]. ^{195}Pt satellites have also been observed for resonances corresponding to protons on the X ligand, such as the α protons of coordinated picoline [127]. The ^{1}H NMR spectrum of the dinuclear complex cation $[\{(terpy)Pt\}_2SMe]^{3+}$ displays a unique 1:8:18:18:8:1 coupling pattern due to methyl protons coupled to two ^{195}Pt centers [124].

^{195}Pt NMR spectroscopy has been conducted on some systems [131,180], with ^{195}Pt chemical shifts found between −2500 and −3200 ppm [38,52,56,130,142] relative to $K_2[PtCl_4]$ in D_2O. The ^{195}Pt chemical shift is sensitive to the nature of the X ligand, shifting from −2694 to −3150 ppm upon displacement of X = Cl^- by a thiolate ligand [141] and shifting ∼70 ppm upfield upon displacement by nitrogen donor, but not changing significantly among guanidine vs. imidazole ligands [178].

5.2. Infrared spectroscopy

Ring mode vibrations of the terpy ligand are affected by coordination to Pt(II), corresponding to shift in energy for bands in the 1100–1600 cm^{-1} region of IR spectra [23]. In IR spectra of $[Pt(terpy)X]^{n+}$ complexes, these bands are also slightly sensitive to the nature of the X ligand [67]. In addition, a band near 520 cm^{-1} due to the N^1–Pt–N^3 asymmetric stretch and another near 460 cm^{-1} due to the Pt–N^2 stretch have been reported [23,26,176]. Bands corresponding to a Pt–Cl stretch (∼345 cm^{-1}) [23,26,176] and Pt–S stretch (∼355 cm^{-1}) [43,182] have also been assigned.

5.3. Electrospray ionization mass spectrometry

Electrospray ionization of a dilute solution of [Pt(terpy)Cl]Cl(aq) results in the formation of several ions, including $[Pt(terpy)Cl]^+$ (base peak), $[Pt(terpy)(OH)]^+$, $[Pt(terpy)(OH_2)]^+$ and a number of other minor ions, possibly including $[Pt(terpy)N_2]^{2+}$ [183].

6. Conclusions

An explosion of interest in platinum terpyridine complexes has produced a large and growing family of coordination compounds with interesting properties and a wide range of potential applications. Fertile research in this burgeoning field has revealed versatile methods of preparation, and characterized important details of complex structure and bonding. Investigations of the thermodynamics and kinetics of ligand-substitution reactions and the factors affecting stacking in the solid state and in solution can inform and guide studies to employ platinum terpyridine complexes as probes of biomolecular structure and activity or as luminescent and redox-active materials.

References

[1] A. Juris, V. Balzani, F. Barigelletti, S. Campagna, P. Belser, A. Vonzelewsky, Coordin. Chem. Rev. 84 (1988) 85.
[2] E. Coronado, J.R. Galan-Mascaros, C. Marti-Gastaldo, E. Palomares, J.R. Durrant, R. Vilar, M. Gratzel, M.K. Nazeeruddin, J. Am. Chem. Soc. 127 (2005) 12351.
[3] B.J. Coe, T.J. Meyer, P.S. White, Inorg. Chem. 32 (1993) 4012.
[4] R. Langen, I.J. Chang, J.P. Germanas, J.H. Richards, J.R. Winkler, H.B. Gray, Science 268 (1995) 1733.
[5] J. Limburg, J.S. Vrettos, L.M. Liable-Sands, A.L. Rheingold, R.H. Crabtree, G.W. Brudvig, Science 283 (1999) 1524.
[6] Y. Chen, Q.L. Fan, P. Wang, B. Zhang, Y.Q. Huang, G.W. Zhang, X.M. Lu, H.S.O. Chan, W. Huang, Polymer 47 (2006) 5228.
[7] G. Dimarco, M. Lanza, S. Campagna, Adv. Mater. 7 (1995) 468.
[8] Photosensitization and Photocatalysis Using Inorganic and Organometallic Compounds, Kluwer Academic Publishers, Dordrecht, Boston, 1993.
[9] M.K. Nazeeruddin, P. Pechy, T. Renouard, S.M. Zakeeruddin, R. Humphry-Baker, P. Comte, P. Liska, L. Cevey, E. Costa, V. Shklover, L. Spiccia, G.B. Deacon, C.A. Bignozzi, M. Gratzel, J. Am. Chem. Soc. 123 (2001) 1613.
[10] S. Flores-Torres, G.R. Hutchison, L.J. Soltzberg, H.D. Abruna, J. Am. Chem. Soc. 128 (2006) 1513.
[11] A. Harriman, R. Ziessel, Chem. Commun. (1996) 1707.
[12] E.C. Constable, Prog. Inorg. Chem. 42 (1994).
[13] G.R. Newkome, P.S. Wang, C.N. Moorefield, T.J. Cho, P.P. Mohapatra, S.N. Li, S.H. Hwang, O. Lukoyanova, L. Echegoyen, J.A. Palagallo, V. Iancu, S.W. Hla, Science 312 (2006) 1782.
[14] U.S. Schubert, H. Hofmeier, G.R. Newkome, Modern Terpyridine Chemistry, Wiley-VCH, Weinheim, 2006.
[15] G.T. Morgan, F.H. Burstall, J. Chem. Soc. (1934) 1498.
[16] E.C. Constable, Adv. Inorg. Chem. 30 (1986) 69.
[17] W. Sliwa, M. Deska, Collect. Czech. Chem. Commun. 64 (1999) 435.
[18] D.M. Lawson, Acta Crystallogr. Sect. D: Biol. Cryst. 50 (1994) 332.
[19] N.M. Kostic, Comments Inorg. Chem. 8 (1988) 137.
[20] S.J. Lippard, Acc. Chem. Res. 11 (1978) 211.
[21] D.R. McMillin, J.J. Moore, Coordin. Chem. Rev. 229 (2002) 113.
[22] M. Howe-Grant, S.J. Lippard, in: D.E. Busch (Ed.), Inorg. Synth. 20 (1980).
[23] R.J. Mureinik, M. Bidani, Inorg. Nucl. Chem. Lett. 13 (1977) 625.
[24] D.R. Baghurst, S.R. Cooper, D.L. Greene, D.M.P. Mingos, S.M. Reynolds, Polyhedron 9 (1990) 893.
[25] F.T. Esmadi, M.K. Dohaidel, Indian J. Chem. Sect. A: Inorg. Bio-Inorg. Phys. Theor. Anal. Chem. 33 (1994) 875.
[26] G. Annibale, M. Brandolisio, B. Pitteri, Polyhedron 14 (1995) 451.
[27] R. Cini, A. Donati, R. Giannettoni, Inorg. Chim. Acta 315 (2001) 73.
[28] S. Chakraborty, T.J. Wadas, H. Hester, C. Flaschenreim, R. Schmehl, R. Eisenberg, Inorg. Chem. 44 (2005) 6284.
[29] G. Lowe, T. Vilaivan, J. Chem. Res. Synop. (1996) 386.
[30] G. Arena, L.M. Scolaro, R.F. Pasternack, R. Romeo, Inorg. Chem. 34 (1995) 2994.
[31] G. Arena, G. Calogero, S. Campagna, L.M. Scolaro, V. Ricevuto, R. Romeo, Inorg. Chem. 37 (1998) 2763.
[32] A. Doppiu, G. Minghetti, M.A. Cinellu, S. Stoccoro, A. Zucca, M. Manassero, Organometallics 20 (2001) 1148.
[33] R. Buchner, J.S. Field, R.J. Haines, C.T. Cunningham, D.R. McMillin, Inorg. Chem. 36 (1997) 3952.
[34] T. Yutaka, I. Mori, M. Kurihara, J. Mizutani, N. Tamai, T. Kawai, M. Irie, H. Nishihara, Inorg. Chem. 41 (2002) 7143.
[35] G. Annibale, B. Pitteri, M.H. Wilson, D. McMillin, in: J.R. Shapley (Ed.), Inorg. Synth. 34 (2004).
[36] S.A. Ross, C.A. Carr, J.W. Briet, G. Lowe, Anti-Cancer Drug Design 15 (2000) 431.
[37] J.D. Crowley, I.M. Steele, B. Bosnich, Eur. J. Inorg. Chem. (2005) 3907.
[38] A.J. Goshe, I.M. Steele, B. Bosnich, J. Am. Chem. Soc. 125 (2003) 444.
[39] S.K. Thomson, G.B. Young, Polyhedron 7 (1988) 1953.
[40] K.G. Strothkamp, S.J. Lippard, Proc. Natl. Acad. Sci. U.S.A. 73 (1976) 2536.
[41] M.G. Hill, M.J. Irwin, C.J. Levy, L.M. Rendina, R.J. Puddephatt, in: M.Y. Darensbourg (Ed.), Inorg. Synth. 32 (1998).
[42] C.A. Bessel, R.F. See, D.L. Jameson, M.R. Churchill, K.J. Takeuchi, J. Chem. Soc., Dalton Trans. (1992) 3223.
[43] K.W. Jennette, J.T. Gill, J.A. Sadownick, S.J. Lippard, J. Am. Chem. Soc. 98 (1976) 6159.
[44] H.K. Yip, L.K. Cheng, K.K. Cheung, C.M. Che, J. Chem. Soc., Dalton Trans. (1993) 2933.
[45] J.A. Bailey, M.G. Hill, R.E. Marsh, V.M. Miskowski, W.P. Schaefer, H.B. Gray, Inorg. Chem. 34 (1995) 4591.
[46] Y. Wong, S.J. Lippard, J. Chem. Soc., Chem. Commun. (1977) 824.
[47] B.C. Tzeng, G.H. Lee, S.M. Peng, Inorg. Chem. Commun. 6 (2003) 1341.
[48] T.K. Aldridge, E.M. Stacy, D.R. McMillin, Inorg. Chem. 33 (1994) 722.
[49] X.M. Liu, S.L. Renard, C.A. Kilner, M.A. Halcrow, Inorg. Chem. Commun. 6 (2003) 598.
[50] B.C. Tzeng, W.F. Fu, C.M. Che, H.Y. Chao, K.K. Cheung, S.M. Peng, J. Chem. Soc., Dalton Trans. (1999) 1017.
[51] Z.D. Bugarcic, F.W. Heinemann, R. van Eldik, Dalton Trans. (2004) 279.
[52] S. Cosar, M.B.L. Janik, M. Flock, E. Freisinger, E. Farkas, B. Lippert, J. Chem. Soc., Dalton Trans. (1999) 2329.
[53] H. Tannai, K. Tsuge, Y. Sasaki, O. Hatozaki, N. Oyama, Dalton Trans. (2003) 2353.
[54] V.W.W. Yam, R.P.L. Tang, K.M.C. Wong, C.C. Ko, K.K. Cheung, Inorg. Chem. 40 (2001) 571.
[55] Z.D. Bugarcic, G. Liehr, R. van Eldik, J. Chem. Soc., Dalton Trans. (2002) 2825.
[56] S. Wee, M.J. Grannas, W.D. McFadyen, R.A.J. O'Hair, Aust. J. Chem. 54 (2001) 245.
[57] J.A. Bailey, V.J. Catalano, H.B. Gray, Acta Crystallogr. Sect. C: Cryst. Struct. Commun. 49 (1993) 1598.
[58] A.W. Roszak, O. Clement, E. Buncel, Acta Crystallogr. Sect. C: Cryst. Struct. Commun. 52 (1996) 1645.
[59] K. Sakai, M. Kurashima, M. Osada, S. Takahashi, Acta Crystallogr. Sect. A: Struct. Rep. Online 59 (2003) M515.
[60] R. Romeo, L.M. Scolaro, M.R. Plutino, A. Albinati, J. Organomet. Chem. 594 (2000) 403.
[61] M. Akiba, Y. Sasaki, Inorg. Chem. Commun. 1 (1998) 61.
[62] H. Jude, J.A.K. Bauer, W.B. Connick, J. Am. Chem. Soc. 125 (2003) 3446.
[63] V.W.W. Yam, R.P.L. Tang, K.M.C. Wong, K.K. Cheung, Organometallics 20 (2001) 4476.

[64] V.W.W. Yam, K.H.Y. Chan, K.M.C. Wong, N.Y. Zhu, Chem. Eur. J. 11 (2005) 4535.
[65] V.W.W. Yam, K.M.C. Wong, N.Y. Zhu, J. Am. Chem. Soc. 124 (2002) 6506.
[66] V.W.W. Yam, R.P.L. Tang, K.M.C. Wong, X.X. Lu, K.K. Cheung, N.Y. Zhu, Chem. Eur. J. 8 (2002) 4066.
[67] E.M.A. Ratilla, B.K. Scott, M.S. Moxness, N.M. Kostic, Inorg. Chem. 29 (1990) 918.
[68] K.M.C. Wong, W.S. Tang, X.X. Lu, N.Y. Zhu, V.W.W. Yam, Inorg. Chem. 44 (2005) 1492.
[69] C.H. Tao, K.M.C. Wong, N.Y. Zhu, V.W.W. Yam, New J. Chem. 27 (2003) 150.
[70] K.M.C. Wong, W.S. Tang, B.W.K. Chu, N.Y. Zhu, V.W.W. Yam, Organometallics 23 (2004) 3459.
[71] V.W.-W. Yam, C.-K. Hui, S.-Y. Yu, N. Zhu, Inorg. Chem. 43 (2004) 812.
[72] C.K. Hui, B.W.K. Chu, N.Y. Zhu, V.W.W. Yam, Inorg. Chem. 41 (2002) 6178.
[73] M. Heller, U.S. Schubert, Eur. J. Org. Chem. (2003) 947.
[74] A. Thompson, Coordin. Chem. Rev. 160 (1997) 1.
[75] S.E. Hobert, J.T. Carney, S.D. Cummings, Inorg. Chim. Acta 318 (2001) 89.
[76] S. Bonse, J.M. Richards, S.A. Ross, G. Lowe, R.L. Krauth-Siegel, J. Med. Chem. 43 (2000) 4812.
[77] S.A. Ross, G. Lowe, D.J. Watkin, Acta Crystallogr. Sect. C: Cryst. Struct. Commun. 57 (2001) 275.
[78] C.A. Carr, J.M. Richards, S.A. Ross, G. Lowe, J. Chem. Res. Synop. (2000) 566.
[79] J.F. Michalec, S.A. Bejune, D.G. Cuttell, G.C. Summerton, J.A. Gertenbach, J.S. Field, R.J. Haines, D.R. McMillin, Inorg. Chem. 40 (2001) 2193.
[80] D. Sielemann, A. Winter, U. Floerke, N. Risch, Org. Biomol. Chem. 2 (2004) 863.
[81] S.W. Lai, M.C.W. Chan, K.K. Cheung, C.M. Che, Inorg. Chem. 38 (1999) 4262.
[82] X.M. Liu, E.J.L. McInnes, C.A. Kilner, M. Thornton-Pett, M.A. Halcrow, Polyhedron 20 (2001) 2889.
[83] R. Buchner, C.T. Cunningham, J.S. Field, R.J. Haines, D.R. McMillin, G.C. Summerton, J. Chem. Soc., Dalton Trans. (1999) 711.
[84] J.S. Field, R.J. Haines, D.R. McMillin, G.C. Summerton, Dalton Trans. (2002) 1369.
[85] J.S. Field, J.A. Gertenbach, R.J. Haines, L.P. Ledwaba, N.T. Mashapa, D.R. McMillin, O.Q. Munro, G.C. Summerton, Dalton Trans. (2003) 1176.
[86] J.J. Moore, J.J. Nash, P.E. Fanwick, D.R. McMillin, Inorg. Chem. 41 (2002) 6387.
[87] R. Okamura, T. Wada, K. Aikawa, T. Nagata, K. Tanaka, Inorg. Chem. 43 (2004) 7210.
[88] V.W.W. Yam, K.M.C. Wong, N.Y. Zhu, Angew. Chem. Int. Ed. Engl. 42 (2003) 1400.
[89] S.C.F. Lam, V.W.W. Yam, K.M.C. Wong, E.C.C. Cheng, N.Y. Zhu, Organometallics 24 (2005) 4298.
[90] A. Chernega, A.S. Droz, K. Prout, T. Vilaivan, G.W. Weaver, G. Lowe, J. Chem. Res. Synop. (1996) 402.
[91] Y.Z. Hu, M.H. Wilson, R.F. Zong, C. Bonnefous, D.R. McMillin, R.P. Thummel, Dalton Trans. (2005) 354.
[92] G.T. Morgan, F.H. Burstall, J. Chem. Soc. (1938) 1672.
[93] H.C. Lip, R.A. Plowman, Aust. J. Chem. 28 (1975) 893.
[94] E.C. Constable, S.M. Elder, M.J. Hannon, A. Martin, P.R. Raithby, D.A. Tocher, J. Chem. Soc., Dalton Trans. (1996) 2423.
[95] C.-W. Chan, C.-M. Che, M.-C. Cheng, Y. Wang, Inorg. Chem. 31 (1992) 4874.
[96] A. von Zelewsky, Coordin. Chem. Rev. 192 (1999) 811.
[97] H.C. Clark, L.E. Manzer, Inorg. Chem. 11 (1972) 2749.
[98] E.W. Ainscough, A.M. Brodie, A.K. Burrell, A. Derwahl, G.B. Jameson, S.K. Taylor, Polyhedron 23 (2004) 1159.
[99] E.W. Abel, N.J. Long, K.G. Orrell, A.G. Osborne, H.M. Pain, V. Sik, J. Chem. Soc., Chem. Commun. (1992) 303.
[100] E.W. Abel, V.S. Dimitrov, N.J. Long, K.G. Orrell, A.G. Osborne, V. Sik, M.B. Hursthouse, M.A. Mazid, J. Chem. Soc., Dalton Trans. (1993) 291.
[101] E.W. Abel, K.G. Orrell, A.G. Osborne, H.M. Pain, V. Sik, M.B. Hursthouse, K.M.A. Malik, J. Chem. Soc., Dalton Trans. (1994) 3441.
[102] R. Romeo, M.R. Plutino, L.M. Scolaro, S. Stoccoro, G. Minghetti, Inorg. Chem. 39 (2000) 4749.
[103] E. Rotondo, G. Giordano, D. Minniti, J. Chem. Soc., Dalton Trans. (1996) 253.
[104] E.W. Abel, K.G. Orrell, A.G. Osborne, H.M. Pain, V. Sik, M.B. Hursthouse, K.M.A. Malik, J. Chem. Soc., Dalton Trans. (1996) 253.
[105] E.W. Abel, A. Gelling, K.G. Orrell, A.G. Osborne, V. Sik, Chem. Commun. (1996) 2329.
[106] A. Gelling, K.G. Orrell, A.G. Osborne, V. Sik, J. Chem. Soc., Dalton Trans. (1998) 937.
[107] A. Gelling, M.D. Olsen, K.G. Orrell, A.G. Osborne, V. Sik, J. Chem. Soc., Dalton Trans. (1998) 3479.
[108] A. Gelling, K.G. Orrell, A.G. Osborne, V. Sik, Polyhedron 18 (1999) 1285.
[109] M. Hissler, R. Ziessel, J. Chem. Soc., Dalton Trans. (1995) 893.
[110] M.S. Khan, M.R.A. Al-Mandhary, M.K. Al-Suti, A.K. Hisahm, P.R. Raithby, B. Ahrens, M.F. Mahon, L. Male, E.A. Marseglia, E. Tedesco, R.H. Friend, A. Kohler, N. Feeder, S.J. Teat, J. Chem. Soc., Dalton Trans. (2002) 1358.
[111] E.C. Constable, C.E. Housecroft, M. Neuburger, A.G. Schneider, B. Springler, M. Zehnder, Inorg. Chim. Acta 300 (2000) 49.
[112] B. Pitteri, G. Marangoni, L. Cattalini, T. Bobbo, J. Chem. Soc., Dalton Trans. (1995) 3853.
[113] F. Basolo, H.B. Gray, R.G. Pearson, J. Am. Chem. Soc. 82 (1960) 4200.
[114] R.J. Mureinik, M. Bidani, Inorg. Chim. Acta 29 (1978) 37.
[115] B.V. Petrovic, M.I. Djuran, Z.D. Bugarcic, Metal-Based Drugs 6 (1999) 355.
[116] G. Annibale, M. Brandolisio, Z. Bugarcic, L. Cattalini, Transit. Met. Chem. 23 (1998) 715.
[117] G. Annibale, L. Cattalini, A. Cornia, A. Fabretti, F. Guidi, Inorg. React. Mech. 2 (2000) 185.
[118] T. Abe, K. Hirano, Y. Shiraishi, N. Toshima, M. Kaneko, Eur. Polym. J. 37 (2001) 753.
[119] C. Diver, G.A. Lawrance, J. Chem. Soc., Dalton Trans. (1988) 931.
[120] S.L. Pinnow, H.M. Brothers, N.M. Kostic, Croat. Chem. Acta 64 (1991) 519.
[121] Z.D. Bugarcic, B.V. Djordjevic, M.I. Djuran, J. Serb. Chem. Soc. 62 (1997) 1031.
[122] C.C. Cheng, Y.L. Lu, Chem. Commun. (1998) 253.
[123] A.K. Fazlur-Rahman, J.G. Verkade, Inorg. Chem. 31 (1992) 2064.
[124] G. Annibale, P. Bergamini, V. Bertolasi, M. Cattabriga, A. Lazzaro, A. Marchi, G. Vertuani, J. Chem. Soc., Dalton Trans. (1999) 3877.
[125] W.D. McFadyen, L.P. Wakelin, I.A. Roos, V.A. Leopold, J. Med. Chem. 28 (1985) 1113.
[126] B. Pitteri, G. Marangoni, F.V. Viseutim, L. Cattalini, T. Bobbo, Polyhedron 17 (1998) 475.
[127] A. McCoubrey, H.C. Latham, P.R. Cook, A. Rodger, G. Lowe, FEBS Lett. 380 (1996) 73.
[128] Q.Z. Yang, L.Z. Wu, Z.X. Wu, L.P. Zhang, C.H. Tung, Inorg. Chem. 41 (2002) 5653.
[129] F.Q. Guo, W.F. Sun, Y. Liu, K. Schanze, Inorg. Chem. 44 (2005) 4055.
[130] J.A. Todd, L.M. Rendina, Inorg. Chem. 41 (2002) 3331.
[131] J.A. Todd, P. Turner, E.J. Ziolkowski, L.M. Rendina, Inorg. Chem. 44 (2005) 6401.
[132] G. Annibale, G. Marangoni, B. Pitteri, F. Visentin, T. Bobbo, Transit. Met. Chem. 25 (2000) 485.
[133] G. Lowe, A.S. Droz, T. Vilaivan, G.W. Weaver, L. Tweedale, J.M. Pratt, P. Rock, V. Yardley, S.L. Croft, J. Med. Chem. 42 (1999) 999.
[134] A. Hofmann, D. Jaganyi, O.Q. Munro, G. Liehr, R. van Eldik, Inorg. Chem. 42 (2003) 1688.
[135] D. Jaganyi, A. Hofmann, R. van Eldik, Angew. Chem. Int. Ed. Engl. 40 (2001) 1680.
[136] C.S. Peyratout, T.K. Aldridge, D.K. Crites, D.R. McMillin, Inorg. Chem. 34 (1995) 4484.
[137] M. Cusumano, M.L. Di Pietro, A. Giannetto, Inorg. Chem. 38 (1999) 1754.
[138] M. Cusumano, M.L. Di Pietro, A. Giannetto, F. Romano, Inorg. Chem. 39 (2000) 50.
[139] G. Lowe, T. Vilaivan, J. Chem. Soc., Perkin Trans. 1 (1996) 1499.
[140] G. Lowe, A.S. Droz, J.J. Park, G.W. Weaver, Bioorg. Chem. 27 (1999) 477.
[141] E.L. Crossley, D. Caiazza, L.M. Rendina, Dalton Trans. (2005) 2825.
[142] S.L. Woodhouse, E.J. Ziolkowski, L.M. Rendina, Dalton Trans. (2005) 2827.
[143] H.M. Brothers, N.M. Kostic, Inorg. Chem. 27 (1988) 1761.
[144] C.F. Weber, R. van Eldik, Eur. J. Inorg. Chem. (2005) 4755.
[145] D. Jaganyi, D. Reddy, J.A. Gertenbach, A. Hofmann, R. van Eldik, Dalton Trans. (2004) 299.
[146] D. Jaganyi, F. Tiba, Transit. Met. Chem. 28 (2003) 803.
[147] B. Pitteri, G. Marangoni, L. Cattalini, F. Visentin, V. Bertolasi, P. Gilli, Polyhedron 20 (2001) 869.
[148] A. Hofmann, L. Dahlenburg, R. van Eldik, Inorg. Chem. 42 (2003) 6528.
[149] J.M. Richards, Oxford University, 2000.
[150] M.H. Wilson, L.P. Ledwaba, J.S. Field, D.R. McMillin, Dalton Trans. (2005) 2754.
[151] A.M.F. Gameiro, R.D. Gillard, N.H. Rees, J. Schulte, A. Sengul, Croat. Chem. Acta 74 (2001) 641.
[152] G. Lowe, J.A. McCloskey, J.S. Ni, T. Vilaivan, Bioorg. Med. Chem. 4 (1996) 1007.
[153] G. Lowe, S.A. Ross, M. Probert, A. Cowley, Chem. Commun. (2001) 1288.
[154] J.A. Bailey, H.B. Gray, Acta Crystallogr. Sect. C: Cryst. Struct. Commun. 48 (1992) 1420.
[155] J.A. Bailey, V.M. Miskowski, H.B. Gray, Acta Crystallogr. Sect. C: Cryst. Struct. Commun. 49 (1993) 793.
[156] J.A. Bailey, V.M. Miskowski, H.B. Gray, Inorg. Chem. 32 (1993) 369.
[157] M. Kato, A. Toshikawa, S. Kishi, Acta Crystallogr. Sect. A: Struct. Rep. Online 58 (2002) M248.
[158] H.K. Yip, C.M. Che, Z.Y. Zhou, T.C.W. Mak, J. Chem. Soc., Chem. Commun. (1992) 1369.
[159] M. Akiba, K. Umakoshi, Y. Sasaki, Chem. Lett. (1995) 607.
[160] K. Becker, C. Herold-Mende, J.J. Park, G. Lowe, R.H. Schirmer, J. Med. Chem. 44 (2001) 2784.
[161] J.C. Dewan, S.J. Lippard, W.R. Bauer, J. Am. Chem. Soc. 102 (1980) 858.
[162] A.H.J. Wang, G.J. Quigley, F.J. Koipak, A. Rich, Abstr. Am. Crystallogr. Assoc. 6 (1979) 50.
[163] P.B. Glover, P.R. Ashton, L.J. Childs, A. Rodger, M. Kercher, R.M. Williams, L. De Cola, Z. Pikramenou, J. Am. Chem. Soc. 125 (2003) 9918.
[164] M.C. DeRosa, F. Al-mutlaq, R. Crutchley, J. Inorg. Chem. 40 (2001) 1406.
[165] W.D. McFadyen, L.P.G. Wakelin, I.A.G. Roos, B.L. Hillcoat, Biochem. J. 238 (1986) 757.
[166] A.M. Bray, D.P. Kelly, P.O.L. Mack, R.F. Martin, L.P.G. Wakelin, Aust. J. Chem. 43 (1990) 629.
[167] D. Sielemann, A. Winter, N. Risch, Heterocycles 65 (2005) 1663.
[168] M.G. Hill, J.A. Bailey, V.M. Miskowski, H.B. Gray, Inorg. Chem. 35 (1996) 4585.
[169] L.P.G. Wakelin, W.D. McFadyen, A. Walpole, I.A.G. Roos, Biochem. J. 222 (1984) 203.
[170] W.D. McFadyen, L.P.G. Wakelin, I.A.G. Roos, B.L. Hillcoat, Biochem. J. 242 (1987) 177.
[171] R. Romeo, G. Arena, L.M. Scolaro, R.F. Pasternack, Nuovo Cimento Della Societa Italiana Di Fisica D-Condens. Matter Atomic Mol. Chem. Phys. Fluids Plasmas Biophys. 16 (1994) 1523.
[172] M. Casamento, G.E. Arena, C. Lo Passo, I. Pernice, A. Romeo, L.M. Scolaro, Inorg. Chim. Acta 276 (1998) 242.

[173] C. Yu, K.M.C. Wong, K.H.Y. Chan, V.W.W. Yam, Angew. Chem. Int. Ed. Engl. 44 (2005) 791.
[174] H. Kurosaki, N. Yamakawa, M. Sumimoto, K. Kimura, M. Goto, Bioorg. Med. Chem. Lett. 13 (2003) 825.
[175] J.D. Crowley, I.M. Steele, B. Bosnich, Inorg. Chem. 44 (2005) 2989.
[176] R.D. Gillard, A. Sengul, A. Oldroyd, Transit. Met. Chem. 26 (2001) 339.
[177] A.H. Wang, J. Nathans, G. van der Marel, J.H. van Boom, A. Rich, Nature (London) 276 (1978) 471.
[178] E.M.A. Ratilla, H.M. Brothers, N.M. Kostic, J. Am. Chem. Soc. 109 (1987) 4592.
[179] E.J. Gabbay, M.A. Adkins, S. Yen, Nucleic Acids Res. 7 (1979) 1081.
[180] R.T.C. Brownlee, W.D. McFadyen, M.J. Oconnor, T.J. Rook, I.A.G. Roos, L.P.G. Wakelin, Magn. Reson. Chem. 25 (1987) 492.
[181] A. Romerosa, P. Bergamini, V. Bertolasi, A. Canella, M. Cattabriga, R. Gavioli, S. Manas, N. Mantovani, L. Pellacani, Inorg. Chem. 43 (2004) 905.
[182] W. Huang, C.D. Li, J.X. Wang, L.G. Zhu, Spectrosc. Lett. 31 (1998) 1793.
[183] R.A.J. O'Hair, Eur. Mass Spectrom. 3 (1997) 390.